



Calhoun: The NPS Institutional Archive

Theses and Dissertations

Thesis Collection

2006-06

Hit-to-kill guidance algorithm for the interception of ballistic missiles during the boost phase

Lukacs, John A.

Monterey California. Naval Postgraduate School

<http://hdl.handle.net/10945/2829>



Calhoun is a project of the Dudley Knox Library at NPS, furthering the precepts and goals of open government and government transparency. All information contained herein has been approved for release by the NPS Public Affairs Officer.

Dudley Knox Library / Naval Postgraduate School
411 Dyer Road / 1 University Circle
Monterey, California USA 93943

<http://www.nps.edu/library>



**NAVAL
POSTGRADUATE
SCHOOL**

MONTEREY, CALIFORNIA

THESIS

**HIT-TO-KILL GUIDANCE ALGORITHM FOR THE
INTERCEPTION OF BALLISTIC MISSILES IN THE
BOOST PHASE**

by

John A. Lukacs IV

June 2006

Thesis Advisor:

Oleg Yakimenko

Approved for public release; distribution is unlimited.

THIS PAGE INTENTIONALLY LEFT BLANK

REPORT DOCUMENTATION PAGE			<i>Form Approved OMB No. 0704-0188</i>
Public reporting burden for this collection of information is estimated to average 1 hour per response, including the time for reviewing instruction, searching existing data sources, gathering and maintaining the data needed, and completing and reviewing the collection of information. Send comments regarding this burden estimate or any other aspect of this collection of information, including suggestions for reducing this burden, to Washington headquarters Services, Directorate for Information Operations and Reports, 1215 Jefferson Davis Highway, Suite 1204, Arlington, VA 22202-4302, and to the Office of Management and Budget, Paperwork Reduction Project (0704-0188) Washington DC 20503.			
1. AGENCY USE ONLY (Leave blank)	2. REPORT DATE June 2006	3. REPORT TYPE AND DATES COVERED Master's Thesis	
4. TITLE AND SUBTITLE Hit-to-Kill Guidance Algorithm for the Interception of Ballistic Missiles During the Boost Phase		5. FUNDING NUMBERS	
6. AUTHOR(S) John A. Lukacs IV		8. PERFORMING ORGANIZATION REPORT NUMBER	
7. PERFORMING ORGANIZATION NAME(S) AND ADDRESS(ES) Naval Postgraduate School Monterey, CA 93943-5000		10. SPONSORING/MONITORING AGENCY REPORT NUMBER	
9. SPONSORING /MONITORING AGENCY NAME(S) AND ADDRESS(ES) N/A		11. SUPPLEMENTARY NOTES The views expressed in this thesis are those of the author and do not reflect the official policy or position of the Department of Defense or the U.S. Government.	
12a. DISTRIBUTION / AVAILABILITY STATEMENT Approved for public release; distribution is unlimited.		12b. DISTRIBUTION CODE	
13. ABSTRACT (maximum 200 words) A near-optimal guidance law has been developed using the direct method of calculus of variations that maximizes the kinetic energy transfer from a surface-launched missile upon interception to a ballistic missile target during the boost phase of flight. Mathematical models of a North Korean Taep'o-dong II (TD-2) medium-range ballistic missile and a Raytheon Standard Missile 6 (SM-6) interceptor are used to demonstrate the guidance law's performance. This law will utilize the SM-6's onboard computer and active radar sensors to independently predict an intercept point, solve the two-point boundary value problem, and determine a near-optimal flight path to that point. Determining a truly optimal flight path would require significant computing power and time, while a near-optimal flight path can be calculated onboard the interceptor and updated in real time without significant changes to the interceptor's hardware. That near-optimal guidance path is then converted into a set of command functions and fed back into the control computer of the interceptor. By modifying the second and third derivatives of the two-point boundary value problem, the intercept conditions can be varied to study their effects upon the optimal flight path regarding the maximization of kinetic energy upon impact.			
14. SUBJECT TERMS Missile Guidance Laws, Direct Methods, Optimal Control, Boost Phase Intercept, Hit-to-Kill		15. NUMBER OF PAGES 157	
		16. PRICE CODE	
17. SECURITY CLASSIFICATION OF REPORT Unclassified	18. SECURITY CLASSIFICATION OF THIS PAGE Unclassified	19. SECURITY CLASSIFICATION OF ABSTRACT Unclassified	20. LIMITATION OF ABSTRACT UL

NSN 7540-01-280-5500

Standard Form 298 (Rev. 2-89)
Prescribed by ANSI Std. Z39-18

THIS PAGE INTENTIONALLY LEFT BLANK

Approved for public release; distribution is unlimited.

**HIT-TO-KILL GUIDANCE ALGORITHM FOR THE INTERCEPTION OF
BALLISTIC MISSILES IN THE BOOST PHASE**

John A. Lukacs IV
Lieutenant, United States Navy
B.S., Drexel University, 1999

Submitted in partial fulfillment of the
requirements for the degree of

MASTER OF SCIENCE IN MECHANICAL ENGINEERING

from the

**NAVAL POSTGRADUATE SCHOOL
June 2006**

Author: John A. Lukacs IV

Approved by: Oleg Yakimenko
Thesis Advisor

Anthony J. Healey
Chairman
Department of Mechanical & Astronautical Engineering

THIS PAGE INTENTIONALLY LEFT BLANK

ABSTRACT

A near-optimal guidance law has been developed using the direct method of calculus of variations that maximizes the kinetic energy transfer from a surface-launched missile upon interception to a ballistic missile target during the boost phase of flight. Mathematical models of a North Korean Taep'o-dong II (TD-2) medium-range ballistic missile and a Raytheon Standard Missile 6 (SM-6) interceptor are used to demonstrate the guidance law's performance. This law will utilize the SM-6's onboard computer and active radar sensors to independently predict an intercept point, solve the two-point boundary value problem, and determine a near-optimal flight path to that point. Determining a truly optimal flight path would require significant computing power and time, while a near-optimal flight path can be calculated onboard the interceptor and updated in real time without significant changes to the interceptor's hardware. That near-optimal guidance path is then converted into a set of command functions and fed back into the control computer of the interceptor. By modifying the second and third derivatives of the two-point boundary value problem, the intercept conditions can be varied to study their effects upon the optimal flight path regarding the maximization of kinetic energy upon impact.

THIS PAGE INTENTIONALLY LEFT BLANK

TABLE OF CONTENTS

I.	INTRODUCTION.....	1
	A. BACKGROUND	1
	B. THESIS ORGANIZATION.....	3
II.	MODELING AND SIMULATION.....	5
	A. TARGET MODELING	6
	1. Basic Definitions and Assumptions	6
	2. The Ballistic Missile Model Program.....	8
	3. Results	12
	B. INTERCEPTOR MODELING	15
	1. Basic Definitions and Assumptions	15
	2. Interceptor Missile Model Program.....	18
	3. Results	21
	C. HIGH-FIDELITY MODELING	22
	1. Initialization.....	23
	2. The Flight Program	28
	3. Results	39
	D. COMMON FUNCTIONS	39
	1. ZLDragC.m	39
	2. SAtmos.m	40
III.	EXISTING GUIDANCE LAWS	43
	A. UNACCEPTABLE GUIDANCE LAWS.....	43
	1. Beam Rider	43
	2. Pure Pursuit.....	43
	B. LESS THAN OPTIMAL GUIDANCE LAWS	44
	1. True Proportional Navigation	44
	2. Compensated Proportional Navigation.....	45
	3. Augmented Proportional Navigation	45
	C. KEY FATAL CHARACTERISTICS	46
	1. Control System Time Constant.....	46
	2. End-game Environment	47
	3. Controlling the Interception Geometry	47
IV.	PROPOSED ALGORITHM.....	49
	A. PROBLEM STATEMENT	49
	B. CALCULUS OF VARIATIONS	50
	C. PROGRAM DEVELOPMENT	55
	1. Boundary Conditions.....	55
	2. Separating and Recombining Space and Time	57
	3. Reference Trajectory	58
	4. Inverse Dynamics	60
	5. Cost and Penalty Functions.....	61
	4. Simulation Outline.....	62

D.	SIMULATION RESULTS	64
V.	CONCLUSIONS	69
A.	VERIFICATION OF OPTIMALITY	69
B.	APPLICABILITY	78
C.	SUGGESTIONS FOR FUTURE RESEARCH.....	78
APPENDIX A:	MODELING PROGRAMS.....	81
A.	3DOF TARGET	81
1.	BRParams3.m.....	81
2.	BRFlight3.m	82
B.	3DOF INTERCEPTOR.....	85
1.	SMParams3.m	85
2.	SMFlight3.m	87
C.	6DOF MODEL	92
1.	BRDetails6.m.....	92
2.	BRParams6.m.....	94
3.	BRFlight6.m	97
3.	SMDetails6.m	101
5.	SMParams6.m	103
6.	SMFlight6.m	106
7.	ACoeff.m	110
8.	Animation.m	112
D.	COMMON PROGRAMS.....	117
1.	ZLDragC.m	117
2.	SAtmos.m	117
APPENDIX B:	GUIDANCE PROGRAMS	121
A.	DEMONSTRATION	121
B.	GUIDANCE ALGORITHMS.....	123
1.	SMGuidance.m.....	123
2.	SMGuidanceCost.m	129
3.	SMTrajectory.m.....	131
LIST OF REFERENCES		139
INITIAL DISTRIBUTION LIST		141

LIST OF FIGURES

Figure 1.	Engagement Sequence Groups [From Ref 9]	1
Figure 2.	Taep'o-dong 2 and SM-6 size comparison (after [Ref 9]).....	5
Figure 3.	Ballistic Missile Flight Path.....	9
Figure 4.	TD-2 Thrust Generated (Boost Phase Only).....	10
Figure 5.	TD-2 Rocket Mass (Boost Phase Only).....	11
Figure 6.	TD-2 Flyout Range	12
Figure 7.	TD-2 Acceleration and Velocity Profiles (Entire Flight)	13
Figure 8.	TD-2 Acceleration and Velocity Profiles (Boost Phase only)	13
Figure 9.	TD-2 Altitude Profile (Entire Flight and Boost Phase only)	14
Figure 10.	SM-2 Configuration Details (Missile Only)	18
Figure 11.	SM-6 Interceptor Thrust Profile.....	20
Figure 12.	SM-6 Interceptor Mass (Boost Phase Only).....	21
Figure 13.	Interceptor Velocity Profile	22
Figure 14.	Pitch plane stability data	33
Figure 15.	Yaw stability and control derivatives	34
Figure 16.	Roll control derivatives.....	34
Figure 17.	Roll control Coupling Derivatives	35
Figure 18.	Yaw control Derivatives	35
Figure 19.	Pitch control effects on roll stability.....	36
Figure 20.	Pitch control derivatives	36
Figure 21.	6DOF Orientation Animation	39
Figure 22.	Drag Coefficient by Mach Number and Flight Phase.....	40
Figure 23.	Atmospheric Temperature Variation by Altitude	41
Figure 24.	Atmospheric Density by Altitude	41
Figure 25.	Atmospheric Pressure Variation by Altitude	42
Figure 26.	Variation of Path with τ_f and x_{10}''' (after [Ref 18]).....	54
Figure 27.	Variation of First Derivative of Path with τ_f and x_{10}'''	54
Figure 28.	X-axis Flight Path and Derivatives	65
Figure 29.	Y-axis Flight Path and Derivatives	65
Figure 30.	Z-axis Flight Path and Derivatives	66
Figure 31.	3D Optimal Flight Path.....	67
Figure 32.	3D Optimal Flight Path.....	68
Figure 33.	Final Interception Geometry	69
Figure 34.	2D (X-Y axis) Optimum Flight Path	70
Figure 35.	2D (X-Z axis) Optimum Flight Path.....	70
Figure 36.	2D (Y-Z axis) Optimum Flight Path.....	71
Figure 37.	Heading (Ψ) and Flight Path Angle (θ) Time History	72
Figure 38.	Control Forces Time History	73
Figure 39.	Penalty Function Values	74
Figure 40.	Iterative Value of the Cost Function.....	75
Figure 41.	Iterative Value of the Cosine of the Impact Angle	76

Figure 42.	Iterative Value of Intercept Time.....	77
Figure 43.	Iterative Value of τ_f	77

LIST OF TABLES

Table 1.	Known Information Regarding the TD-2	6
Table 2.	Theoretical Velocity Capability of the Target Model.....	8
Table 3.	Known Information Regarding the SM-6	15
Table 4.	Range of Possible Interceptor Thrust Values.....	17
Table 5.	WGS-84 Values	24
Table 6.	Frame References used in the 6DOF Model (After [Ref 14])	25
Table 7.	Interceptor Known Data.....	55

THIS PAGE INTENTIONALLY LEFT BLANK

ACKNOWLEDGMENTS

The author wishes to acknowledge the immense patience of his wife, Sarah, while he spent numerous hours in the computer lab. Her unfailing belief in my abilities often surpassed my own, and without that support this would not have been possible.

The author also wishes to acknowledge the assistance of his advisor, who patiently answered every question, no matter how minor. His efforts in assisting me to troubleshoot pages and pages of MATLAB code are greatly appreciated.

THIS PAGE INTENTIONALLY LEFT BLANK

I. INTRODUCTION

A. BACKGROUND

For many years now, the United States Department of Defense has expended great effort to develop an integrated ballistic missile defense system through a layered, defense in depth strategy. A ballistic missile's speed and altitude leave little room for error by the defender, and any strategy must include systems capable of defeating a ballistic missile at each of its three distinct phases – boost, midcourse, and terminal - which the Missile Defense Agency labels "Engagement Sequence Groups" (ESG) as shown in Figure 1 [Ref 9].



Figure 1. Engagement Sequence Groups [From Ref 9]

It is the portion of the effort directed toward the boost phase of the Ballistic Missile Defense Programs that is the focus this paper. The boost phase ESG is concerned with developing methods and technologies to conduct Boost Phase Intercept (BPI). Intercepting a missile in its boost phase is the ideal solution for a ballistic missile defense, since the missile is very vulnerable during this phase of its flight. The missile is relatively slow while struggling to overcome gravity, has a very visible exhaust plume, and cannot deploy countermeasures [Refs 9, 11]. Yet the challenges needing to be overcome are immense: countering the large acceleration rates, reliable scanning and tracking, and very short reaction time being the most daunting [Refs 9, 11]. A variety of weapon systems are under development for conducting boost phase interception, including airborne lasers, space-based intercept missiles, and ground-based intercept missiles. None of these systems is totally operational, though several look promising.

This paper is applicable to surface-based interceptors, specifically the United States Navy's Standard Missile. The SM-6 very quickly reaches its top speed of Mach 3+ [Ref 6, 12], allowing it to catch up and maneuver around a boosting ballistic missile. The SM-6 is not currently configured for missile defense options, as the United States Navy has not yet decided on appropriate requirements for surface ship based BPI [Ref 6]. Yet, the SM-6 missile contains the necessary capabilities to conduct such ballistic missile defense missions, including Advanced Medium Range Air-to-Air Missile (AMRAAM) signal processing capabilities that enable the use of active and semi active radar, AMRAAM guidance and control systems, and advanced fusing techniques [Ref 12]. Given the correct guidance laws and programming, these systems combine to make the missile very effective out to the maximum kinetic range. This paper analyzes one method for developing such a guidance law.

A missile's guidance law is one of the largest single factors affecting its ability to intercept a target. Yet, regarding the BPI ESG, intercepting the target is only one factor; the other major consideration is the ability to kill the target. Early ballistic missile defense concepts recognized that a simple warhead effect is not sufficient to destroy an ICBM and initiated development of hit to kill technologies [Ref 2, 3]. The relative sizes of a nominal ICBM and an SM-6 means that the interception must maximize the kinetic energy transferred to the ICBM in order to be effective, which suggests the need to control the geometry of the interception. Current guidance laws do not address this aspect, leaving the actual intercept geometry to be the result of the guidance law and the relative capabilities of the missiles, instead of an input into the guidance law. This is a reasonable course of action when all that is necessary to kill the target is to get the missile within the limits of the proximity fuse, the case with most surface-to-air engagements. It breaks down, however, when dealing with ballistic missiles. The desire for hit-to-kill end game conditions, coupled with the need to maximize the kinetic energy transfer, means the interception geometry cannot be left to chance and must be controlled as an input of the guidance law.

The objective of this thesis is to design a guidance law that will generate the interceptor's entire flight path in order to minimize the distance traveled, minimize the time to intercept, and maximize kinetic energy transfer by controlling the interception

geometry while providing near-optimal flight path to interception. This will be done by utilizing the direct method of calculus of variations combined with inverse dynamics theory to reverse engineer in real time an optimal flight path using the missile's onboard sensors and computers [Ref 18].

B. THESIS ORGANIZATION

Chapter II develops the simulation models for the ballistic missile target and the Standard Missile interceptor, generating a mathematical Three Degree-of-Freedom (3DOF) model of each. This paper will focus on the Taep'o-dong Two (TD2) ballistic rocket in development by the People's Democratic Republic of Korea (DPRK), which is believed to be an intercontinental ballistic missile (ICBM) capable of reaching at least Alaska or Hawaii from launch sites within North Korea [Ref 4]. The SM-6 is the US Navy's latest Extended Range Anti-Air Warfare missile that includes Active-Homing Terminal Guidance – the key feature that allows for the accuracy necessary to intercept an ICBM in the boost phase. Finally, a full Six Degree-of-Freedom (6DOF) model is presented for future research to capitalize upon.

Chapter III discusses several modern guidance laws, describing and evaluating for their effectiveness at intercepting and killing an ICBM. Two families of guidance laws, Pursuit and Proportional Navigation, are examined. The reasons for the necessity of a new guidance law are presented.

Chapter IV develops and describes the new guidance law and test program. The guidance law is continuously calculated onboard the missile as a two point boundary value problem, using Direct Methods of Calculus of Variation to calculate a near-optimal flight path and the control commands necessary to achieve it.

Chapter V summarizes the results and discusses the feasibility of employing such methods in a real-world scenario.

The Appendices include a listing of all MATLAB functions and scripts used in the simulation.

Throughout the remainder of this paper, the term "rocket", "target", and "TD2" will be used to refer to the Taep'o-dong 2, while the term "missile", "interceptor", and "SM-6" will refer to the Standard Missile 6.

II. MODELING AND SIMULATION

This chapter develops a three-dimensional target model that operates in the Earth's gravitational field, using the TD-2 rocket for reference data. The simulation models a two-stage, boosting target that reaches intercontinental velocities. Then a three-dimensional interceptor model is developed that operates in the Earth's gravitational field, using the SM-6 missile for reference data. The simulation models a two-stage, boosting missile that reaches nominal velocities. Figure 2 shows a comparison of the relative sizes of the missiles involved.



Figure 2. Taep'o-dong 2 and SM-6 size comparison (after [Ref 9])

A. TARGET MODELING

1. Basic Definitions and Assumptions

Table 1 shows the basic details of a Taep'o-dong two (TD-2) rocket [Ref 4].

	Overall		Stage 1	Stage 2
Length	32 m	Diameter	2.2 m	1.335 m
Payload	750-1000 kg	Length	16 m	14 m
Range	3500–4300 km	Launch Weight	~60,000 kg	15,200 kg
Stages	2	Thrust	~103,000 kg _f	13,350 kg _f
Thrust Chambers	4,1	Fuel / Oxidizer	TM-185 / AK-27I	TM-185 / AK-27I
Type	LR ICBM	Propellant Mass	-	12,912 kg
		Burn Time	~125 s	110 s

Table 1. Known Information Regarding the TD-2

The limited data must be extrapolated into a complete missile picture. This required several assumptions, which will be discussed during the course of the extrapolation.

The first assumption was that of a linear ratio between the fuel and the thrust. The thrust developed was assumed to be a weak function of fuel consumption and the number of thrust chambers, and a strong function of the specifics of the engines. Stage one has four chambers while stage two has one chamber; therefore the ratio of the fuel consumption rates should not be greater than 4. The total propellant mass of stage two is 12,912 kg while the total mass of the stage is 15,200 kg, for a fuel mass fraction of 0.849 and a fuel consumption rate (for 110 s) of 117.38 kg/s. This value is appropriate for a ballistic missile [Ref 21]. Assuming the same ratio for stage one results in a fuel mass of 50,970 kg and a fuel consumption rate (for 125 s) of 407.8 kg/s.

The fuel used is a combination of a liquid fuel and a liquid oxidizer. TM-185 is composed of 20% Gasoline (737.22 kg/m³) and 80% Kerosene (817.15 kg/m³) [Ref 4],

which results in a fuel density of 801.164 kg/m³. The oxidizer, AK-27I, is composed of 27% N₂O₄ (1,450 kg/m³) and 73% HNO₃ (1,580 kg/m³) [Ref 4], which results in an oxidizer density of 1,544 kg/m³. Finally, the fuel to oxidizer ratio (F/O) for this fuel combination is 4.05:1 [Ref 16], yielding a cumulative density of 1,182.62 kg/m³. Given the density of the fuel, the total volume for each stage is easily determined. For stage one the required volume of fuel is 43.1 m³, while for stage two the required volume of fuel is 10.9 m³. Since the total available volume of stage one is 60.82 m³, and the total available volume of stage two is 19.6 m³, the values are reasonable.

Given that both stages use the same fuel, the specific impulse (I_{sp}) should be the same for both stages, which is expressed as [Ref 21]

$$I_{sp} = \frac{T}{\dot{W}} \quad (2.A.1)$$

where \dot{W} is the in-stage fuel consumption rate (in kg/s) and T is the thrust produced. The first stage I_{sp} is 252.57 s, which is reasonable for an intercontinental ballistic missile. Yet the second stage I_{sp} using the given thrust data is only 113.73 s, which is too low to accelerate the rocket to intercontinental speeds [Ref 21]. The second stage I_{sp} will therefore be assumed to be 252.57 s, and the resultant thrust is then 29,650 kgf.

Under these assumptions, it is possible to determine the resultant increase in velocity ΔV (in m/s) by the rocket equation [Ref 21]

$$\Delta V_n = I_{sp} g \ln \left(\frac{1}{1 - m_{f,n}} \right), \text{ where } m_{f,n} = \frac{m_{p,n}}{\sum_{i=n}^2 m_{t,i} + m_{pay}} \quad (2.A.2)$$

where n is the stage number, $m_{p,n}$ (in kg) is the stage propellant mass, $m_{t,i}$ (in kg) is the total stage mass, and m_{pay} (in kg) is the payload mass. In each stage, all masses except the propellant mass in that stage is considered part of the structural mass. Each of the stages yields a separate ΔV where the total velocity capability of the overall system is

$$\Delta V = \sum_{i=1}^n \Delta V_i \quad (2.A.3)$$

where n is the number of stages.

This value does not account for drag or the variation of gravity, so it is only a theoretical estimate of the final value that will be used to verify the model is working correctly. The theoretical values are listed in Table 2.

	Stage 1	Stage 2	Total
Stage Mass Fraction	0.671	0.809	-
ΔV (in m/s)	2755.21	4108.68	6863.90

Table 2. Theoretical Velocity Capability of the Target Model

The final velocity from the model should therefore be less than 6863 m/s, since both gravity and drag will be working against the launch.

2. The Ballistic Missile Model Program

The 3DOF model presented here is a series of MATLAB functions on a repeating integration loop, using four function files to accomplish the modeling (the “3” at the end of each title refer to the 3DOF model).

1. BRFlight3.m - integrates each time step to determine the current position, attitude, and aerodynamic forces acting on the rocket/missile;
2. BRParams3.m - determines the mass of the rocket and the surface reference area;
3. ZLDragC.m - determines the drag coefficient (described in section D);
4. SAtmos.m – determines the properties of the local atmosphere (described in section D);

The program BRFlight3.m generates a ballistic flight path that will be intercepted by the SM-6 based on the model developed by Zarchan [Ref 21]. The main difference is that Zarchan developed a two-dimensional x-y model, whereas this paper requires a three-dimensional model. The mapping to a three dimensional system is done simply by employing the x-y equations as x-z equations and making the y-values a constant, in this

case zero. Thus a three-dimensional flight path is created entirely contained within the x-z plane as shown in Figure 3, where the asterisks represent the staging events.

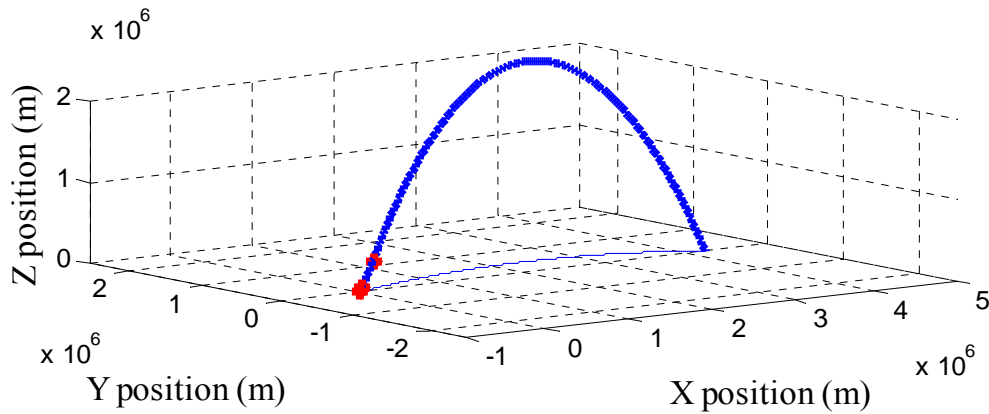


Figure 3. Ballistic Missile Flight Path

The launch position is at

$$\begin{aligned} x_0 &= 0 \\ y_0 &= 0 \\ z_0 &= R_e \end{aligned} \tag{2.A.4}$$

where R_e is the WGS-84 radius of the Earth, 6,378,137 m.

The initial velocities are:

$$\begin{aligned} \dot{x}_0 &= V_0 \cos \theta \cos \Psi \\ \dot{y}_0 &= V_0 \cos \theta \sin \Psi \\ \dot{z}_0 &= V_0 \sin \theta \end{aligned} \tag{2.A.5}$$

where V_0 is the initial velocity, θ is the initial elevation angle, and Ψ is the initial heading. A heading of $\Psi = 0$ will result in an initial y velocity of 0 as required for this model. The launch angle, θ , is 85 degrees, which was chosen to maximize the range while still recognizing the restrictions on launching such a large missile as the TD-2 (45-60 degrees is not a feasible launch angle) [Ref 21].

The program first calculates the axial force on the missile, a_T , which is based on the thrust and drag forces acting on the missile. The thrust is a given set of time-based values based on the previously articulated known data and assumptions, shown in Figure

4. The thrust also drops sharply at 130 seconds and 240 seconds to represent the staging events. Following the completion of the boost phase, the thrust is zero, though the axial force is not due to the continuous presence of drag.

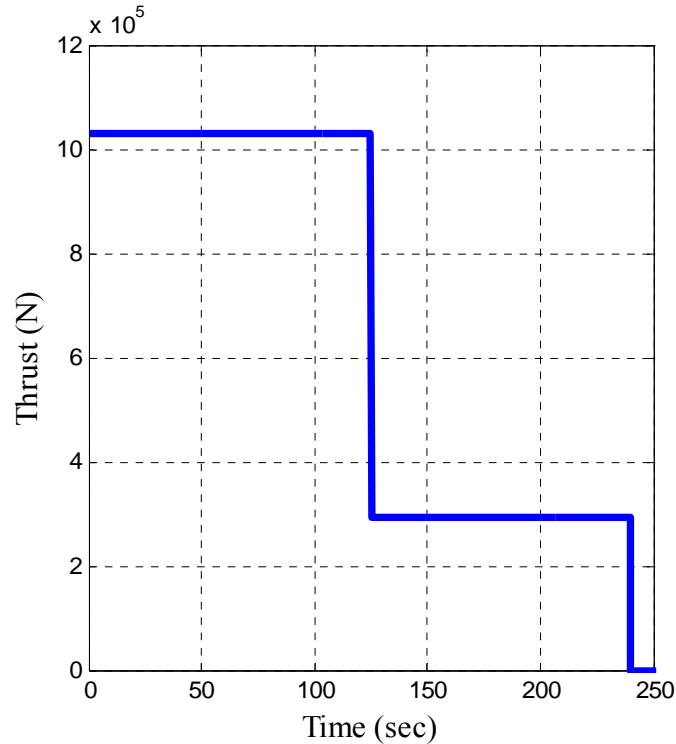


Figure 4. TD-2 Thrust Generated (Boost Phase Only)

The drag requires several steps to calculate, including determination of the local atmospheric density and temperature (using the function `Statmos.m`), the atmospheric drag constant (using the function `ZLDragC.m`), and the reference surface area (using the function `BRParams3.m`). `Statmos.m` and `ZLDragC.m` are described in section D of this chapter.

The rocket's mass is a simple function of time (using the function `BRParams3.m`), shown in Figure 5. The mass drops sharply at 130 seconds and at 240 seconds, which represent the staging events. After the completion of the boost phase, the mass remains constant for the duration of the flight.

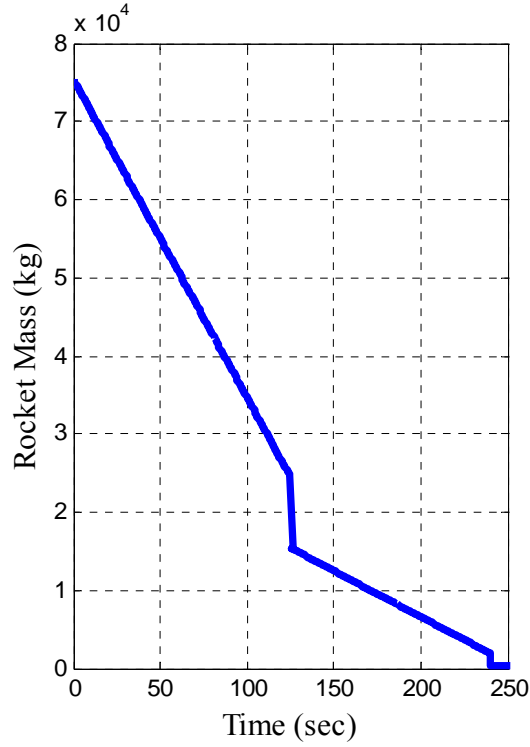


Figure 5. TD-2 Rocket Mass (Boost Phase Only)

The axial thrust force is then the difference between the thrust and drag, and the axial acceleration is given by

$$a_T = \frac{(T-D)}{mg} \quad (2.A.6)$$

Using the nominal two-stage booster design, a simple gravity turn is generated by aligning the thrust vector with the velocity vector, keeping in mind the flight path is entirely contained within the x-z plane [Ref 21]

$$\begin{aligned} \ddot{x} &= \frac{-gm x}{(x^2 + z^2)^{1.5}} + \frac{a_T \dot{x}}{(\dot{x}^2 + \dot{z}^2)^{0.5}} \\ \ddot{y} &= 0 \\ \ddot{z} &= \frac{-gm z}{(x^2 + z^2)^{1.5}} + \frac{a_T \dot{z}}{(\dot{x}^2 + \dot{z}^2)^{0.5}} \end{aligned} \quad (2.A.7)$$

where gm is the WGS-84 Earth's gravitational constant, $3.986 \times 10^{14} \text{ m}^3/\text{s}^2$ [Ref 14]. Equations (2.A.7) are integrated for the duration of the rocket flight.

3. Results

The two dimensional graph of the x-z plane, shown in figure 6, clearly shows the altitude and range of the rocket, which compares favorably with the known data presented earlier and Zarchan [Ref 21], where the asterisks again represent the location of the staging events. As noted in Zarchan, the flat earth equations used here are only moderately accurate over the course of the rocket's entire flight, but since the focus of this paper is only on the boost phase, the accuracy of the termination position is irrelevant. During the boost phase the accuracy of the flat earth equations is very good.

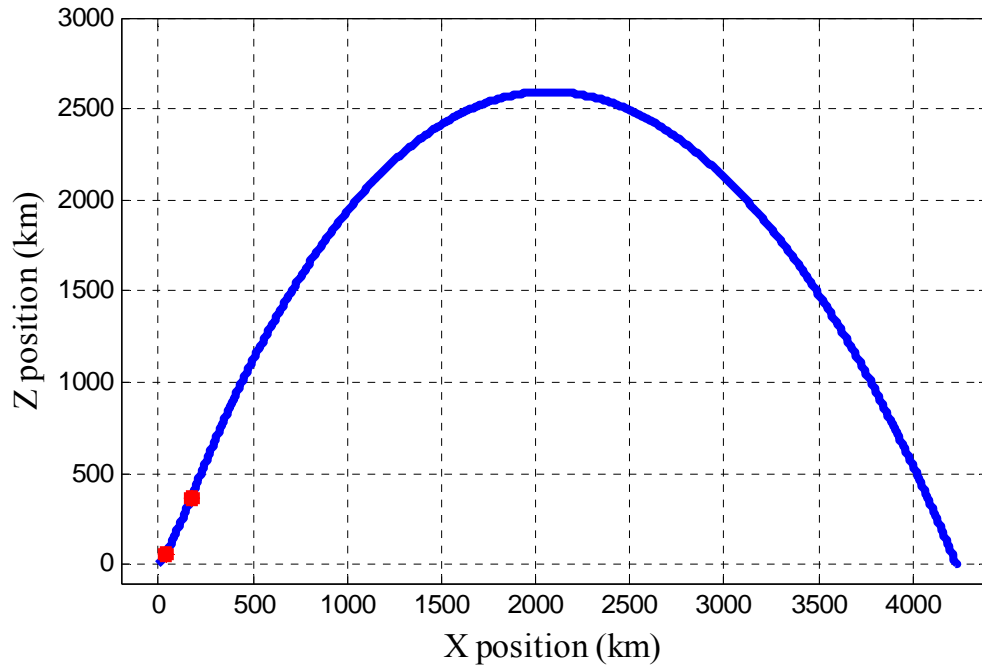


Figure 6. TD-2 Flyout Range

The acceleration required to achieve these ranges is on the order of 6.5 km/s [Ref 21]. Figures 7 and 8 clearly show that this speed has been achieved at the end of the boost phase, and thus the range values are appropriate. Figure 7 shows the velocity profile for the entire flight. The rocket reaches a velocity of nearly 6 km/s at the end of the boost phase. After burnout it decelerates due to gravity until it reaches its apogee, after which point it begins to accelerate due to gravity.

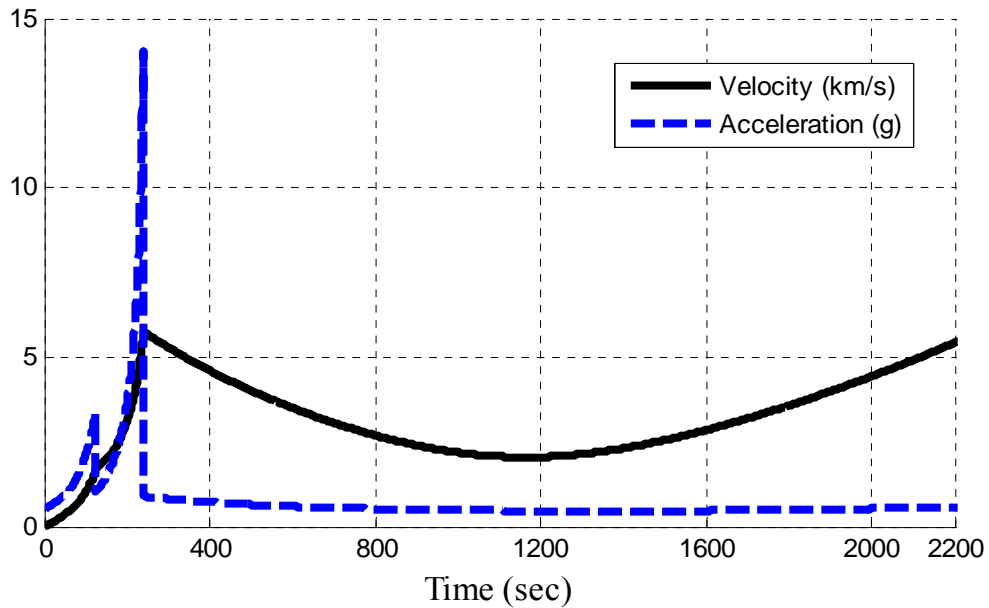


Figure 7. TD-2 Acceleration and Velocity Profiles (Entire Flight)

Figure 7 shows a closer look at the boost phase acceleration and velocity profiles. The effects of staging are readily apparent. It is clear that the values are consistent with, but slightly less than, the predictions from Table 2, as expected due to the presence of gravity and drag.

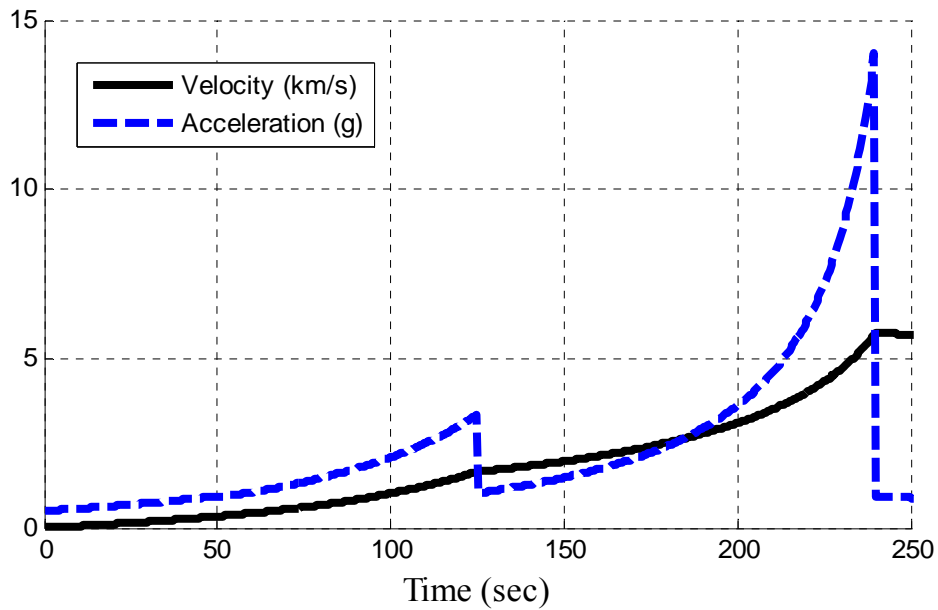


Figure 8. TD-2 Acceleration and Velocity Profiles (Boost Phase only)

The determination of the available time for a surface-launched missile to intercept the target is one of the critical values that can now be determined. Figure 9 shows the altitude profile for the TD-2 for the entire flight and the boost phase only. The effects of acceleration are quite apparent. The uppermost limit of the atmosphere according to the WGS-84 standard atmospheric model is 86 km. Even at 86 km, however, an endoatmospheric missile has a hard time maneuvering due to the low density of the local atmosphere. Thus the maximum allowable intercept value must be lowered; in this case 50-60 km will be considered the upper limit. The target achieves this altitude between 130 s and 140 s. This is one of the most significant limitations on the BPI problem, since a US Navy ship on station and actively monitoring the launch area will still need 45-60 seconds to detect, track, analyze, and engage the target. This paper will assume a 60 second delay in the interceptor launch.

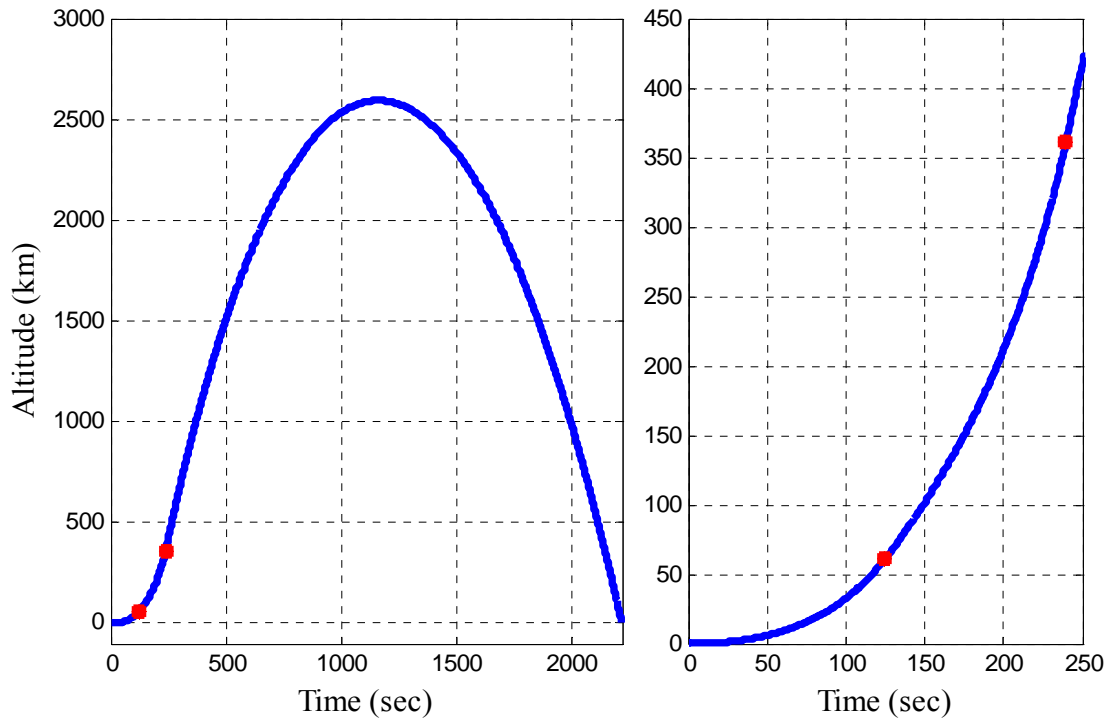


Figure 9. TD-2 Altitude Profile (Entire Flight and Boost Phase only)

The final step of the program is to record all the data for the rocket. This data will be called by the interceptor simulation to mimic the missile’s onboard sensors. The missile will “see” the location and velocity of the rocket at the appropriate intervals by coordinating the launch time of the interceptor with the launch time of the ballistic missile.

B. INTERCEPTOR MODELING

1. Basic Definitions and Assumptions

The following are the basic details of a Raytheon Standard Missile 6 (SM-6) [Refs 6, 12].

	Overall		Stage 1	Stage 2
Length	6.5 m	Diameter	0.53 m	0.34 m
Payload	115 kg	Length	1.72 m	4.78 m
Range	150 km	Launch Weight	712 kg	686 kg
Stages	2	Thrust	-	-
Thrust Chambers	1,1	Fuel / Oxidizer	HTPB-AP	TP-H1205/6
Type	ERAAW	Propellant Mass	468 kg	360 kg
		Burn Time	6 s	-

Table 3. Known Information Regarding the SM-6

Again, the limited data must be extrapolated into a complete missile picture. Several assumptions were again made, which will be discussed during the course of the extrapolation.

The two stages have dissimilar fuels, so very few assumptions can be correlated between the two. One assumption that can be made and applied to both solid propellants is the grain pattern. It has been assumed that both motors use a star grain pattern, which was designed to and is known to very effectively provide a constant stable burn throughout the flight. A star grain pattern produces thrust variations of less than 4% for the duration of the burn [Ref 10]. This grain pattern typically has a volume loading

fraction of 60-80%, which will be the assumed range for both stages. The final value will be determined by what gives a reasonable value for structural thickness.

The Stage 1 fuel is HTPB-AP. The presence of smoke during launch, in addition to the massive thrust required, strongly suggests the presence of a metal (probably aluminum). The density of the combination of those three components that yields the highest specific impulse is 1860 kg/m³. A fuel with a mass of 468 kg with a density of 1860 kg/m³ has a volume of 0.25 m³. Applying the loading fraction of 60% to the volume and subtracting from the total volume of the Mk-72 engine leaves 0.0208 m (~4/5 in) average thickness for the structural components. This will be the assumed average value for the external structure of the SM-6.

When applied to Stage 2, the density of the TP-H1205/6 fuel is roughly 3000 kg/m³, which is too high. Assuming a volumetric fraction of 80% yields a density of 2267 kg/m³, a more realistic value.

Solid fuel motors used aboard U.S. Navy ships must have a Department of Defense (DOD) Hazard Classification of 1.1 or 1.3. Typical solid rocket fuels of this category have a specific impulse, I_{sp} , in the range of 180-270 seconds [Ref 3]. The thrust produced by such a rocket motor is given by

$$F = I_{sp} \dot{m} g \quad (2.B.1)$$

where \dot{m} is the change in mass over time or the stage fuel consumption rate $\frac{dm}{dt}$ (in kg/s) and g is the gravitational acceleration at the current distance from the center of the Earth (in m/s²). Using the known masses and burntimes, and assuming a fifteen second burntime for the second stage, results in the range of possible thrust values given in Table 4. Since open source literature details the SM-3 (which uses the same engines) speed capability as 4000 m/s [Ref 6], the final implemented values will be chosen to accelerate the SM-6 to that speed in a reasonable time.

	Stage 1	Stage 2
Mass (kg)	468	360
Burntime (s)	6	15
Thrust Range (N)	137,732.4 – 206,598.6	42,379.2 – 63,568.8

Table 4. Range of Possible Interceptor Thrust Values

The density of the structural components must be calculated by omission, since the assumption can be made that the material is some form of composite vice anything like common structural steel. The volume of each component was calculated assuming simple geometric shapes – tangent ogive nosecone, cylindrical body sections, trapezoidal wingforms, and triangular tail control surfaces. No detailed specifications are available for the SM-6, but it is similar enough to the SM-2, shown in Figure 10 [Ref 1], for the purposes of calculating the sizes of structural components. An additional modifying assumption to account for the sensor and computer equipment inside the radome was included by adding 30% of the volume of the radome as structural weight. The total volume of structural components was 0.162 m³, and the total weight of structure and miscellaneous components was 685 kg (everything except fuel and warhead), resulting in a structural density of 4220 kg/m³, which is a realistic value for a high strength composite material.

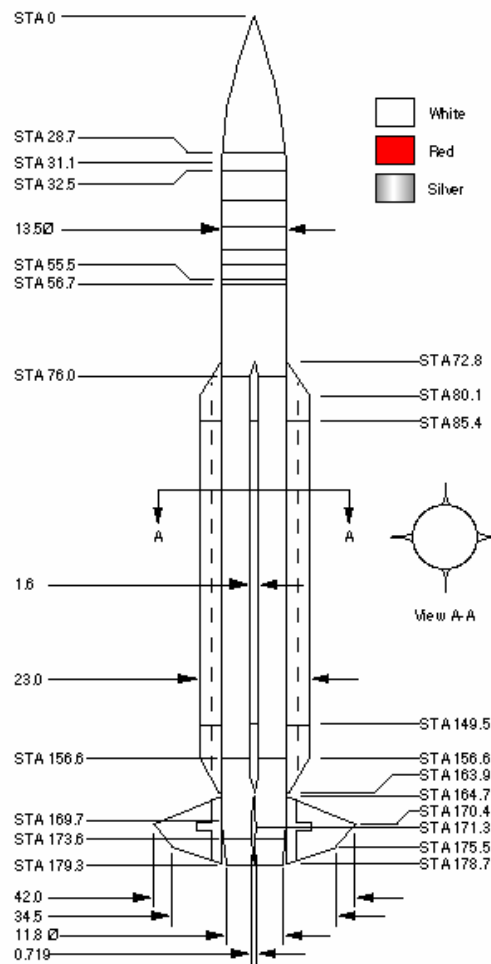


Figure 10. SM-2 Configuration Details (Missile Only)

2. Interceptor Missile Model Program

The 3DOF model presented here is a series of MATLAB functions on a repeating integration loop, using four function files to accomplish the modeling. (the “3” at the end of each title refer to the 3DOF model).

1. SMFlight3.m - integrates each time step to determine the current position, attitude, and aerodynamic forces acting on the rocket/missile;
2. SMParams3.m - determines the mass of the rocket and the surface reference area;
3. ZLDragC.m - determines the drag coefficient (described in section D);

4. STatmos.m – determines the properties of the local atmosphere (described in section D);

The program SMFlight.m generates the flight plan using the axial velocity, V , the heading angle, Ψ , and the flight path angle, θ , related through the kinematic equations [Ref 19]

$$\begin{aligned}\dot{x} &= V \cos \theta \cos \Psi \\ \dot{y} &= V \cos \theta \sin \Psi \\ \dot{z} &= V \sin \theta\end{aligned}\tag{2.B.2}$$

The three components are the result of the forces acting on the missile, related through the dynamics equations [Ref 19]

$$\begin{aligned}\dot{V} &= g (n_x - \sin \theta) \\ \dot{\theta} &= \frac{g}{V} (n_y - \cos \theta) \\ \dot{\Psi} &= \frac{g}{V \cos \theta} n_z\end{aligned}\tag{2.B.3}$$

where n_x is the axial force, n_y is the yaw force, and n_z is the lift force.

Further, the acceleration components are found from the derivatives of equation (2.B.2).

$$\begin{aligned}\ddot{x}_1 &= \dot{V} \cos \theta \cos \Psi - \dot{\theta} V \sin \theta \cos \Psi - \dot{\Psi} V \cos \theta \sin \Psi \\ \ddot{x}_2 &= \dot{V} \cos \theta \sin \Psi - \dot{\theta} V \sin \theta \sin \Psi + \dot{\Psi} V \cos \theta \cos \Psi \\ \ddot{x}_3 &= \dot{V} \sin \theta + \dot{\theta} V \cos \theta\end{aligned}\tag{2.B.4}$$

The axial forces are calculated in the same manner as the axial force of the ballistic missile, in fact re-using both the STatmos.m and ZLDragC.m functions. STatmos.m and ZLDragC.m are described in section D of this chapter. The SMPParams.m function uses the same methodology as the BRParams.m function to calculate the reference surface area and the mass.

The thrust is a given set of time-based values based on the known data and the assumptions, shown in Figure 11. The thrust drops sharply at 6 s and 26 s, again to represent the staging events.

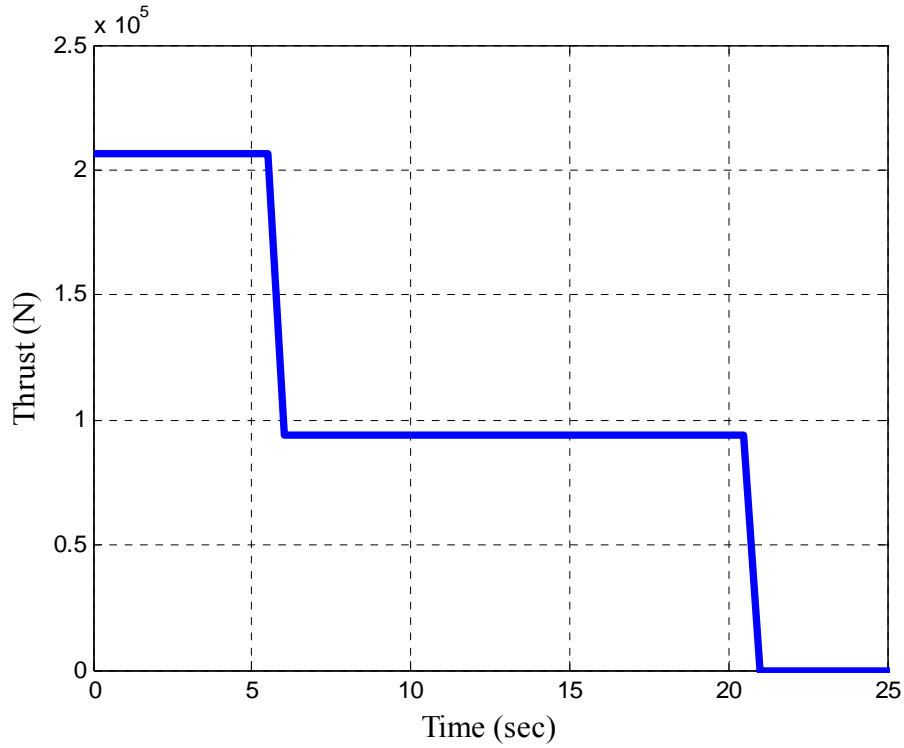


Figure 11. SM-6 Interceptor Thrust Profile

The mass is again a simple function of time (using the function SMPParams.m), shown in Figure 12. The mass drops sharply at 6 seconds and at 26 seconds, again to represent the staging events.

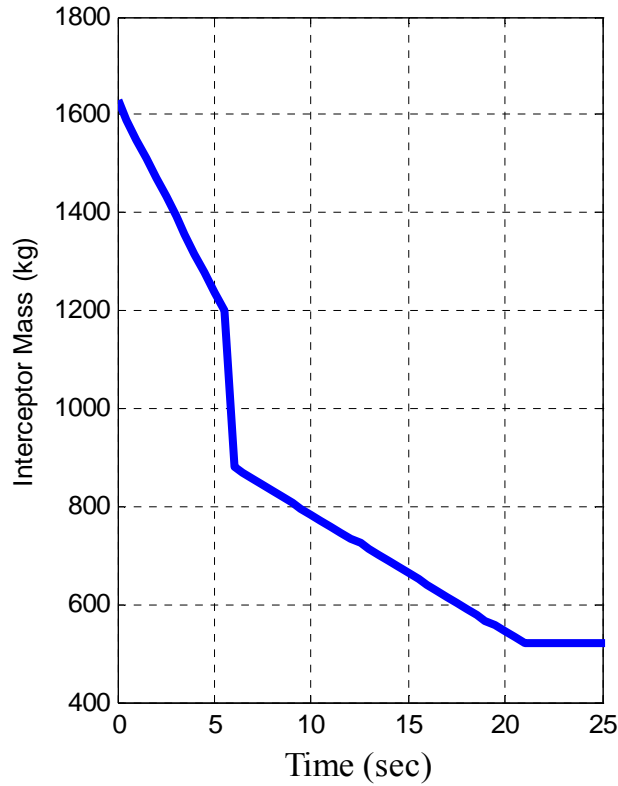


Figure 12. SM-6 Interceptor Mass (Boost Phase Only)

The axial thrust force is then the difference between the thrust and drag, and the axial acceleration is given by

$$n_x = \frac{(T - D)}{mg} \quad (2.B.5)$$

The remaining two forces, n_y, n_z , are returned from the guidance laws and applied by integrating equations (2.B.3).

3. Results

Many of the results are specifically dependant on the guidance law, but several are relatively independent, such as the Velocity, Acceleration, and generic flight profile. The I_{sp} of both stages was maximized but still unable to accelerate the SM-6 beyond a speed of 3,500 m/s. This speed was not detrimental to the simulation and was determined to be the most accurate value considering all the data. Figure 13 shows the generic

Velocity and Acceleration profile produced by the model, which will change slightly with each run due to the guidance law in effect and specifics of the simulation.

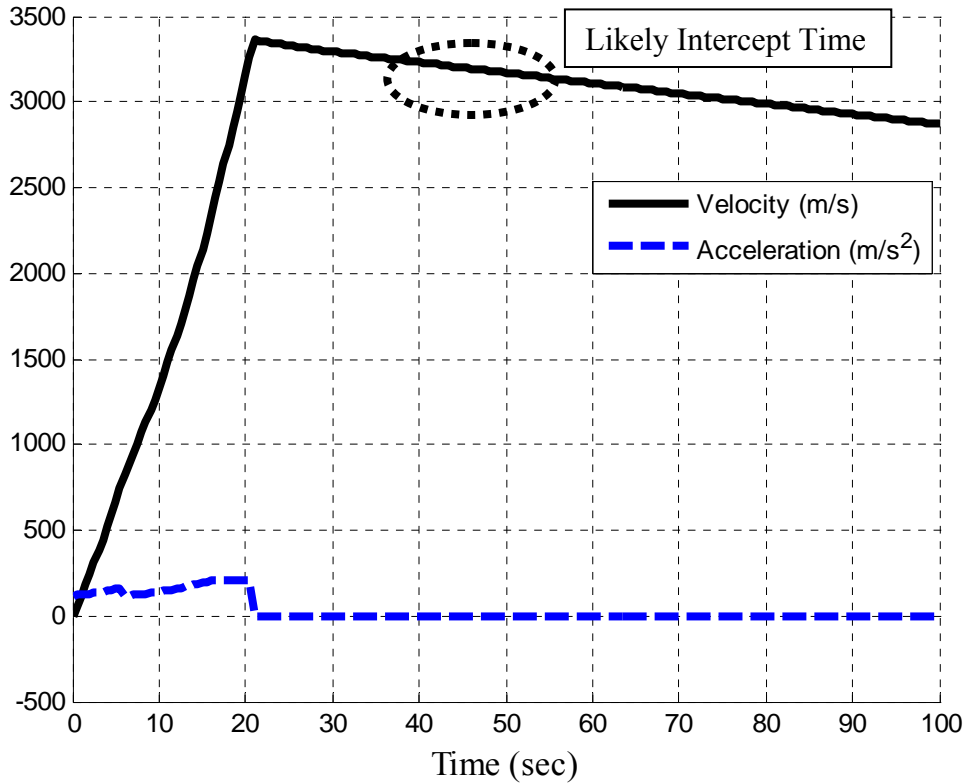


Figure 13. Interceptor Velocity Profile

C. HIGH-FIDELITY MODELING

Although the guidance law modeled and developed in sections III and IV deals with a 3DOF models discussed earlier, the follow-on research will require a higher fidelity model, such as a Six-Degree-of-Freedom (6DOF) model of the interceptor missile presented here. This model uses the same fundamental algorithm for the guidance law, but instead of treating the interceptor as a point mass and considering only position, velocity, and acceleration, it will also consider attitude and orientation. It also goes one step further than the algorithm presented by converting acceleration commands into aileron commands.

The higher fidelity modeling was also addressed in this study. The 6DOF model presented here is a series of MATLAB functions on a repeating integration loop. It uses

seven function files to accomplish the modeling, each applying to their respective simulations (the “6” at the end of each title refer to the 6DOF model). The programs are very similar, only the control inputs and physical parameters differ.

1. BRInitialize6.m and SMInitialize6.m, which initializes the first step values based on launch conditions;
2. BRDetail6.m and SMDetail6.m, which describes the rocket/missile characteristics such as structural thickness, sizes, and fuel weights, etc.
3. BRFlight6.m and SMFlight6.m, which repeats for each time step to determine the current position, attitude, and aerodynamic forces acting on the rocket/missile;
4. BRParams6.m and SMPParams6.m, which determines the mass of the rocket/missile and moment of inertia based on time, and several aerodynamic derivatives;
5. AeroC.m, which interpolates to determine several aerodynamic values based on angle of attack, altitude, and control surface deflections;
6. ZLDragC.m;
7. SAtmos.m;

The output of the model is utilized by the guidance law program, SMGuidance.m, to determine the necessary inputs to the interceptor missile auto-pilot.

1. Initialization

In order to increase the accuracy of the simulation, the Earth is NOT assumed to be a perfect, non-rotating spheroid. Based on the World Geographic Survey of 1984, the following values were used in the program [Ref 14].

Earth's Radius, R_e	6,378,137 m
Earth's Semi-Minor Axis, b	6,356,752 m
Earth's Flattening (1/Ellipticity), f	1/298.257223563
Earth's Rotation Rate (Ω_{ZE})	7.292116 e-5 rad/sec
Earth's Gravitational Constant, GM	3.986004418e14 m ³ /s ²

Table 5. WGS-84 Values

A launch point was needed from North Korea, and Pyongyang was chosen arbitrarily. The coordinates for the launch point (μ_l, λ_l) are (40°54' North, 129°34' East). A suitable US city was needed within the maximum estimated range of the TD-2 missile, 3,500-4,000 km, so Pearl Harbor, at 4,260 km at a bearing of 010°, was selected. The coordinates for the target point (μ_t, λ_t) are 22°03' North by 159°09' West [Ref 5]. The geocentric launch latitude is found by converting from the geodetic latitude according to [Ref 8, 14]

$$\tan \mu_s = (1 - f)^2 \tan \mu_g \quad (2.C.1)$$

The coordinates of the launch point were converted from Geodetic into Rectangular coordinates according to [Ref 14]

$$R_s = \frac{R_e^2}{\sqrt{1 - e^2 \sin^2 \mu_s}}, \text{ where } e = \sqrt{\frac{a^2 - b^2}{a^2}}, \quad (2.C.2)$$

and

$$p(0) = \begin{bmatrix} p_x(0) \\ p_y(0) \\ p_z(0) \end{bmatrix} = \begin{bmatrix} R_s \cos \mu_s \\ 0 \\ R_s \sin \mu_s \end{bmatrix} \quad (2.C.3)$$

The initial velocity was defined as

$$v(o) = \begin{bmatrix} 0 \\ 0 \\ 0 \end{bmatrix} \quad (2.C.4)$$

Several different coordinate systems are involved in the flight of the interceptor missile. The propulsive forces act on the missile at its center of gravity, while the aerodynamic forces act relative to the movement of the missile with respect to the atmosphere, and the gravitational forces depend on the position of the missile. In order to apply all forces equally and appropriately it is necessary to define convenient coordinate systems for each and then rotate those coordinate systems into a common one. Five reference frames will be utilized in the model: two geocentric; two geographic; and a body fixed (subscripted *b*).

Frame Category	Frame of Reference	Coordinate System
Geocentric	F_i , an "inertial frame", non-rotating but translating with Earth's cm	ECI (Earth Centered Inertial), origin at Earth's cm, axes in the equatorial plane and along the spin axis
Geocentric	F_e , a frame defined by the "rigid" Earth	ECEF (Earth-centered, Earth-fixed), origin at Earth's cm, axes in the equatorial plane and along the spin axis
Geographic		Tangent-plane system, a geographic system with its origin on the Earth's surface
Geographic	F_{NED} (also F_{ENU}), a frame translating with the vehicle cm, in which the axes represent fixed directions	Vehicle-carried system, a geographic system with its origin at the vehicle cm
Body	F_b , a "body" frame defined by the "rigid" vehicle	Vehicle body-fixed system, origin at the vehicle cm, axes aligned with vehicle reference directions

Table 6. Frame References used in the 6DOF Model (After [Ref 14])

The initial reference frame is Earth Centered Inertial (F_i). This frame includes the rotation of the earth as a translational motion. The earth's rotation can be removed from the equation, thereby simplifying the rest of the problem, by rotating the frame about the z -axis through the angle

$$\mu = \lambda_0 - Llong + Wz_E t \quad (2.C.5)$$

The celestial longitude, λ_0 , is arbitrary and can be chosen to be zero. The resulting rotation matrix is [Ref 8,14]

$$R_{e/i} = \begin{bmatrix} \cos(ILong + Wz_E t) & \sin(ILong + Wz_E t) & 0 \\ -\sin(ILong + Wz_E t) & \cos(ILong + Wz_E t) & 0 \\ 0 & 0 & 1 \end{bmatrix} \quad (2.C.6)$$

where e and i are used to designation ECI and ECEF systems, respectively.

The system must now be rotated into the navigational reference system, normally designated North-East-Down for the directions that x - y - z point, respectively. However, an intermediate step is required to rotate from ECEF to Up-East-North first. This is accomplished by rotating first through the geocentric longitude,

$$R_{u/e} = \begin{bmatrix} \cos(latgc) & 0 & \sin(latgc) \\ 0 & 1 & 0 \\ -\sin(latgc) & 0 & \cos(latgc) \end{bmatrix} \quad (2.C.7)$$

then through the y -axis to point the x -axis North and the z -axis Down,

$$R_{n/u} = \begin{bmatrix} 0 & 0 & 1 \\ 0 & 1 & 0 \\ -1 & 0 & 0 \end{bmatrix} \quad (2.C.8)$$

In order to rotate the NED system into the body-fixed system, the initial roll (φ), pitch (θ), and yaw (ψ) angles must be defined. The initial roll is defined as zero, as the missile is not rotating about its x -axis on the launch pad. The initial pitch is the elevation of the launch direction with respect to the horizon. The initial yaw is the initial heading with respect to north. With these terms defined, the rotation matrices for each variable are [Ref 22]

$$\begin{aligned}
R_\phi &= \begin{bmatrix} 1 & 0 & 0 \\ 0 & \cos \phi & \sin \phi \\ 0 & -\sin \phi & \cos \phi \end{bmatrix} \\
R_\theta &= \begin{bmatrix} \cos \theta & 0 & -\sin \theta \\ 0 & 1 & 0 \\ \sin \theta & 0 & \cos \theta \end{bmatrix} \\
R_\psi &= \begin{bmatrix} \cos \psi & \sin \psi & 0 \\ -\sin \psi & \cos \psi & 0 \\ 0 & 0 & 1 \end{bmatrix}
\end{aligned} \tag{2.C.9}$$

and the total rotation from NED to body-centered system is

$$R_{b/n} = R_\phi R_\theta R_\psi \tag{2.C.10}$$

The final complete rotational transformation is the combination of all the rotations

$$R_{b/i} = R_{b/n} R_{n/u} R_{u/e} R_{e/i} \tag{2.C.11}$$

This rotation matrix allows for the computation of several important variables, notably the angular velocity and the Euler angles which will lead directly to the Quaternion of this system.

The initial angular velocity is found by transforming the Earth's rotation into the body system according to [Ref 8]

$$\omega_{b_0} = R_{b/i} \begin{bmatrix} 0 \\ 0 \\ Wz_E \end{bmatrix} \tag{2.C.12}$$

It is often preferable to track the system orientation through the use of the Quaternion instead of using other methods such as Euler Kinematic Equations or Poisson Kinematic Equations. The initialization of the Quaternion is derived from the initial Euler angles. The Euler angles are defined from the rotation matrix $R_{b/i}$ (a 3x3 Matrix)

$$\begin{aligned}
\phi_E &= \tan^{-1} \left(\frac{R_{b/i}(2,3)}{R_{b/i}(3,3)} \right) \\
\theta_E &= -\sin^{-1} (R_{b/i}(1,3)) \\
\psi_E &= \tan^{-1} \left(\frac{R_{b/i}(1,2)}{R_{b/i}(1,1)} \right)
\end{aligned} \tag{2.C.13}$$

The initial Quaternion is calculated from Euler angles [Ref 14]

$$\begin{aligned}
q_0 &= \cos\left(\frac{\phi}{2}\right) \cos\left(\frac{\theta}{2}\right) \cos\left(\frac{\psi}{2}\right) + \sin\left(\frac{\phi}{2}\right) \sin\left(\frac{\theta}{2}\right) \sin\left(\frac{\psi}{2}\right) \\
q_1 &= \sin\left(\frac{\phi}{2}\right) \cos\left(\frac{\theta}{2}\right) \cos\left(\frac{\psi}{2}\right) - \cos\left(\frac{\phi}{2}\right) \sin\left(\frac{\theta}{2}\right) \sin\left(\frac{\psi}{2}\right) \\
q_2 &= \cos\left(\frac{\phi}{2}\right) \sin\left(\frac{\theta}{2}\right) \cos\left(\frac{\psi}{2}\right) + \sin\left(\frac{\phi}{2}\right) \cos\left(\frac{\theta}{2}\right) \sin\left(\frac{\psi}{2}\right) \\
q_3 &= \cos\left(\frac{\phi}{2}\right) \cos\left(\frac{\theta}{2}\right) \sin\left(\frac{\psi}{2}\right) - \sin\left(\frac{\phi}{2}\right) \sin\left(\frac{\theta}{2}\right) \cos\left(\frac{\psi}{2}\right)
\end{aligned} \tag{2.C.14}$$

To check the validity of the Quaternion, the rotation matrix $R_{b/i}$ can be re-evaluated [Ref 14]

$$R_{b/i}^b = \begin{bmatrix} (q_0^2 + q_1^2 - q_2^2 - q_3^2) & 2(q_1q_2 + q_0q_3) & 2(q_1q_3 - q_0q_2) \\ 2(q_1q_2 - q_0q_3) & (q_0^2 - q_1^2 + q_2^2 - q_3^2) & 2(q_2q_3 + q_0q_1) \\ 2(q_1q_3 + q_0q_2) & 2(q_2q_3 - q_0q_1) & (q_0^2 - q_1^2 - q_2^2 + q_3^2) \end{bmatrix} \tag{2.C.15}$$

The results should be the same as before.

All the required initial values have now been calculated, and the resulting output is [Ref 14]

$$X_0 = \begin{bmatrix} p_0 \\ v_0 \\ wb_0 \\ q \end{bmatrix} \tag{2.C.16}$$

2. The Flight Program

Once the previous iteration (or the initialization) has been integrated, it is returned to the program as the current values. The program uses these values to calculate all the

descriptive values of the system, apply the corrective time- and position- dependant factors, and calculate the derivatives for the next iteration.

The angle of attack is $\tan^{-1}\left(\frac{v_z}{v_x}\right)$ and the sideslip angle is $\tan^{-1}\left(\frac{v_y}{v_x}\right)$. The program then calculates the necessary control surface deflections to zero the angle of attack and the sideslip angle, to maintain the alignment of the missile axis and its velocity vector.

The geocentric latitude is derived from the Cartesian coordinates of the position [p]

$$latgc = \tan^{-1}\left(\frac{p_z}{\sqrt{p_x^2 + p_y^2}}\right) \quad (2.C.17)$$

The celestial longitude is derived from rectangular coordinates of [p] with time-dependant correction factors, subject to a principle value requirement (between -180 and +180)

$$\lambda_g = \tan^{-1}\left(\frac{p_y}{p_x}\right) + lLong + W_{z_E}t \quad (2.C.18)$$

Determining the geodetic coordinates requires an iterative process because the prime radius of curvature, N , is a function of the geodetic latitude, φ , [Ref 14]

$$\begin{aligned}
\phi &= \tan^{-1} \left[\frac{z}{\sqrt{x^2 + y^2} \left(1 - \frac{Ne^2}{N+h} \right)} \right] \\
N &= \frac{\text{Re}}{\sqrt{1 - e^2 \sin^2 \phi}} \\
(N+h) &= \frac{\sqrt{x^2 + y^2}}{\cos \phi} \\
\Delta h &= (N+h) - N - h \quad \leftarrow \text{iterated while } \text{abs}(\Delta h) < 0.1 \\
h &= h + \Delta h
\end{aligned} \tag{2.C.19}$$

The ranges and required accuracy of this model prohibit the assumption of a flat earth with a constant gravitational acceleration vector. The gravitational forces on the missile are a position dependant correction factor.

$$\frac{-GM}{r^2} \begin{bmatrix} [1 + 1.5J_2(\text{Re}/r)^2(1 - 5\sin^2 \psi)]p_x / r \\ [1 + 1.5J_2(\text{Re}/r)^2(1 - 5\sin^2 \psi)]p_y / r \\ [1 + 1.5J_2(\text{Re}/r)^2(3 - 5\sin^2 \psi)]p_z / r \end{bmatrix} \tag{2.C.20}$$

The atmospheric affects on the missile are dependant on the altitude, which is derived using the SAtmos.m function described in section D.

The missiles speed in m/s is determined by the normalization of the velocity vector, vb. The missiles Mach number is determined by dividing the speed by the local Mach number which is determined by the local temperature from the SAtmos.m program ($M = \sqrt{\gamma RT}$).

The moment matrix and missile mass is determined as a function of time and is based on assumed fuel usage parameters. The missile program calls a separate function, either SMPParams.m, to evaluate the specific descriptive parameters of the ballistic

missile. The program assumes a cruciform missile in two stages plus a conical nosecone section, where only the first stage separates after completion.

The dimensions of the remaining fuel are critical to the purposes of calculating the center of gravity. For the interceptor, the first stage is active for 6 s while the stage 1 fuel is consumed. The fuel is solid, so the only parameters to change are the length of the fuel and the inner radius as it is consumed. Once the fuel is totally consumed in stage 1, the booster separates and stage 2 takes over in a similar manner. Stage 2 lasts for an additional 20 s. For the rocket, the first stage is active for 125 s while the stage 1 fuel is consumed. The canister the fuel is contained in is assumed to be a constant size and diameter, so the only parameter to change is the length of the fuel as it is consumed. The missile is in a constant forward acceleration, so the fuel is assumed to remain in the rear of the canister for the purposes of calculating its center of gravity. Thus the center of gravity of the fuel tends toward the rear of the missile through the flight. Once the fuel is totally consumed in stage 1, the booster separates and stage 2 takes over in a similar manner. Stage 2 lasts for 110 seconds.

The center of gravity (CG) is determined by the parallel axis theorem applied independently to the x , y , and z axes. The missile was separated into five separate pieces: nosecone, stage 1 structure, stage 2 structure, stage 1 fuel, and stage 2 fuel. Each CG was separately calculated and then combined. The CG of the individual structural components was a simple matter of their distance from the nosecone. The center of gravity of the fuel was then based on the fuel remaining in the canister, referenced to the base of the missile section. The missile CG is calculated from the locations and masses of the component sections:

$$M_{missile} CG_{missile} = M_{nose} CG_{nose} + M_{st1_str} CG_{st1_str} + M_{st1_fuel} CG_{st1_fuel} + M_{st2_str} CG_{st2_str} + M_{st2_fuel} CG_{st2_fuel} \quad (2.C.21)$$

The moments of inertia for the x , y , and z -axes are calculated using the CG and the remaining fuel length using a similar methodology of components. For the rocket the equations are

	J_{xx}	$J_{yy} = J_{zz}$
Nosecone	$\frac{3}{10} M_{nose} r^2$	$\frac{3}{5} M_{nose} \left(\frac{r^2}{4} + h^2 \right) + M_{nose} \left(CG - \frac{5}{8} L_{nose} \right)^2$
Stage 1 Structure	$\frac{M_{str}}{2} (r_0^2 + r_i^2)$	$\frac{M_{str}}{12} [3(r_0^2 + r_i^2) + L_{st1}^2] + M_{str} (CG - 24)^2$
Stage 1 Fuel	$\frac{M_{fuel} r^2}{2}$	$\frac{M_{fuel}}{12} (3r^2 + L_{st1}^2) + M_{fuel} (CG - (32 - L_{fuel}))$ (2.C.22)
Stage 2 Structure	$\frac{M_{str}}{2} (r_0^2 + r_i^2)$	$\frac{M_{str}}{12} [3(r_0^2 + r_i^2) + L_{st2}^2] + M_{str} (CG - 9)^2$
Stage 2 Fuel	$\frac{M_{fuel} r^2}{2}$	$\frac{M_{fuel}}{12} (3r^2 + L_{st2}^2) + M_{fuel} (CG - (16 - L_{fuel}))$

The equations for the interceptor are similar.

The J matrix returned is the symmetrical matrix, since the ballistic missile itself is symmetric:

$$J = \begin{bmatrix} J_{xx} & 0 & 0 \\ 0 & J_{yy} & 0 \\ 0 & 0 & J_{zz} \end{bmatrix} \quad (2.C.23)$$

The BRParams.m and SMPParams.m functions also determine the reference areas for the control surfaces and missile planform areas using simple equations from Zarchan [Ref 21]. The function returns the base diameter (dia), reference area (S_{ref}), planform area (S_{plan}), wing area (S_{wing}), tail area (S_{tail}), nose area (A_n), body area (A_b), nose center of pressure (X_{cpn}), and body center of pressure (X_{cpb}) according to

$$\begin{aligned}
S_{ref} &= \frac{\pi d^2}{4} \\
S_{plan} &= L_{st1} d_{st1} + L_{st2} d_{st2} + 0.67 L_{nose} d_{nose} \\
S_{wing} &= 0.5 h_T (C_{TT} + C_{RT}) \\
S_{tail} &= 0.5 h_T (C_{TT} + C_{RT}) \\
A_n &= 0.67 L_{nose} d_{nose} \\
X_{cpn} &= 0.67 L_{nose} \\
A_b &= L_{st1} d_{st1} + L_{st2} d_{st2} \\
X_{cpb} &= \frac{0.67 A_{nose} L_{nose} + A_{body} (L_{nose} + 0.5(L_{st1} + L_{st2}))}{A_{nose} + A_{body}}
\end{aligned} \tag{2.C.24}$$

The program then calls the function ACoeff.m to determine several necessary aerodynamic coefficients. The function inputs are angle of attack, altitude, and pitch control surface deflection. The pitch control surface is specifically included because it alone varies over the spectrum of possible angles, from -20^0 to $+20^0$, whereas the roll and yaw derivatives can be assumed to be constant over that range of possible angles. The pitch deflections therefore require a second interpolation to determine their actual value at each time step.

Figures 14-20 detail the range of values of the variables returned after interpolation (all figures after [Ref 7]). Some variables require multiple interpolations, such as in Figures 14 and 19.

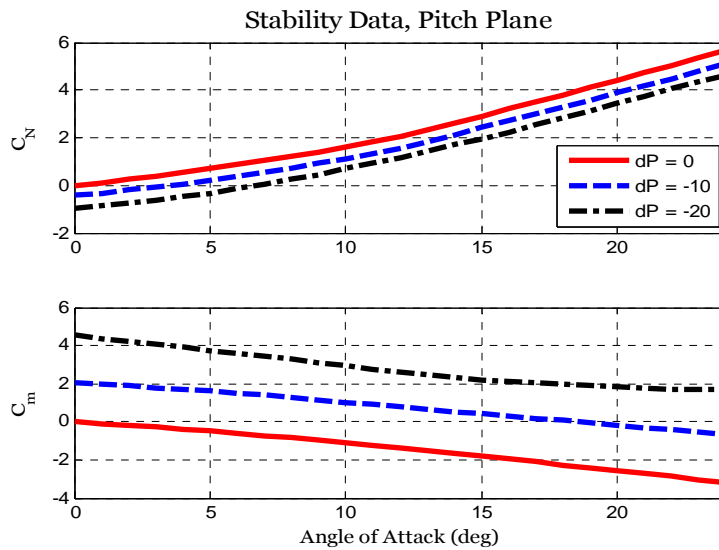


Figure 14. Pitch plane stability data

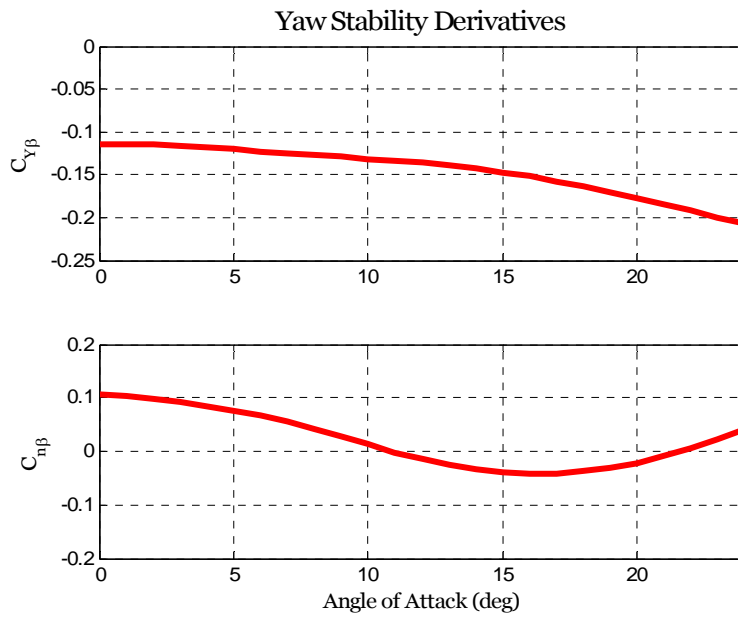


Figure 15. Yaw stability and control derivatives

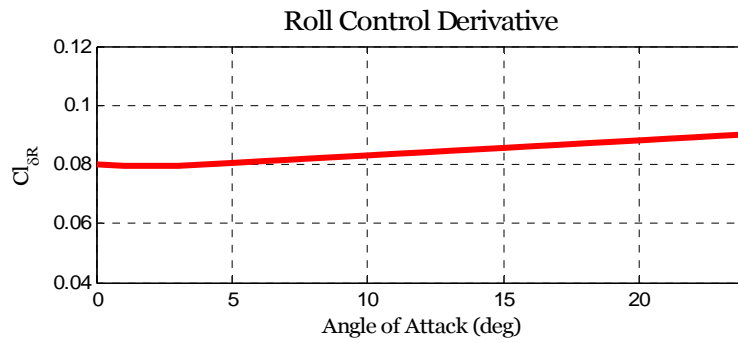


Figure 16. Roll control derivatives

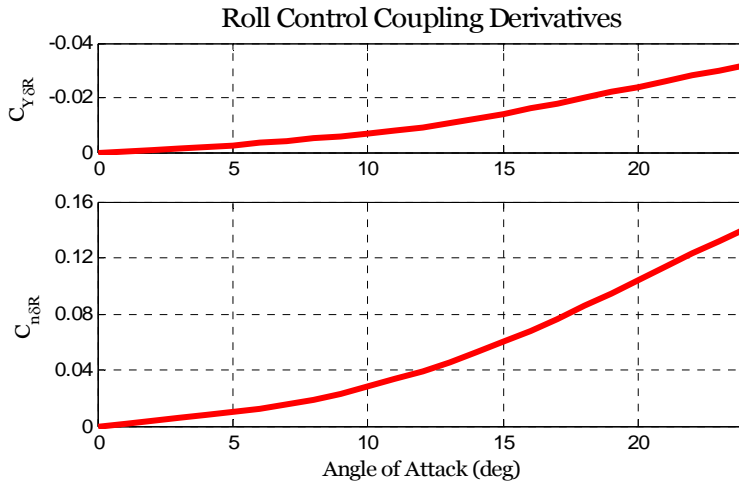


Figure 17. Roll control Coupling Derivatives

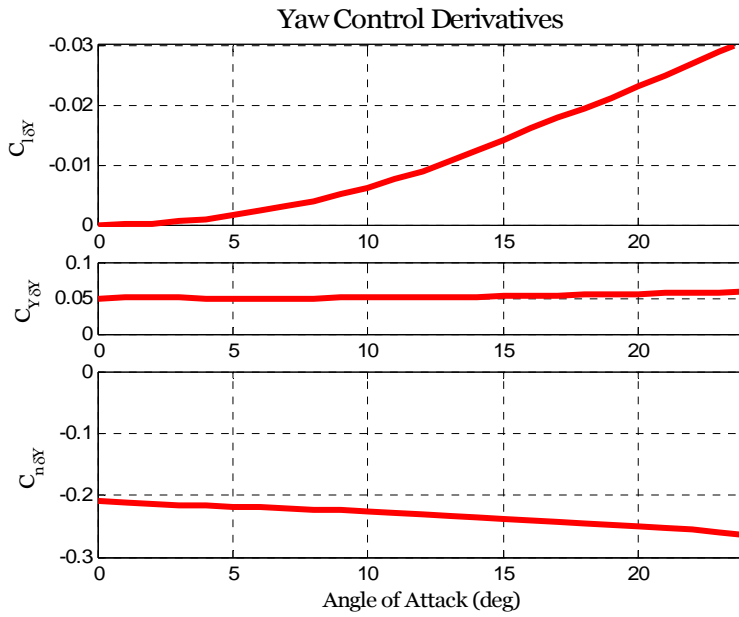


Figure 18. Yaw control Derivatives

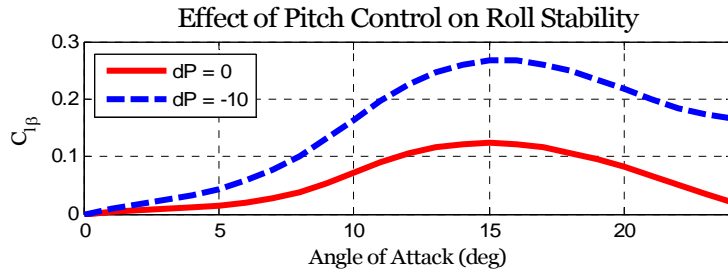


Figure 19. Pitch control effects on roll stability

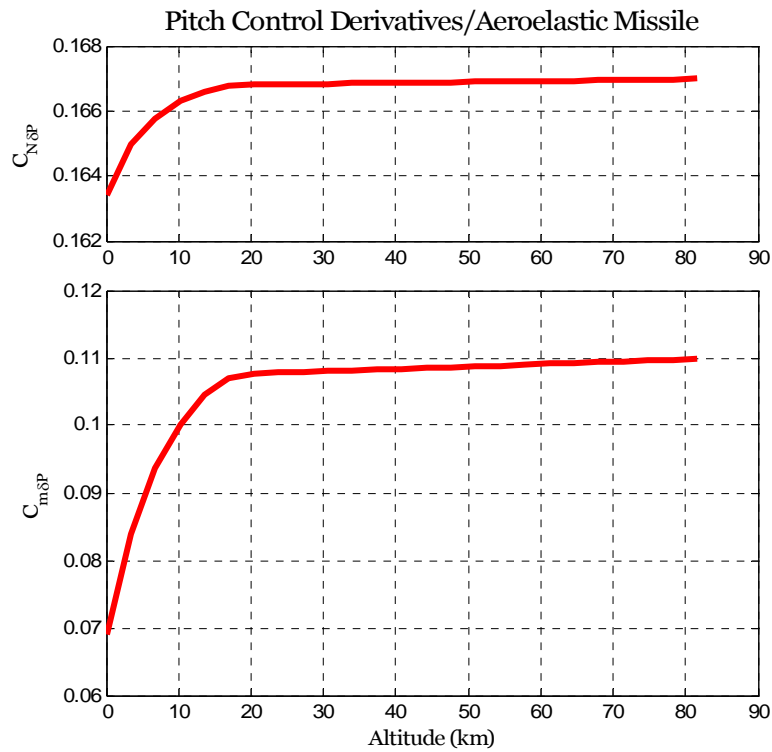


Figure 20. Pitch control derivatives

The returned values are combined together to calculate the force and moment coefficients [Ref 7]

$$\begin{aligned}
C_Y(\alpha, \beta, \delta P, \delta Y, \delta R) &= C_{Y\beta} \beta + C_{Y\delta Y} \delta Y + C_{Y\delta R} \delta R \\
C_N(\alpha, \delta P) &= C_{N\alpha} \alpha + C_{N\delta P} \delta P \\
C_l(\alpha, \beta, \delta P, \delta Y, \delta R) &= C_{l\beta} \beta + C_{l\delta Y} \delta Y + C_{l\delta R} \delta R \\
C_m(\alpha, \delta P) &= C_{m\alpha} \alpha + C_{m\delta P} \delta P \\
C_n(\alpha, \beta, \delta P, \delta Y, \delta R) &= C_{n\beta} \beta + C_{n\delta Y} \delta Y + C_{n\delta R} \delta R
\end{aligned} \tag{2.C.25}$$

The program calls the function ZLDragC.m to determine the value of the drag coefficient. The Thrust is determined exactly as before, by simple time dependence. The total force on the body of the missile from all lift, drag, thrust, and aerodynamic forces is then [Ref 22]

$$[f]^b = \begin{bmatrix} f_x \\ f_y \\ f_z \end{bmatrix} = \begin{bmatrix} -q_{ro} S_{ref} C_N \sin \alpha \\ q_{ro} S_{ref} \\ q_{ro} S_{ref} C_N \cos \alpha \end{bmatrix} + \begin{bmatrix} Thrust \\ 0 \\ 0 \end{bmatrix} - \frac{\rho}{2} \begin{bmatrix} V_x \\ V_y \\ V_z \end{bmatrix}^2 \tag{2.C.26}$$

The torque experienced by the missile from all moment forces is [Ref 7]

$$T = q_{ro} S_{ref} d \begin{bmatrix} C_l \\ C_m \\ C_n \end{bmatrix} \tag{2.C.27}$$

The inertial-body centered rotation matrix is determined using the quaternion

$$R_{b/i}^b = \begin{bmatrix} (q_0^2 + q_1^2 - q_2^2 - q_3^2) & 2(q_1 q_2 + q_0 q_3) & 2(q_1 q_3 - q_0 q_2) \\ 2(q_1 q_2 - q_0 q_3) & (q_0^2 - q_1^2 + q_2^2 - q_3^2) & 2(q_2 q_3 + q_0 q_1) \\ 2(q_1 q_3 + q_0 q_2) & 2(q_2 q_3 - q_0 q_1) & (q_0^2 - q_1^2 - q_2^2 + q_3^2) \end{bmatrix} \tag{2.C.28}$$

Also, as before, the ECI-inertial rotation matrix is determined as

$$R_{e/i} = \begin{bmatrix} \cos(lLong + Wz_E t) & \sin(lLong + Wz_E t) & 0 \\ -\sin(lLong + Wz_E t) & \cos(lLong + Wz_E t) & 0 \\ 0 & 0 & 1 \end{bmatrix} \tag{2.C.29}$$

The total rotation matrix is then

$$R_{b/n} = (R_{n/e} R_{e/i} R_{i/b})^T \tag{2.C.30}$$

The Euler angles with respect to the ECEF system are [Ref 8]

$$\begin{aligned}
\phi &= \tan^{-1} \left(\frac{R_{b/n}(2,3)}{R_{b/n}(3,3)} \right) \\
\theta &= -\sin^{-1} (R_{b/n}(1,3)) \\
\psi &= \tan^{-1} \left(\frac{R_{b/n}(1,2)}{R_{b/n}(1,1)} \right)
\end{aligned} \tag{2.C.31}$$

The quaternion rotation matrix is calculated is [Ref 14]

$$\Omega_{b/i}^b = \begin{bmatrix} 0 & -P & -Q & -R \\ P & 0 & R & -Q \\ Q & -R & 0 & P \\ R & Q & -P & 0 \end{bmatrix} \tag{2.C.32}$$

The centripetal acceleration due to the rotation of the missile and its velocity is the vector product [Ref 14]

$$\Omega_{b/i} = \begin{bmatrix} 0 & -R & Q \\ R & 0 & P \\ -Q & P & 0 \end{bmatrix} \tag{2.C.33}$$

The centripetal acceleration due to the Earth's angular velocity and the rotation in the ECI frame is the vector triple product [Ref 14]

$$\Omega_{e/i}^i = \begin{bmatrix} 0 & -Wz_E & 0 \\ Wz_E & 0 & 0 \\ 0 & 0 & 0 \end{bmatrix}^{-2} \tag{2.C.34}$$

All values, coefficient, and matrices have been determined. The full state parameters can be calculated as [Ref 14]

$$\begin{aligned}
{}^i \dot{p}_{CM/O}^i &= R_{b/i} * v_b + \Omega_{e/i} * p_i \\
{}^b v_{CM/e}^b &= \frac{1}{m} F_{A,T}^b + R_{b/i} * (G^i - \Omega_{e/i}^i * p_{CM/O}^i) - (\Omega_{b/i}^b + R_{b/i} \Omega_{e/i} R_{b/i}^T) * v_{CM/e}^b \\
{}^b \dot{\omega}_{b/i}^b &= (J^b)^{-1} * (M_{A,T}^b - \Omega_{b/i}^b J^b \omega^b) \\
\dot{q}_{b/i} &= \frac{1}{2} q_{b/i} * \Omega_{b/i}^b
\end{aligned} \tag{2.C.35}$$

3. Results

In order to fully visualize the geometry of the intercept, an animation function was developed that shows side-by-side the orientation of the target and the interceptor. A screen shot of the plot is shown in Figure 21. The animation shows the stage changes of the missile as well, dropping the used stages at the appropriate moment.

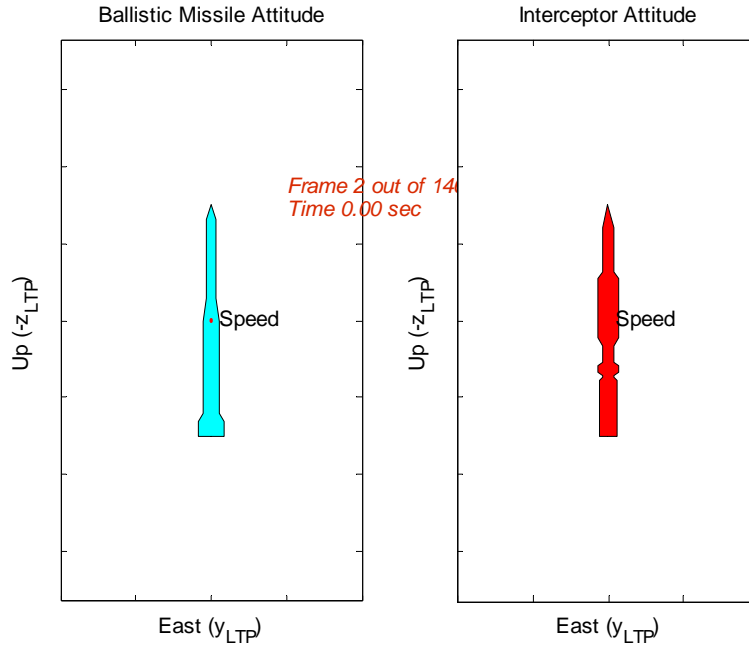


Figure 21. 6DOF Orientation Animation

D. COMMON FUNCTIONS

Two functions were common to all the models, ZLDragC.m and SAtmos.m.

1. ZLDragC.m

The drag on the missile is dependant on two conditions, the Mach number and whether the missile is in the boost or glide phase. The phase of the missile is easily determinable from the time.

The reason the values differ is the presence or absence of the base drag. When the rocket is under power, the thrust pressure is balanced to atmospheric, so there are no parasitic drag effects from the tail section. After the engine shuts down, there is no longer any pressure generated, so the sharp end of the tail section generates a drag effect.

Parasitic drag from the rest of the missile is relatively constant in both phases of the missile flight.

There is a sharp increase in the drag effects at Mach one, after which the drag drops considerably [Ref 8]. Figure 22 shows the effect of speed on the drag coefficient.

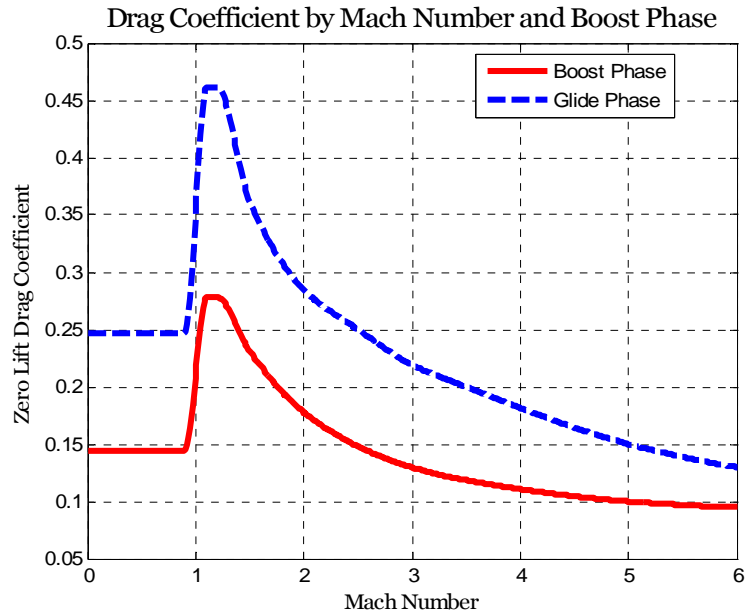


Figure 22. Drag Coefficient by Mach Number and Flight Phase

The drag force is then calculated from

$$Drag = C_D \frac{\rho V^2}{2} \quad (2.D.1)$$

and the atmospheric dynamic pressure is calculated from

$$q_{ro} = \frac{\rho V^2}{2} \quad (2.D.2)$$

2. STatmos.m

Many of the atmospheric affects on the missile are dependant on the altitude. The missile program calls a separate script, STAtmos.m, to determine the density, pressure, and temperature of the local atmosphere. The script is based on the 1976 standard

atmospheric survey, and includes values up to 86 km in a tabular format. Figures 23-25 show the details of the values returned.

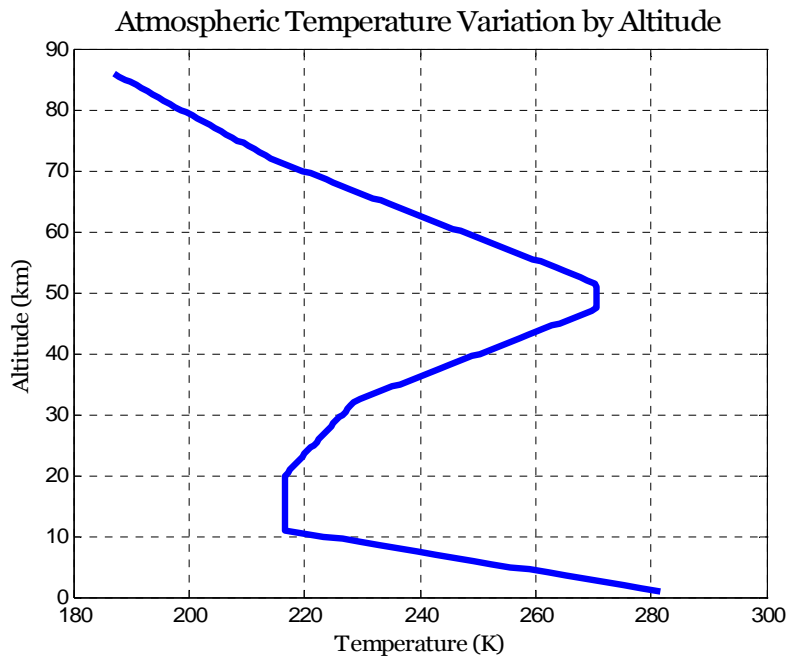


Figure 23. Atmospheric Temperature Variation by Altitude

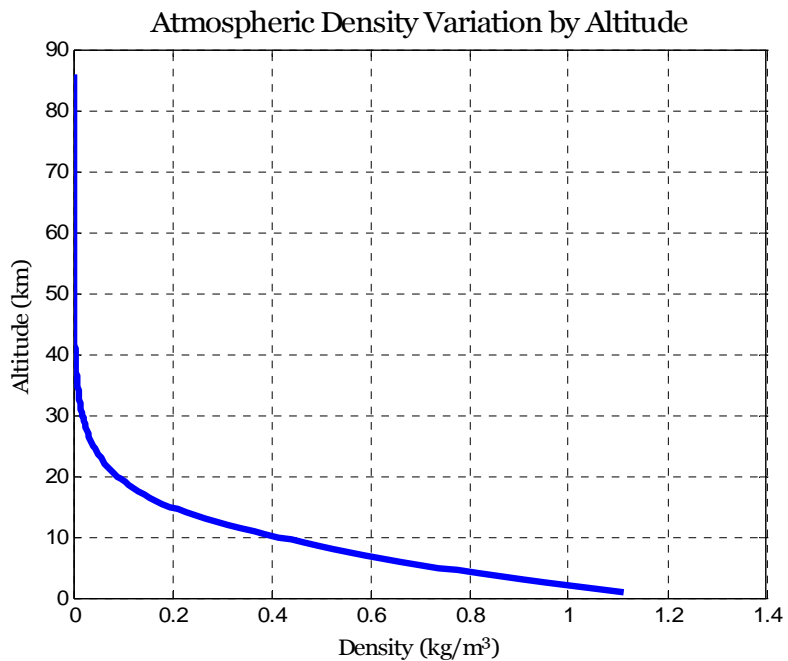


Figure 24. Atmospheric Density by Altitude

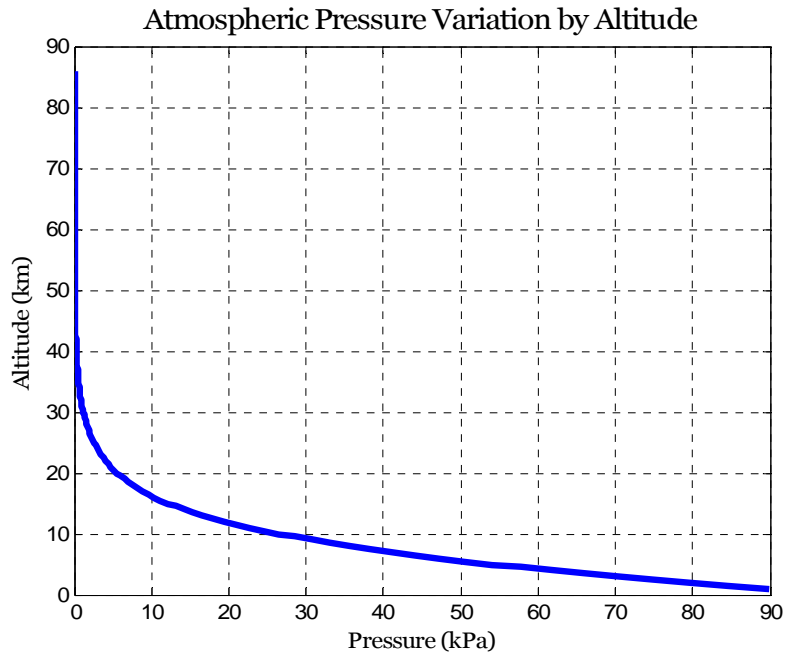


Figure 25. Atmospheric Pressure Variation by Altitude

III. EXISTING GUIDANCE LAWS

There are a wide variety of guidance laws available for missile guidance processing. Many of them are not acceptable for this application such as Beam Rider and Pure Pursuit, while others are acceptable though not optimal such as Proportional Navigation and its variants.

A. UNACCEPTABLE GUIDANCE LAWS

1. Beam Rider

Beam Rider (also called Command Line-of-Sight) is among the simplest forms of command guidance. The missile simply flies along a tracker beam that is continuously pointed at the target. In other words, the inertial velocity vector is continuously pointed at the target. The beam and the missile generally originate from the same position, but not always. The guidance commands are proportional to the angular error between the missile and the beam, and if the missile remains exactly on the beam it will hit the target. There is no consideration for the capabilities of the target, and the missile is not directed to orient itself to lead the target in order to anticipate its movements. The missile therefore requires much greater maneuvering capabilities in the moments just prior to interception. This form of guidance law also assumes that the shooter will have a direct line of sight for the entire engagement, and that the diffraction of the beam will be negligible, which is obviously not true over the distances required for a BPI. [Ref 2]

2. Pure Pursuit

Pure Pursuit overcomes this limitation by having the missile supply the targeting data instead of a third-party observer. This is, in effect, Beam Rider Guidance where the beam is generated onboard the missile. As before, the missile only follows the beam and the guidance commands are proportional to the angular error between the missile and the line of sight to the target. This overcomes the diffraction of the beam, but still does not command the missile to orient itself to lead the target. It thus requires similarly large maneuvering capabilities to complete the interception.

Both of these guidance laws are severely limited in their effectiveness, are used only at short range against non-maneuvering or relatively slow targets, and require

significant interceptor capabilities relative to the target. This is not an accurate description of the requirements for a BPI, and both laws are therefore discounted for use here. [Ref 2]

B. LESS THAN OPTIMAL GUIDANCE LAWS

1. True Proportional Navigation

Another family of guidance laws involves Proportional Navigation (PN) and its derivatives. Of the three basic guidance laws, proportional navigation is the most versatile, and therefore most frequently implemented, making it the guidance law of choice in nearly all modern guided missiles. In proportional navigation the rate of change of the missile heading is proportional to the rate of rotation of the line-of-sight (LOS) from the missile to the target. The guidance system points the differential velocity vector at the target [Ref 2]

In order for interception to occur, the heading angle and the LOS angle, λ , must remain constant. If the target increases speed, then λ will increase and the interceptor must increase its heading Ψ to compensate. Thus it is apparent that they must be proportional to each other, or more accurately, the rate of change of each must be proportional, [Ref 21]

$$\dot{\Psi} = N\dot{\lambda} \quad (3.B.1)$$

where N is the proportionality constant, which determines the amount of target lead by the interceptor (usually 3-5 depending on the interceptor's maneuvering capabilities). The interceptor maneuvers until $\dot{\lambda} = 0$, at which point $\dot{\Psi} = 0$ and no further maneuvers take place until intercept.

The missile seeker measures the LOS rate and the PN guidance law converts that into an acceleration command by the guidance computer. Using the fact that the acceleration normal to the velocity vector of the interceptor is

$$a = \vec{V}^D \dot{\Psi} \quad (3.B.2)$$

which can be correlated to the LOS rate to develop the steering command for the guidance computer

$$a = N\vec{V}^D \dot{\lambda} \quad (3.B.3)$$

The same method applies to the extension of this law into three dimensions.

Using angular velocity vectors between the target and interceptor, Zipfel [Ref 22] develops a three dimensional PN guidance law as

$$a = N\vec{V}^D\Omega^{OE}u_v - g \quad (3.B.4)$$

where Ω^{VE} is the cross product of the LOS frame with the Earth and the velocity vector with respect to the Earth, u_v is the unit vector of \vec{V}^D , and g is the added gravity bias.

2. Compensated Proportional Navigation

True PN is rarely implemented in this simple form, however. The thrust generated by the interceptors motor creates a parasitic acceleration in the LOS angle that must be compensated for in the autopilot command or intercept errors will occur. Such a guidance law is termed “compensated”. The missile acceleration is projected onto the LOS plane by

$$[a_m]^{LOS} = {}^{LOS}_wR[a_m]^w \quad (3.B.5)$$

and subtracted from the PN command in equation (3.B.4) to obtain the augmented command [Ref 22]

$$a = N\vec{V}^D[\Omega^{OE}]^w[u_v]^w - {}^{LOS}_wR[a_m]^w - {}^w_nR[g]^n \quad (3.B.6)$$

where the rotation matrix ${}^{LOS}_wR$ of the LOS coordinates with respect to the wind frame is defined by the azimuth and elevation angles from the LOS vector.

3. Augmented Proportional Navigation

Zarchan details one further variation of PN, termed Augmented Proportional Navigation which includes an extra term to account for the acceleration of the target [Ref 21].

$$a = N\vec{V}^D\Omega^{OE}u_v + \frac{N}{2}n_T - g \quad (3.B.7)$$

where n_T is the acceleration of the target. However, a detailed knowledge of the target’s acceleration requires an advanced Kalman filter, such as an Extended Kalman Filter or an Alpha-Beta-Gamma Filter, which are not sufficiently accurate [Ref 13] and is not feasible to be implemented onboard an interceptor as small as the Standard Missile. Additionally,

application of the acceleration would require exact knowledge of the target's staging events where the acceleration value changes radically.

C. KEY FATAL CHARACTERISTICS

There are three fatal characteristics of these guidance laws which can preclude the interceptor from impacting the target: the dynamics of the missile controls system, the lack of knowledge of the end-game environment, and the inability to control the intercept geometry.

1. Control System Time Constant

If the dynamics of the seeker, noise filter and flight control system are neglected, a perfect or zero-lag guidance system is achieved and the missile will always hit the target if it is tracked correctly. In reality, guidance commands can not be implemented instantaneously and there will be lags or dynamics within the guidance system. In missile systems, the dominant portion of the total system time constant is usually associated with the flight control system actuators such as the tail fin control surfaces [Ref 21]. Such time lags are generally represented by a time constant

$$\frac{n_L}{n_c} = \frac{1}{1 + sT} \quad (3.B.8)$$

where n_L is the achieved missile acceleration, n_c is the commanded missile acceleration, and T is the flight control system time constant. Zarchan has shown that even a very good 1-second time constant can have a considerable impact on the miss distance [Ref 21]. A system with a small guidance system time constant has the potential for having very small miss distances. However, technology issues limit how small the guidance system time constant can be. Thus all systems that utilize current target information in a homing guidance loop with a feedback control system will have some miss distance due to the flight control system time constant.

2. End-game Environment

The lack of knowledge of end-game environment is also a major problem. Missiles use fuel for a fraction of the flight to generate a set amount of thrust and speed, after which the missile must glide to the target under a constant drag- and gravity-induced deceleration. The amount of available maneuver capability depends on the missile speed and altitude of engagement – higher speeds and lower engagement altitudes work to increase the missile capability [Ref 20]. Therefore trajectories should be flown to maximize the missile velocity and minimize the intercept altitude so that there is sufficient acceleration left to intercept the target.

Yet the above guidance laws do not consider the end-game prior to achieving it. The effect is to guide the missile along the most direct path and hope that the interception will take place under atmospheric conditions that are acceptable to the interceptor and to try to minimize the acceleration at each moment with the hope that there will be enough capability remaining to complete the end-game. The assumption that target maneuvers will be sufficiently small enough that the missile will have enough capability to counter them is usually accurate; however, the immense accelerations involved in a BPI makes active management of the missile's acceleration critical to ensuring the end-game is successful.

3. Controlling the Interception Geometry

The interception geometry of any engagement under the above guidance laws is a result of the relative speeds of the missile and target, the launch geometry, and the maneuvers involved. The above guidance laws have no control over any of these aspects, though this geometry is critical to ensuring the interceptor is capable of destroying the ICBM. An overtaking intercept (the interceptor approaches the target from the rear) is significantly less desirable than a head-on or a right-angle intercept.

Only if the intercept geometry is controllable can it be expected to conform to a pre-determined setup. Since none of these guidance laws can control the geometry, they are not capable of maximizing the kinetic energy transfer via the intercept geometry.

THIS PAGE INTENTIONALLY LEFT BLANK

IV. PROPOSED ALGORITHM

A method that overcomes fatal characteristics of modern guidance laws is the key driving factor in the development of this advanced guidance law. The guidance law will determine the near-optimal flight path from the interceptor position to a predicted target position for the interceptor to follow to intercept, and then derive the set of control commands necessary to execute that flight. This section will describe a method for deriving that trajectory using calculus of variations based on three cues: high-order polynomials as a reference function for the flight path, a preset thrust history as one of the controls, and a few optimization parameters. The trajectory optimization problem is then converted into a nonlinear programming problem and solved numerically.

A. PROBLEM STATEMENT

Among all admissible trajectories,

$$\begin{aligned} \bar{z}(t) &= \{z_1(t), z_2(t), \dots, z_r(t)\}^T \in S \\ S &= \{\bar{z}(t) \in Z^r \subset E^r\}, t \in [t_0, t_f] \end{aligned} \quad (4.A.1)$$

that satisfies:

1. The system of differential equations (dynamic constraints):

$$\dot{z}_i = f_i(t, \bar{z}, \bar{u}, \bar{a}), \quad i = \overline{1, r} \quad (4.A.2)$$

where the vector of controls is

$\bar{u}(t) = \{u_1(t), u_2(t), \dots, u_m(t)\}^T$, $m < r$, $\bar{u} \in U^m \subset E^m$ and the vector of missile parameters is $\bar{a} = (a_1, a_2, \dots, a_p)$, $\bar{a} \in A^p \subset E^p$;

2. The initial conditions:

$$\bar{z}(t_0) \in S_0, \quad S_0 = \{\bar{z}_0 \in Z^r \subset E^r\} \quad (4.A.3)$$

$$\bar{u}(t_0) \in R_0, \quad R_0 = \{\bar{u}_0 \in U^m \subset E^m\} \quad (4.A.4)$$

and the final conditions:

$$\bar{z}(t_f) \in S_f, S_f = \left\{ \bar{z}_f \in Z^r \subset E^r; G_j(\bar{z}(t_f)) = 0, j = \overline{1, l} \right\} \quad (4.A.5)$$

$$\bar{u}(t_f) \in R_f, R_f = \left\{ \bar{u}_f \in U^m \subset E^m \right\} \quad (4.A.6)$$

3. The constraints imposed on the state space

$$\bar{\eta}(t, \bar{z}) = \left\{ \eta_1(t, \bar{z}), \eta_2(t, \bar{z}), \dots, \eta_\mu(t, \bar{z}) \right\}^T \geq \bar{0} \quad (4.A.7)$$

on the controls

$$\bar{\xi}(t, \bar{z}, \bar{u}) = \left\{ \xi_1(t, \bar{z}, \bar{u}), \xi_2(t, \bar{z}, \bar{u}), \dots, \xi_\nu(t, \bar{z}, \bar{u}) \right\}^T \geq \bar{0} \quad (4.A.8)$$

and on the controls derivatives

$$\bar{\pi}(t, \bar{u}, \vec{u}) = \left\{ \pi_1(t, \bar{u}, \vec{u}), \pi_2(t, \bar{u}, \vec{u}), \dots, \pi_\sigma(t, \bar{u}, \vec{u}) \right\}^T \geq \bar{0} \quad (4.A.9)$$

Find the optimal trajectory, $\bar{z}_{opt}(t)$, that minimizes the integral function

$$J = K(x_0, x_f) + \int_{t_0}^{t_f} L(t, \bar{z}, \bar{u}) dt \quad (4.A.10)$$

and the corresponding optimal controls, $\bar{u}_{opt}(t)$, where K, L are defined functions.

B. CALCULUS OF VARIATIONS

Calculus of variations deals with functions of functions, termed functionals, instead of functions of some variable or variables as in ordinary calculus. Specific interest is in the extremals of these functionals - those making the functional attain a maximum or minimum value [Ref 15]. There are two broad categorizations of methods to solve these problems, indirect methods and direct methods.

Indirect methods resolve the problem into a differential equation, usually via the difference of a series of equations of motion and thus solve the general theory of partial differential equations. This method does not assume anything about the solution, leading to a very complete and perfectly precise answer; however, one must integrate the resultant equation to derive the extremals. The precision greatly increases the computational complexity, and therefore the time required to solve, for negligible gain in

optimality. Further, these differential equations are difficult to integrate except in the simplest of cases, and nearly impossible to program [Ref 19]. This approach is further complicated by the need to solve the problem in a specified fixed region instead of in the small neighborhood of some point. These difficulties can be overcome by using direct methods, which do not reduce the variational problems to ones involving differential equations.

The fundamental idea of direct methods is to consider a variational problem as a limit problem of the extreme of a function of a finite number of variables that can be solved by numerical methods. Two basic direct methods are the Rayleigh-Ritz and Galerkin methods, which assume the solution to be an unknown function but of a certain form containing a set of unknown coefficients (themselves functions of the boundary conditions), which are then found by minimization. The practical result is that the problem has been reduced from calculus to algebra, but at the cost of a significant increase in the number of simultaneous equations to be solved. It is for this reason that little work was done in this field until the advent of computer technology. The possible solution set is restricted to a smaller space than the original equation because of the initial assumption regarding the solution, but the resultant problem can be programmed and quickly solved using computers; however, the solutions are only an approximation of the original solution. Therefore these solutions can only be regarded as near-optimal solutions.

Professor Taranenko [Ref 19] first applied the ideas of direct methods and the combination of Ritz and Galerkin methods to the problems of flight dynamics by identifying a reference function for the flight vehicle's motion and velocity

$$x_i = x_{i0} + (x_{if} - x_{i0}) \frac{\tau - \tau_0}{\tau_f - \tau_0} + \Phi_i(\tau), \quad i = \overline{1,4} \quad (2.1)$$

where x_1, x_2, x_3 , are the Cartesian coordinates for the flight path, x_4 is the velocity, and $\Phi_i(\tau)$ is a continuous, unequivocal, differentiable function satisfying the boundary conditions $\Phi_i(\tau_0) = \Phi_i(\tau_f) \equiv 0$. Any function that satisfies those conditions would be acceptable for use. Taranenko called τ a virtual arc. It is this critical variable that allows

the separation of the spatial trajectory from the velocity and thus optimizes one or the other, or both independently. The specific task determines the appropriate choice of τ , but in general any continuous, monatomic function is acceptable: time, path, energy, etc. The remaining state parameters and flight controls are then determined by solving the inverse problem of flight dynamics. Rather than starting with the control time histories and integrating them to determine the flight path, this method starts with a flight path and determines the control time histories necessary to create it.

In order to implement a solution to this problem that can be solved in real time, a further restriction must be made. The continuous problem must be discretized to reduce the infinite variational problem to one of optimization of few parameters at numerous sampling points. This allows for the optimization of the planar trajectory of the missile at several points along the path by presetting the state variables and one of the controls' time histories, and then solving the inverse flight dynamics problem.

These methods have all previously been used for off-line optimization of trajectories, but none has yet been applied to the real-time onboard optimization of a missile flight path. Yakimenko detailed a method called a Direct Method for Rapid Prototyping, which he applied to short term spatial trajectories of aircraft maneuvers using fixed boundary points [Ref 19]. The developed program presented here uses similar numerical method to provide a near-optimal spatial trajectory that is completely defined by a few optimization parameters, but as will be discussed shortly, has fluid final boundary conditions.

Though the method artificially limits the possible trajectory variations, it does guarantee the following [Ref 19]:

1. The boundary conditions are satisfied a priori,
2. The control commands are physically realizable and smooth,
3. Only a few variable parameters are used, thus ensuring that the iterative process converges well,
4. The near-optimal solution is very close to the optimal one.

A simple two dimensional variation program of a similar 7th order system will demonstrate how the direct method varies the flight path according to the boundary conditions. The boundary conditions are

$$\begin{array}{cccc}
 x_{10} = 0 & x_{20} = 0 & x_{1f} = 1 & x_{2f} = 1 \\
 x'_{10} = 0.2 & x'_{20} = 1 & x'_{1f} = 0.1 & x'_{2f} = -1 \\
 x''_{10} = 0.1 & x''_{20} = 0.1 & x''_{1f} = 0.1 & x''_{2f} = 0.1 \\
 x'''_{10} = \text{var} & x'''_{20} = 0.1 & x'''_{1f} = 0.1 & x'''_{2f} = 0.1
 \end{array}$$

where the third derivative of the initial x_1 condition has been set to vary according to

$$x'''_{10} = \{-0.4; -0.1; 0.2; 0.5\}$$

and the length of the virtual arc varies according to

$$\tau_f = 1, 2, \dots, 10$$

The resulting set of paths is shown in Figure 26 and the first derivative of the path is shown in Figure 27. It is important to note that the first derivative is not “velocity” but is instead the “rate of change of the path”. It is proportional but not equal to velocity, specifically because of the virtual variable τ as discussed previously. Each line represents a different choice of τ_f , showing that by varying that value the length of the path can change drastically. The algorithm developed here will use this technique to derive the optimal flight path.

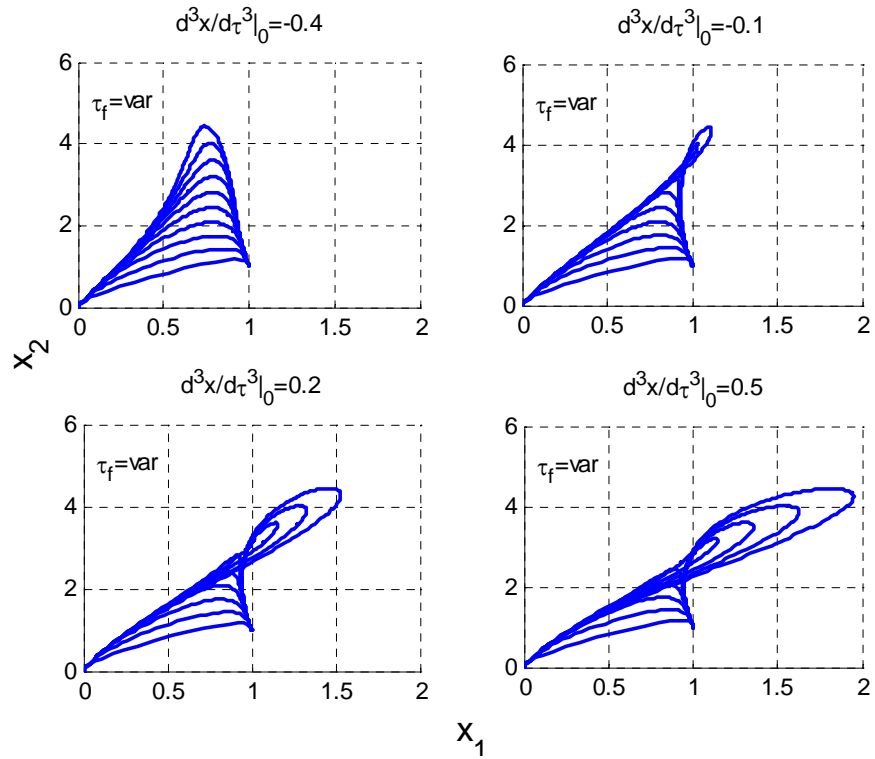


Figure 26. Variation of Path with τ_f and x_{10}''' (after [Ref 18])

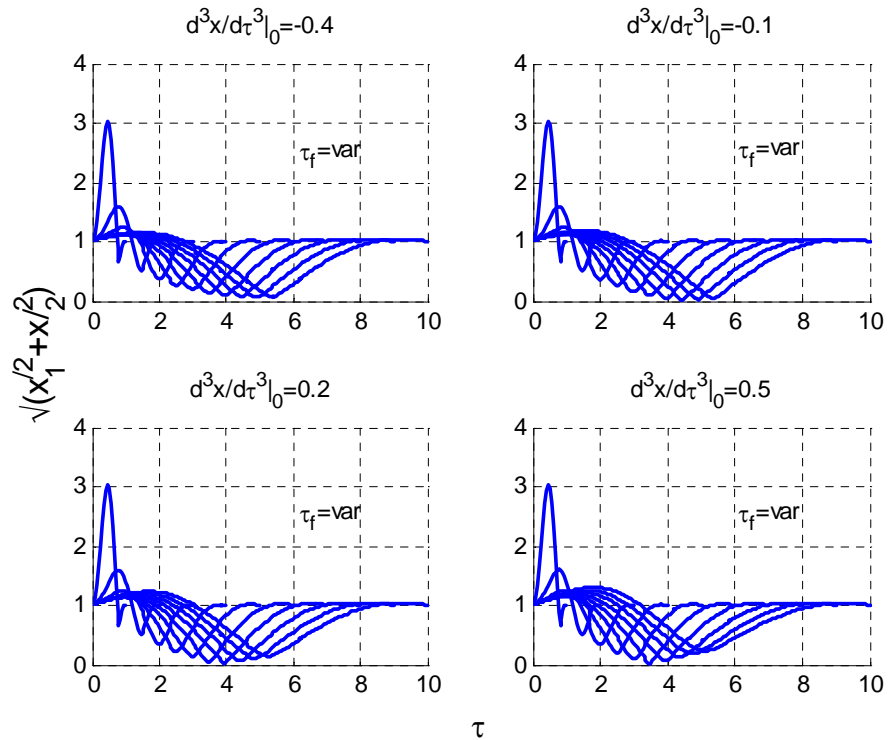


Figure 27. Variation of First Derivative of Path with τ_f and x_{10}'''

C. PROGRAM DEVELOPMENT

1. Boundary Conditions

Using equations (3.2) and (3.3), in addition to the controls n_x, n_y, n_z , it is possible to construct the vector of state variables $z = \{x_1, x_2, x_3, V, \theta, \Psi\}^T$ and the vector of controls $u = \{n_x, n_y, n_z\}^T$. The model for thrust, drag, and missile characteristics is the same as previously used in Chapter 3.

The beginning assumption is that the following data is known by the interceptor's onboard computer:

	Interceptor	Target
Body Frame	$\left. \begin{array}{l} x_1(t_0) = x_{10} \\ x_2(t_0) = x_{20} \\ x_3(t_0) = x_{30} \\ V(t_0) = V_0 \\ \Psi(t_0) = \Psi_0 \\ \theta(t_0) = \theta_0 \\ n_y(t_0) = n_{y0} \\ n_z(t_0) = n_{z0} \end{array} \right\} \begin{array}{l} \dot{x}_{10} \\ \dot{x}_{20} \\ \dot{x}_{30} \end{array} \left. \vphantom{\begin{array}{l} x_1(t_0) = x_{10} \\ x_2(t_0) = x_{20} \\ x_3(t_0) = x_{30} \\ V(t_0) = V_0 \\ \Psi(t_0) = \Psi_0 \\ \theta(t_0) = \theta_0 \\ n_y(t_0) = n_{y0} \\ n_z(t_0) = n_{z0} \end{array}} \right\} \begin{array}{l} \ddot{x}_{10} \\ \ddot{x}_{20} \\ \ddot{x}_{30} \end{array}$	$\left. \begin{array}{l} x_1(t_f) = x_{1f} \\ x_2(t_f) = x_{2f} \\ x_3(t_f) = x_{3f} \\ V(t_f) = V_f \\ \Psi(t_f) = \Psi_f \\ \theta(t_f) = \theta_f \end{array} \right\} \begin{array}{l} \dot{x}_{1f} \\ \dot{x}_{2f} \\ \dot{x}_{3f} \end{array}$
Earth Centered Inertial	$\begin{array}{l} x_1^{SM}(t), x_2^{SM}(t), x_3^{SM}(t) \\ \dot{x}_1^{SM}(t), \dot{x}_2^{SM}(t), \dot{x}_3^{SM}(t) \\ \ddot{x}_1^{SM}(t), \ddot{x}_2^{SM}(t), \ddot{x}_3^{SM}(t) \end{array}$	$\begin{array}{l} x_1^{BR}(t), x_2^{BR}(t), x_2^{BR}(t) \\ \dot{x}_1^{BR}(t), \dot{x}_2^{BR}(t), \dot{x}_3^{BR}(t) \end{array}$

Table 7. Interceptor Known Data

The target data will be used to determine the final boundary conditions of the interceptor missile according to the time until intercept, Δt :

Position:

$$\begin{aligned}
x_{1f}^{SM} &= x_{10}^{BR} + \dot{x}_{10}^{BR} \Delta t \\
x_{2f}^{SM} &= x_{20}^{BR} + \dot{x}_{20}^{BR} \Delta t \\
x_{3f}^{SM} &= x_{20}^{BR} + \dot{x}_{20}^{BR} \Delta t
\end{aligned} \tag{4.C.1}$$

Heading and Flight Path Angle:

$$\begin{aligned}
\theta_f^{SM} &= \frac{\pi}{2} + \theta_f^{BR}, \text{ where } \theta_f^{BR} = \text{arctg} \frac{\dot{x}_3^{BR}}{\sqrt{\dot{x}_1^{BR2} + \dot{x}_2^{BR2}}} \\
\psi_f^{SM} &= \psi_f^{BR}, \text{ where } \psi_f^{BR} = \text{arctg} \frac{\dot{x}_2^{BR}}{\dot{x}_1^{BR}}
\end{aligned} \tag{4.C.2}$$

which, when combined with reasonable estimates of the final values of the velocity, V , and the time rate of change of velocity, \dot{V} , heading ($\dot{\Psi} = 0$), and flight path angle ($\dot{\theta} = 0$), yields the final conditions:

$$\begin{aligned}
\dot{x}_{1f}^{SM} &= V_f \cos \theta_f \cos \psi_f \\
\dot{x}_{2f}^{SM} &= V_f \cos \theta_f \sin \psi_f \\
\dot{x}_{3f}^{SM} &= V_f \sin \theta_f
\end{aligned} \tag{4.C.3}$$

and

$$\begin{aligned}
\ddot{x}_{1f}^{SM} &= \dot{V}_f \cos \theta_f \cos \Psi_f - \dot{\theta}_f V_f \sin \theta_f \cos \Psi_f - \dot{\Psi}_f V_f \cos \theta_f \sin \Psi_f \\
\ddot{x}_{2f}^{SM} &= \dot{V}_f \cos \theta_f \sin \Psi_f - \dot{\theta}_f V_f \sin \theta_f \sin \Psi_f + \dot{\Psi}_f V_f \cos \theta_f \cos \Psi_f \\
\ddot{x}_{3f}^{SM} &= \dot{V}_f \sin \theta_f + \dot{\theta}_f V_f \cos \theta_f
\end{aligned} \tag{4.C.4}$$

In order to ensure a smooth flight path at the initial and final points, an additional constraint of

$$\begin{aligned}
\ddot{x}_{1i}^{SM} &= \ddot{x}_{1f}^{SM} = 0 \\
\ddot{x}_{2i}^{SM} &= \ddot{x}_{2f}^{SM} = 0 \\
\ddot{x}_{3i}^{SM} &= \ddot{x}_{3f}^{SM} = 0
\end{aligned} \tag{4.C.5}$$

will be imposed on the system at the initial and final conditions. This will have the practical result of limiting the initial and final controls on the system to smooth maneuvers, thus avoiding any tendency to conduct a “flair maneuver” at the last second. In current air-to-air engagements, the kill capability of the warhead can be greatly

improved by a last minute change in the orientation of the missile, a rapid jerk of the attitude from the flight path to an optimal angle, which is termed a “flair maneuver”. This focuses the blast effects toward the target and is of great usefulness when it is the warhead damage that kills the target; but in this situation it is the kinetic energy of the missile impact that kills the target. A flair maneuver would only dissipate much of that energy, possibly all of it, in order to achieve the algorithm’s desired impact angle and render the developed flight path useless for the mission. Similarly, an immediate and large maneuver at the start of the flight path would only dissipate the energy. Such maneuvers are discarded by these beginning and ending boundary conditions.

2. Separating and Recombining Space and Time

As discussed previously, in order to independently optimize the spatial trajectory and the velocity, the reference function will be derived as a function of τ . The boundary conditions cannot, therefore, be defined as functions of time derivatives as in equations (4.C.3) – (4.C.5). A connection between the spatial and time domains must therefore be introduced, λ , which is defined as

$$\lambda(\tau) = \frac{d\tau}{dt} \quad (4.C.6)$$

and is termed the virtual speed [Ref 19]. This allows for the independent variation of the speed profile along the same paths according to any other convenient reference. In this case the known thrust profile, n_x , will be utilized by integrating the third equation of (2.B.3) and applying the virtual speed

$$V'(\tau) = g(n_x - \sin \theta) \frac{d\tau}{dt} = \frac{g(n_x - \sin \theta)}{\lambda(\tau)} \quad (4.C.7)$$

Further use of the virtual speed allows the recalculation of the initial and final boundary conditions, transforming them from the time frame to the spatial frame. For this, the obvious relations

$$\begin{aligned}\dot{x}_i(\tau) &= \frac{dx_i}{d\tau} \frac{d\tau}{dt} = x'_i(\tau)\lambda(\tau) \\ \ddot{x}_i(\tau) &= \frac{d(x'_i(\tau)\lambda(\tau))}{d\tau} \frac{d\tau}{dt} = x''_i\lambda^2 + \dot{x}_i\lambda' \quad i=1,2,3\end{aligned}\tag{4.C.8}$$

which when rearranged defines the first and a second derivative of the missile coordinates as

$$x'_i = \lambda^{-1}\dot{x}_i \quad x''_i = \lambda^{-2}[\ddot{x}_i - \dot{x}_i\lambda'] \quad i=1,2,3\tag{4.C.9}$$

Using the values of λ and λ' defined as

$$\lambda_0 = V_0, \quad \lambda'_0 = \dot{V}_0 V_0^{-1} \quad \lambda_f = V_f, \quad \lambda'_f = \dot{V}_f V_f^{-1}\tag{4.C.10}$$

3. Reference Trajectory

The knowledge of the initial and final position plus the initial and final conditions of the first and second time derivatives allows for the construction of a 7th-order polynomial (the maximum orders of the time derivatives of the missile coordinates at the initial and final points plus one) to describe the reference function of the aircraft coordinates x_i ($i=1,2,3$). The following are introduced as the reference functions [Ref 19]:

$$\begin{aligned}x_i(\tau) &= \sum_{k=0}^5 a_{ik} \frac{(\max(1, k-2))! \tau^k}{k!} \\ x'_i(\tau) &= \sum_{k=1}^5 a_{ik} \frac{(\max(1, k-2))! \tau^{k-1}}{(k-1)!} \\ x''_i(\tau) &= \sum_{k=2}^5 a_{ik} \tau^{k-2} \\ x'''_i(\tau) &= \sum_{k=3}^5 (k-2) a_{ik} \tau^{k-3}\end{aligned}\tag{4.C.11}$$

Or written another way,

$$\begin{aligned}
x'''_i(\tau) &= a_{i3} + a_{i4}\tau + a_{i5}\tau^2 + a_{i6}\tau^3 + a_{i7}\tau^4 \\
x''_i(\tau) &= a_{i2} + a_{i3}\tau + \frac{1}{2}a_{i4}\tau^2 + \frac{1}{3}a_{i5}\tau^3 + \frac{1}{4}a_{i6}\tau^4 + \frac{1}{5}a_{i7}\tau^5 \\
x'_i(\tau) &= a_{i1} + a_{i2}\tau + \frac{1}{2}a_{i3}\tau^2 + \frac{1}{6}a_{i4}\tau^3 + \frac{1}{12}a_{i5}\tau^4 + \frac{1}{20}a_{i6}\tau^5 + \frac{1}{30}a_{i7}\tau^6 \\
x_i(\tau) &= a_{i0} + a_{i1}\tau + \frac{1}{2}a_{i2}\tau^2 + \frac{1}{6}a_{i3}\tau^3 + \frac{1}{24}a_{i4}\tau^4 + \frac{1}{60}a_{i5}\tau^5 + \frac{1}{120}a_{i6}\tau^6 + \frac{1}{210}a_{i7}\tau^7
\end{aligned} \tag{4.C.12}$$

The coefficients can be determined by solving the equations simultaneously,

$$\begin{pmatrix}
1 & 0 & 0 & 0 & 0 & 0 & 0 & 0 \\
0 & 1 & 0 & 0 & 0 & 0 & 0 & 0 \\
0 & 0 & 1 & 0 & 0 & 0 & 0 & 0 \\
0 & 0 & 0 & 1 & 0 & 0 & 0 & 0 \\
1 & \tau_f & \frac{1}{2}\tau_f^2 & \frac{1}{6}\tau_f^3 & \frac{1}{24}\tau_f^4 & \frac{1}{60}\tau_f^5 & \frac{1}{120}\tau_f^6 & \frac{1}{210}\tau_f^7 \\
0 & 1 & \tau_f & \frac{1}{2}\tau_f^2 & \frac{1}{6}\tau_f^3 & \frac{1}{12}\tau_f^4 & \frac{1}{20}\tau_f^5 & \frac{1}{30}\tau_f^6 \\
0 & 0 & 1 & \tau_f & \frac{1}{2}\tau_f^2 & \frac{1}{3}\tau_f^3 & \frac{1}{4}\tau_f^4 & \frac{1}{5}\tau_f^5 \\
0 & 0 & 0 & 1 & \tau_f & \tau_f^2 & \tau_f^3 & \tau_f^4
\end{pmatrix}
\begin{pmatrix}
a_{i0} \\
a_{i1} \\
a_{i2} \\
a_{i3} \\
a_{i4} \\
a_{i5} \\
a_{i6} \\
a_{i7}
\end{pmatrix}
=
\begin{pmatrix}
x_{i0} \\
x'_{i0} \\
x''_{i0} \\
x'''_{i0} \\
x_{if} \\
x'_{if} \\
x''_{if} \\
x'''_{if}
\end{pmatrix} \tag{4.C.13}$$

Finally, by substituting the corresponding values of $x_{i0}, x'_{i0}, x''_{i0}$ ($i=1,2,3$) for $\tau_0=0$, and $x_{if}, x'_{if}, x''_{if}$ ($i=1,2,3$) for $\tau=\tau_f$ (where τ_f is the first optimization parameter, the virtual arc), results in a set of 24 linear algebraic equations for 21 unknown coefficients a_{ik} ($i=1,2,3, k=0,1,\dots,7$)

$$\begin{aligned}
a_{i0} &= x_{i0} & a_{i1} &= x'_{i0} & a_{i2} &= x''_{i0} & a_{i3} &= x'''_{i0} \\
a_{i4} &= \frac{-4x'''_{if} + 16x'''_{i0}}{\tau_f} + \frac{60x''_{if} - 120x''_{i0}}{\tau_f^2} + \frac{-360x'_{if} - 480x'_{i0}}{\tau_f^3} + \frac{840x_{if} - 840x_{i0}}{\tau_f^4} \\
a_{i5} &= \frac{30x'''_{if} + 60x'''_{i0}}{\tau_f^2} + \frac{-420x''_{if} + 600x''_{i0}}{\tau_f^3} + \frac{2340x'_{if} - 2700x'_{i0}}{\tau_f^4} + \frac{-5040x_{if} + 5040x_{i0}}{\tau_f^5} \\
a_{i6} &= \frac{-60x'''_{if} - 80x'''_{i0}}{\tau_f^3} + \frac{780x''_{if} - 900x''_{i0}}{\tau_f^4} + \frac{-4080x'_{if} - 4320x'_{i0}}{\tau_f^5} + \frac{8400x_{if} - 8400x_{i0}}{\tau_f^6} \\
a_{i7} &= \frac{35x'''_{if} + 35x'''_{i0}}{\tau_f^4} + \frac{-420x''_{if} + 420x''_{i0}}{\tau_f^5} + \frac{2100x'_{if} + 2100x'_{i0}}{\tau_f^6} + \frac{-4200x_{if} + 4200x_{i0}}{\tau_f^7}
\end{aligned} \tag{4.C.14}$$

4. Inverse Dynamics

The numerical solution develops a reference trajectory over a fixed set of N points equidistantly placed along the virtual arc. The virtual interval is

$$\Delta\tau = \frac{\tau_f}{N-1} \quad (4.C.15)$$

and the corresponding time interval is

$$\Delta t_j = 2 \frac{\left(\sum_1^3 (x_{i;j} - x_{i;j-1})^2 \right)^{\frac{1}{2}}}{V_j + V_{j-1}}, \quad j = 1, 2, \dots, N-1 \quad (4.C.16)$$

where V_j and V_{j-1} is determined by integrating equation (4.C.7). N is any convenient number, chosen to be 100 in this program.

The value of V_j also allows for the determination of both θ and Ψ by rearranging equations (2.B.2) and substituting the virtual velocity

$$\begin{aligned} \theta_j &= \text{arctg} \frac{x'_{3;j}}{\sqrt{x'^2_{1;j} + x'^2_{2;j}}} \\ \psi_j &= \text{arctg} \frac{x'_{2;j}}{x'_{1;j}} \end{aligned} \quad (4.C.17)$$

The controls n_y and n_z are found by rearranging equations (2.B.3) to be

$$\begin{aligned} n_{y;j} &= \frac{V_j}{g} \dot{\Psi}_j \cos \theta_j \\ n_{z;j} &= \frac{V_j}{g} (\dot{\theta}_j + \cos \theta_j) \end{aligned} \quad (4.C.18)$$

where the angular derivatives are determined as

$$\begin{aligned} \dot{\theta}_j &= \cos^2 \theta \frac{x''_3(x_1'^2 + x_2'^2) - x'_3(x''_1 + x''_2)}{(x_1'^2 + x_2'^2)^{3/2}} \\ \dot{\Psi}_j &= \cos^2 \Psi \frac{x'_1 x''_2 - x''_1 x'_2}{x_1'^2} \end{aligned} \quad (4.C.19)$$

5. Cost and Penalty Functions

Finally, the calculation of the flight path results in a set of functions that must be minimized, which occurs through a Cost Function (CF) and a Penalty Function (PF). These functions must be carefully chosen to ensure that the optimal path is truly feasible, desirable, and obtainable. A simple example of a CF is $J \equiv t_f$, the minimal time problem, or $J \equiv |u(t)|$, the minimum fuel problem, though there is no limit to the number or variation of the Cost Function.

In this case, the CF was chosen to optimize three properties simultaneously; minimize the length of the virtual arc, τ_f , minimize the time to intercept, t_{go} , and maximize the impact angle of the interception. The CF for this program is written as

$$J = w_1 k_1 \tau_f + w_2 k_2 t_{go} + w_3 k_3 \frac{\vec{V}^{BR} \cdot \vec{V}^{SM}}{\|\vec{V}^{BR}\| \|\vec{V}^{SM}\|} \quad (4.C.20)$$

Each item must be scaled appropriately using the scaling factors k_1, k_2, k_3 , so that they are all roughly equivalent when optimized, e.g. the anticipated intercept time is counted in tens of seconds while the cosine of the impact angle will vary from zero to one. Failure to weight them properly will skew the results of the cost function. Additionally, through the weighting functions w_1, w_2, w_3 , a trade-off analysis can be conducted and variables can be included or excluded as desired.

The first two variables, τ and t_{go} , are necessary to ensure the system's optimal solution is actually physically realizable. Without them, the system will continue to optimize the intercept well beyond the capabilities of the missile or even physical reality. One example is that, in a purely mathematical sense, there is no problem with a negative velocity (yet in the physical world that makes no sense) and the program might try a program that would intercept after the missile velocity has gone past zero and into negative numbers (of course, the missile would stop flying long before it even reaches zero). One might be tempted to include a myriad of parameters to cover all possible eventualities; however, including these two parameters sufficiently accounts for nearly every physical limitation and eliminates the need for having a long list of cost variables.

The third variable in the CF was chosen in order to maximize the angle of impact upon interception. This reflects the need, described in Chapter 1, to maximize the kinetic energy in order to ensure the interceptor disables the target. The cost is calculated using a simple dot product relationship

$$\cos \theta = \frac{\text{dot}(\vec{x}_f^{SM}, \vec{x}_f^{BR})}{\|\vec{x}_f^{SM}\| \|\vec{x}_f^{BR}\|} \quad (4.C.21)$$

which will have a minimum value of zero when the impact angle is at a maximum.

The PF is chosen to ensure that certain conditions are not violated or exceeded, such as physical limitations. In this case, the PF is on the maximum acceleration in the y and z direction. Zarchan showed that acceleration capability is dependent on altitude and speed [Ref 21]. The PF has been set up to reflect this by varying between 40 g's at sea level to 10 g's at 50,000 ft.

These are not the only CF or PF variables that can be included. The choice of variables to include is situation dependant and may be modified to meet whatever the needs of the situation demand.

4. Simulation Outline

The simulation begins with the definition of the ballistic missile flight path. The data will be used to represent what the missile “sees” when it is defining the boundary conditions. A perfect picture is assumed for this simulation. Once the ballistic flight path has been defined, the interceptor is launched. The interceptor launch point was chosen as $[100000; 100000; \text{Re}]^T$, roughly 150 nm from the launch position.

The first portion of the SM-6 flight is the vertical launch, which was assumed to last 6 s, followed by a 4 s period in which the missile arcs over toward the target, as it would do under guidance from the AEGIS weapon system in normal circumstances. At 10 seconds, the state of the interceptor and the state of the ballistic target is “seen” and input into the system. At this point the missile would not have an independent radar picture of the target, so instead would be fed targeting data from the AEGIS weapon

system. This can continue indefinitely until the interceptor has its own radar fix on the ballistic missile.

A first “guess” at time to go and flight distance is done by a simple iterative process that takes the known velocity profile and iterates an initial intercept time using a first order approximation of the ballistic path. This process uses the known velocity profile of the SM-6 and the known velocity profile of the TD-2 in order to develop an accurate “guess” according to

$$\begin{aligned}
 & t_{go1} = 100; \delta = 5; \\
 & \text{while } \delta > 1 \\
 & \quad \text{if } t_{go1} < 26 \\
 & \quad \quad V_f = \frac{3500}{26} t_{go1} \\
 & \quad \quad V_{ave} = \frac{V_f}{2} \\
 & \quad \text{else} \\
 & \quad \quad V_f = 3500 - 10(t_{go1} - 26) \\
 & \quad \quad V_{ave} = \left(26 * \frac{3500}{2} + \frac{(t_{go1} - 26)(3500 + V_f)}{2t_{go1}} \right) \\
 & \quad \text{end} \\
 & x_f = x_t + \dot{x}_t t_{go1} \\
 & t_{go2} = \frac{\sqrt{\sum_{i=1}^3 (x_{f,i} - x_{0,i})^2}}{\|xdt\| + V_{ave}} \\
 & \delta = |t_{go2} - t_{go1}| \\
 & t_{go1} = \frac{t_{go1} + t_{go2}}{2} \\
 & \text{end} \\
 & t_{go} = t_{go1}
 \end{aligned}$$

Also, the program creates an initial guess at the optimum final values of the flight path angle and heading using (4.C.3). This serves only as an initial start point and must only be mildly accurate, since the program will optimize the time and flight path as it

operates. The accuracy of the initial guesses only serves to decrease the necessary computation time.

The MATLAB function “fminsearch” carries out the optimization by varying the four optimization parameters and evaluating the cost function. Once the minimum value of the CF has been found, the fminsearch returns the required control time history to the missile guidance system, which can then execute the commands and fly the derived flight path. Since the missile system can be programmed with sufficient data to compensate for its control system time constant, the system lag can be effectively negated, thus eliminating a source of error.

Updating the guidance system every several seconds will result in increasingly accurate final intercept positions and further ensure the mission kill.

D. SIMULATION RESULTS

The simulation ran as expected, testing about 80 iterations and different flight paths before arriving in the neighborhood of the final value, and testing about 160 iterations and different flight paths before arriving at the optimal solution.

The three coordinate axes were independently optimized. Figures 28-30 show the flight paths generated and the first and second derivatives of those flight paths in each of the coordinate axes. It is clear that each flight path is smooth, continuous, and satisfies the initial and final boundary conditions.

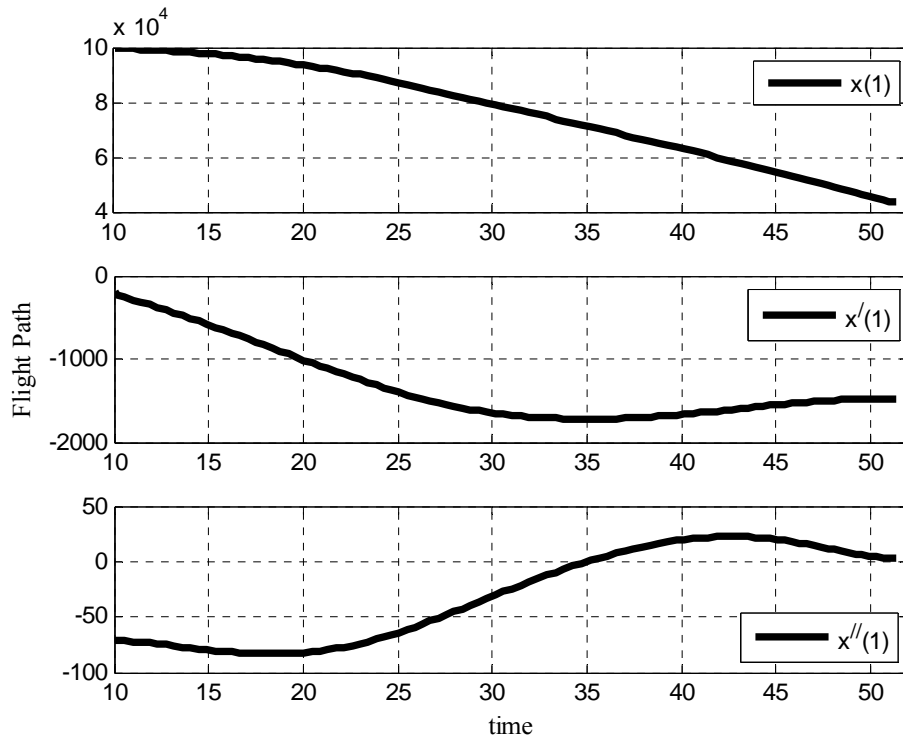


Figure 28. X-axis Flight Path and Derivatives

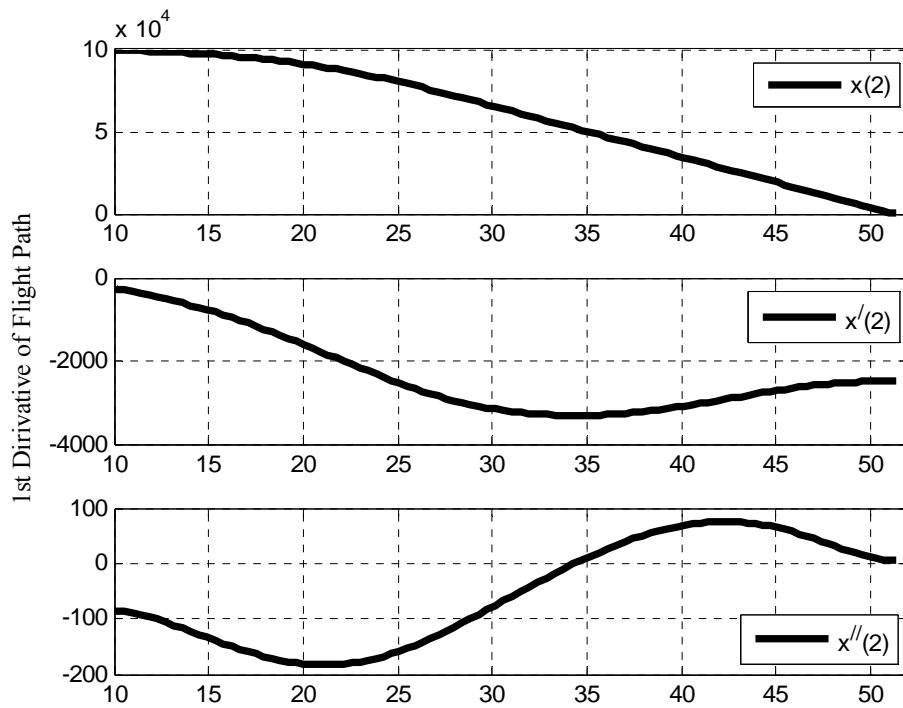


Figure 29. Y-axis Flight Path and Derivatives

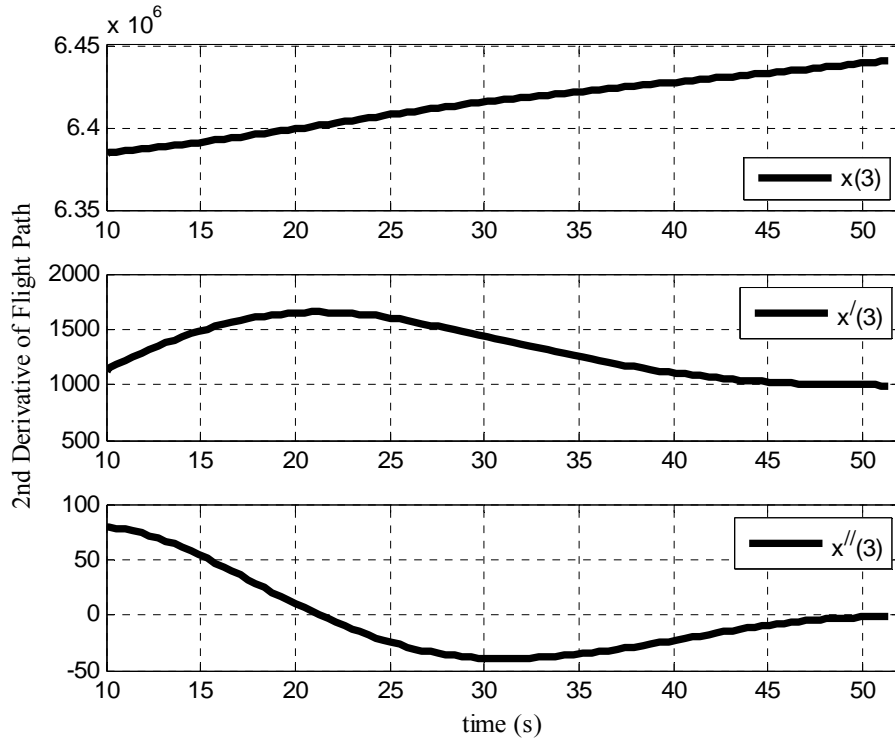


Figure 30. Z-axis Flight Path and Derivatives

It is important to note that the derivatives of the flight path are not the velocity and acceleration in a time-frame sense, but instead are the spatial derivatives. They represent the rate of change of the motion of the flight path. In an abstract sense, the interceptor missile could travel along this optimum path at any chosen speed (though in this case the velocity history is defined), and still be flying along the optimum path. The velocity history is introduced after the optimum path has been derived to determine the flight time and test the boundary conditions.

The final flight path selected is shown in Figures 31-33, in three dimensional plots from various angles. In each figure is a large black star designating the point that the interceptor activated the guidance law and the point that the state of the ballistic rocket was extracted. The only state that the interceptor missile was given was the one represented by the star. The final intercept position is on the ballistic flight path because the algorithm optimized the intercept time and determined the final position based on that optimization. This is the major difference between this program and most predictive intercept guidance laws where the time to intercept is only an educated guess.

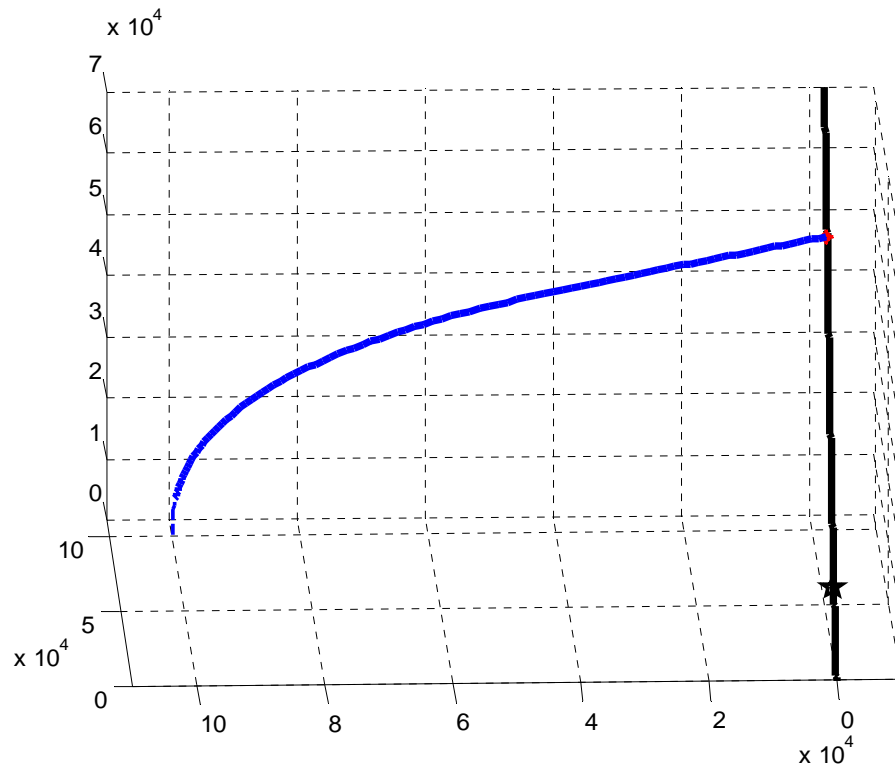


Figure 31. 3D Optimal Flight Path

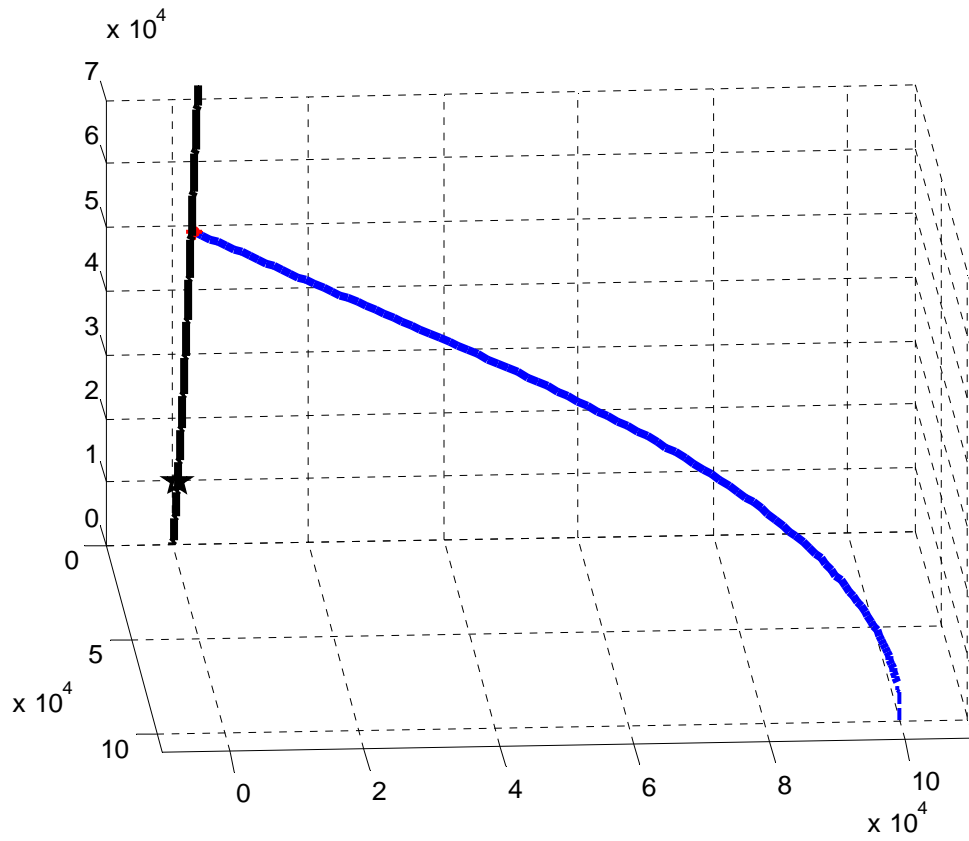


Figure 32. 3D Optimal Flight Path

V. CONCLUSIONS

A. VERIFICATION OF OPTIMALITY

A plot of the position and velocity of the ballistic missile overlaid upon the final optimal flight path shows the final intercept geometry, as shown in Figure 34, where the lines extending from the position point represent the current velocity vector at that moment (the relative scale shows the relative speeds and the circle at the end denotes “forward” for each). It is clear from Figure 34 that the interceptor does indeed intercept the ballistic missile, and at a near right angle as was intended.

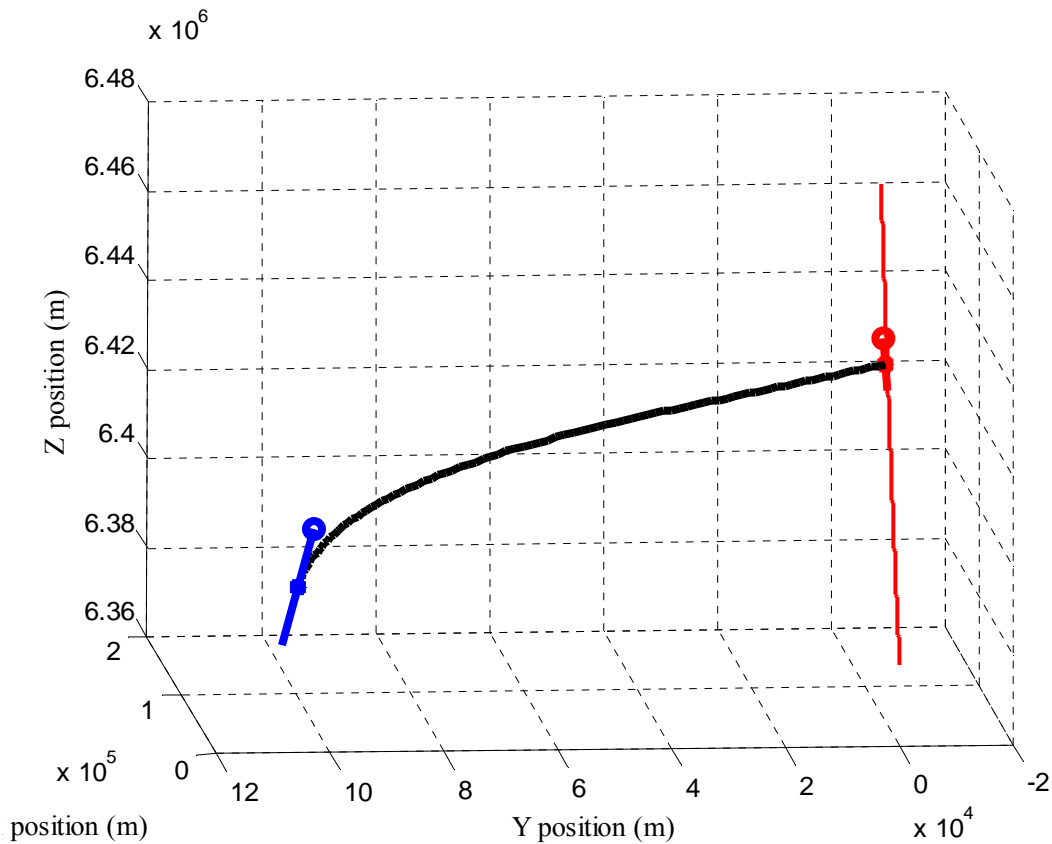


Figure 33. Final Interception Geometry

Another way to verify that the interception is as predicted is to look at each coordinate axis, as shown in Figures 35-37. Again the missile's heading and relative speeds are denoted by the lines extended from the position point, and the line shows the optimum flight path.

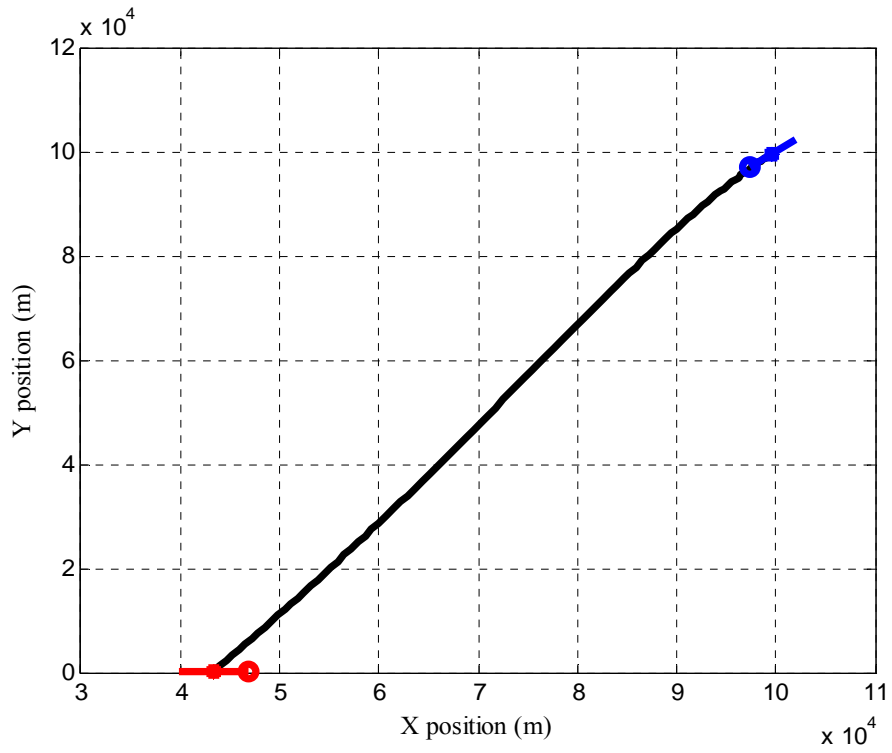


Figure 34. 2D (X-Y axis) Optimum Flight Path

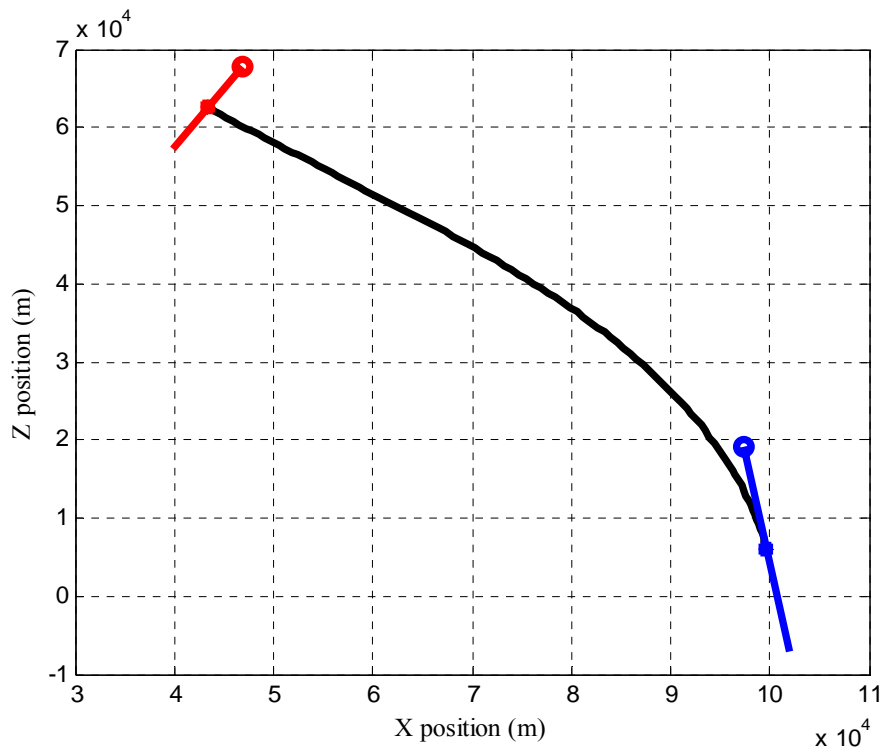


Figure 35. 2D (X-Z axis) Optimum Flight Path

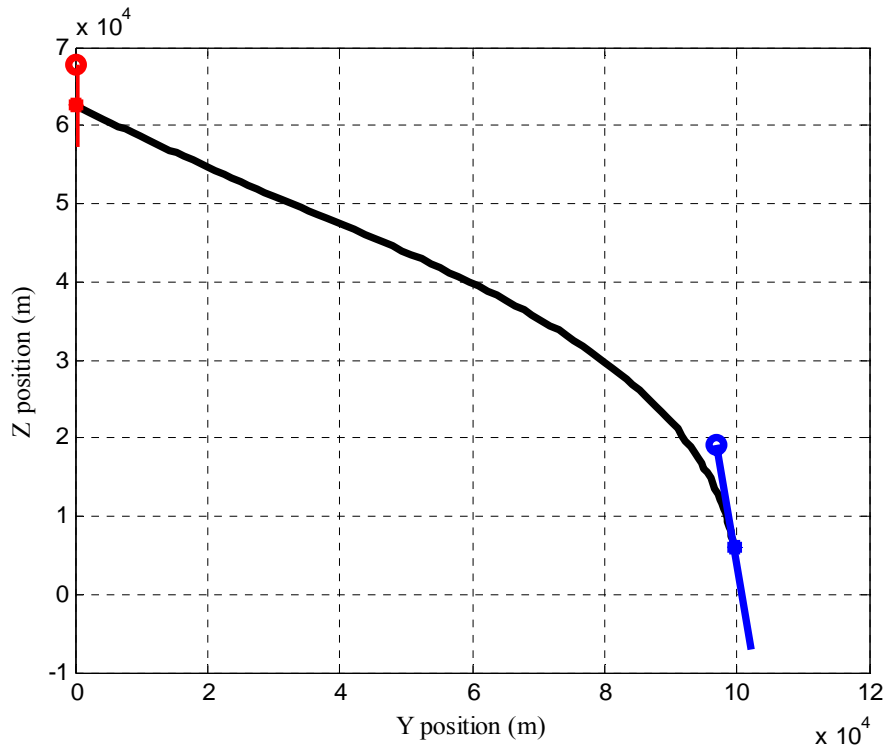


Figure 36. 2D (Y-Z axis) Optimum Flight Path

It is clear that the intercept does occur and that it is at a near right angle. The remaining question is whether it is feasible and physically possible for the interceptor missile to fly the derived path. Figure 38 shows the time history of the heading and flight path angles.

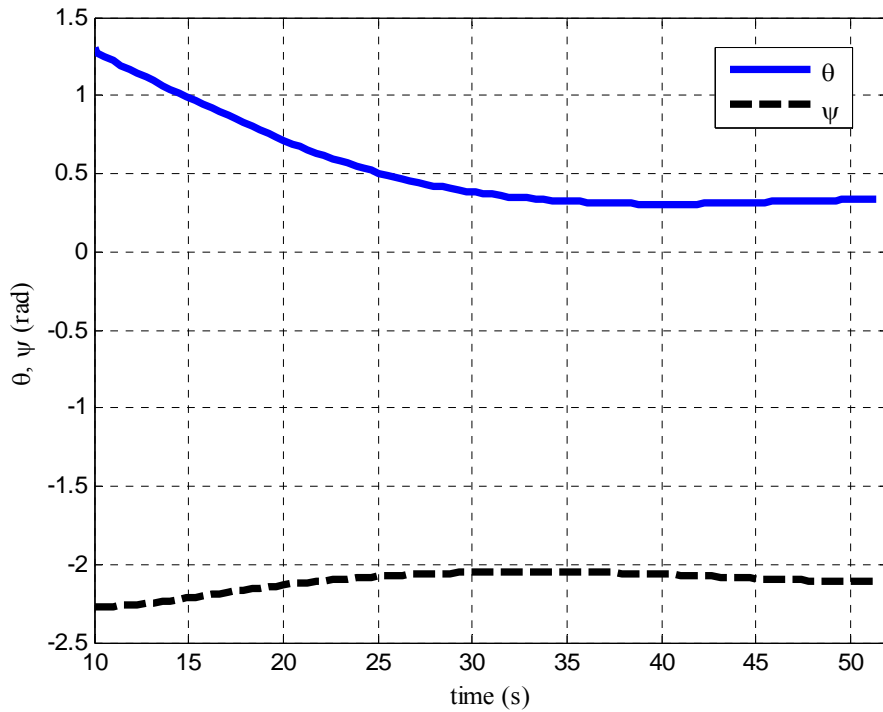


Figure 37. Heading (Ψ) and Flight Path Angle (θ) Time History

It is clear from Figure 38 that the path generated does not require large variations of heading or flight path, suggesting it is a feasible flight path. However, this is not conclusive. Instead, the required axial forces must be verified to be constantly within the limitations of the system. Figure 39 shows the time history of the independent control forces, n_y, n_z . The dashed line represents the maximum capability of the system at each point, based on the altitude of the missile as discussed in Chapter IV.

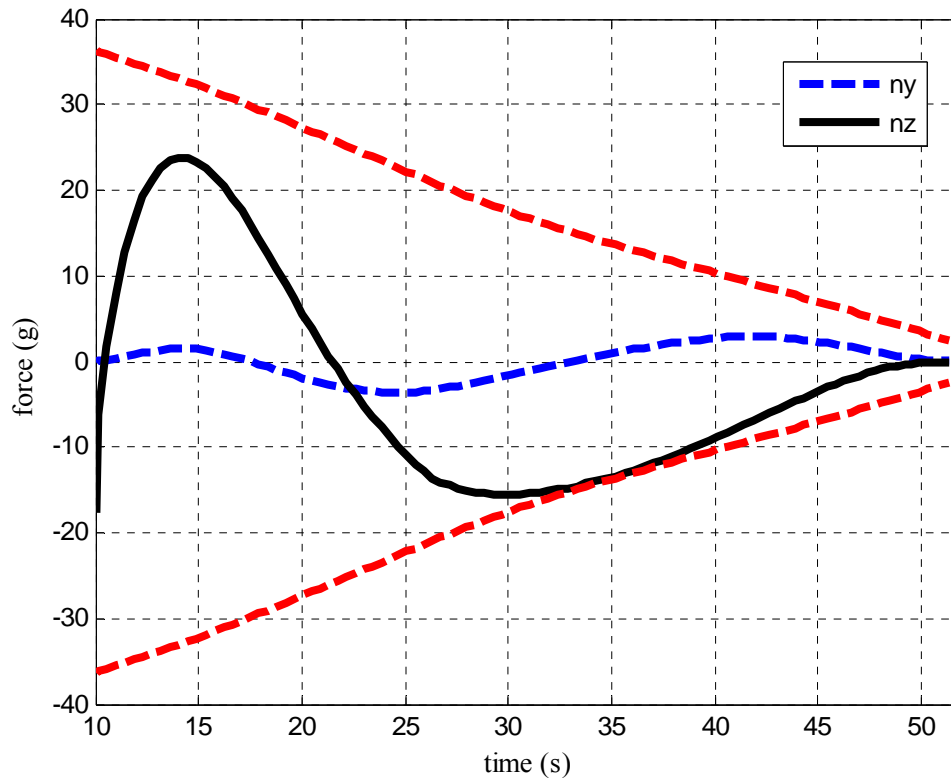


Figure 38. Control Forces Time History

It is clear from Figure 39 that the missile is capable of navigating the generated flight path. Note that it uses the full capabilities of the missile to conduct the interception, which suggests that the program is appropriately accounting for the missile capabilities. Also note that the required forces are near zero at the intercept point, demonstrating no flair maneuver or high-g maneuver was conducted. This suggests that the full kinematic energy of the missile is directed into the target, which was the original intent of the program.

It can be proven that the penalty functions were indeed influencing the choice of trajectory. If the required control effort exceeded the maximum capabilities of the missile the trajectory, the path should be rejected as infeasible. It can be seen from Figure 40 that this is the case, and that the final path has no penalty assigned to it.

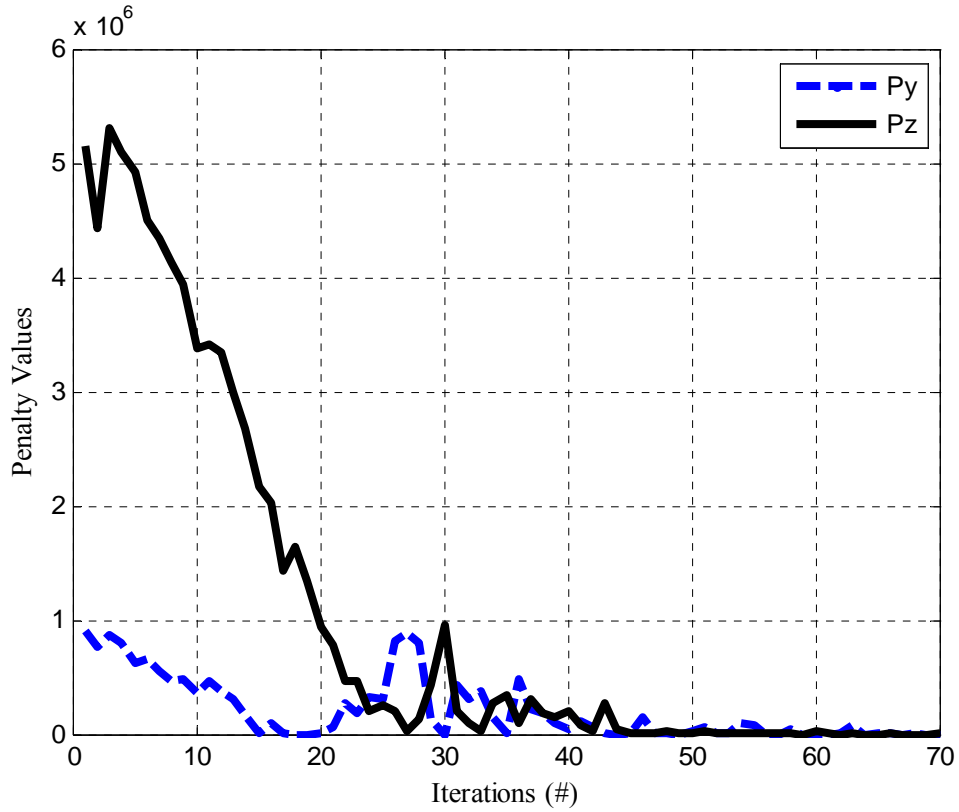


Figure 39. Penalty Function Values

The flight path is feasible, it accomplishes the intended goal, and is within the capabilities of the interceptor missile. The final question, then, is whether the generated flight path is in fact “optimal”, i.e. the best available path. Figure 41 shows the value of the CF after each iteration, with emphasis on the final series of values. The figure clearly demonstrates that the value of the CF quickly gets within the neighborhood of the minimum, and after a short duration reaches the minimum cost function.

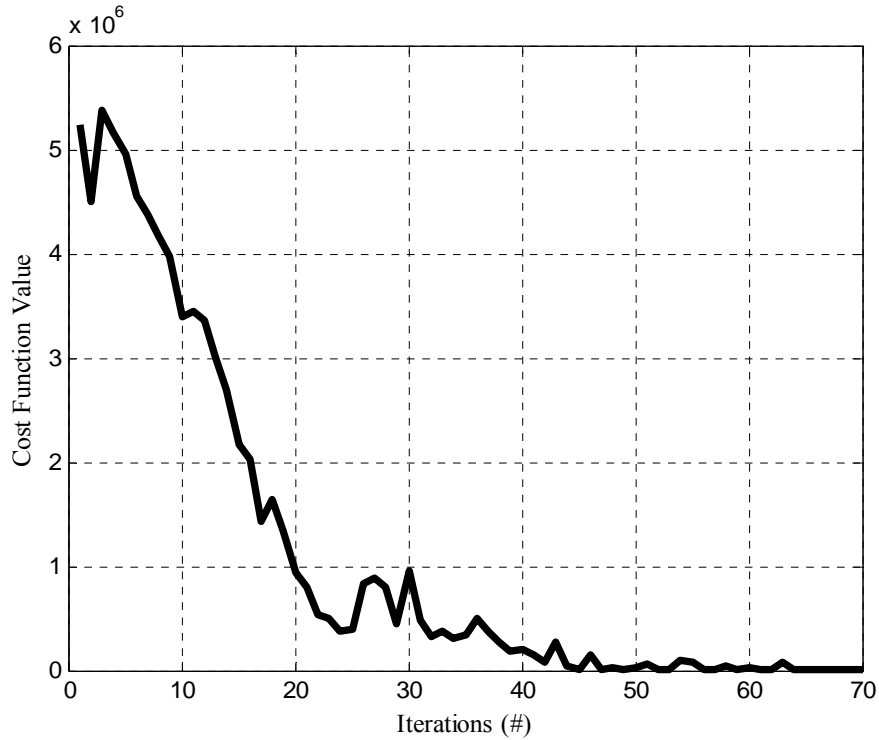


Figure 40. Iterative Value of the Cost Function

It is also important to ensure the impact angle is maximized. It has already been shown from the various graphs that the impact angle is indeed close to 90 degrees. It remains to be seen, however, if it the best one that can be found. It is possible that this flight path is returned as “optimal” not because it maximizes the impact angle, but instead because the values of t_{go} and τ_f dominate to the point that impact angle’s contribution is negligible. Figure 42 shows the value of the impact angle after each iteration of the program, with emphasis on the final values.

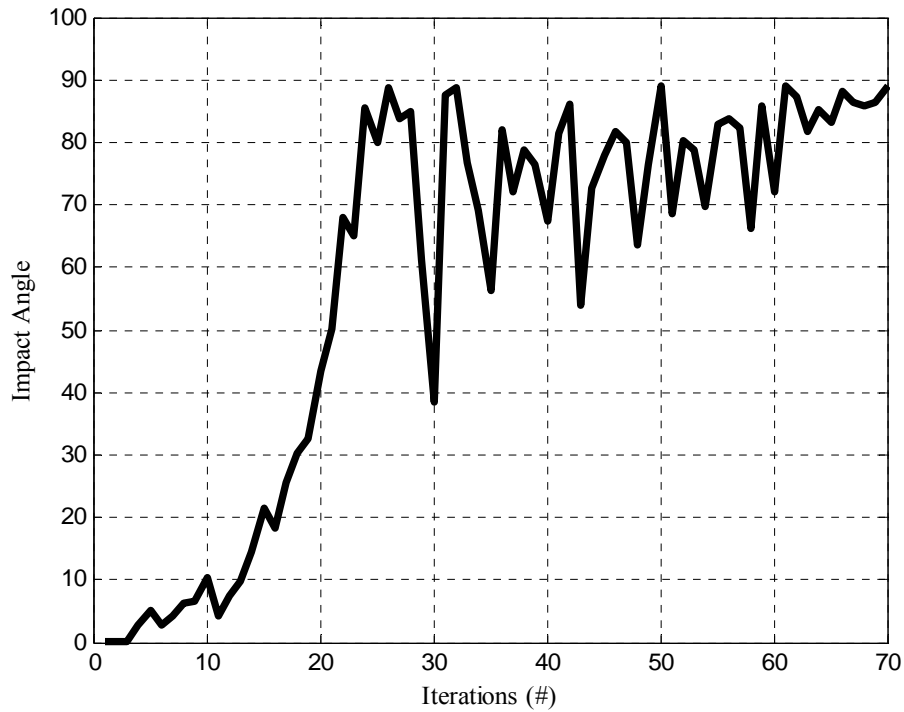


Figure 41. Iterative Value of the Cosine of the Impact Angle

The two remaining variables to be optimized have no target value, as there was with the impact angle. It therefore must only be shown that the algorithm has indeed tried numerous values and found the best one. Figure 43 shows the iterative value of t_{go} , and clearly shows this is occurring. Likewise for Figure 44 regarding τ_f .

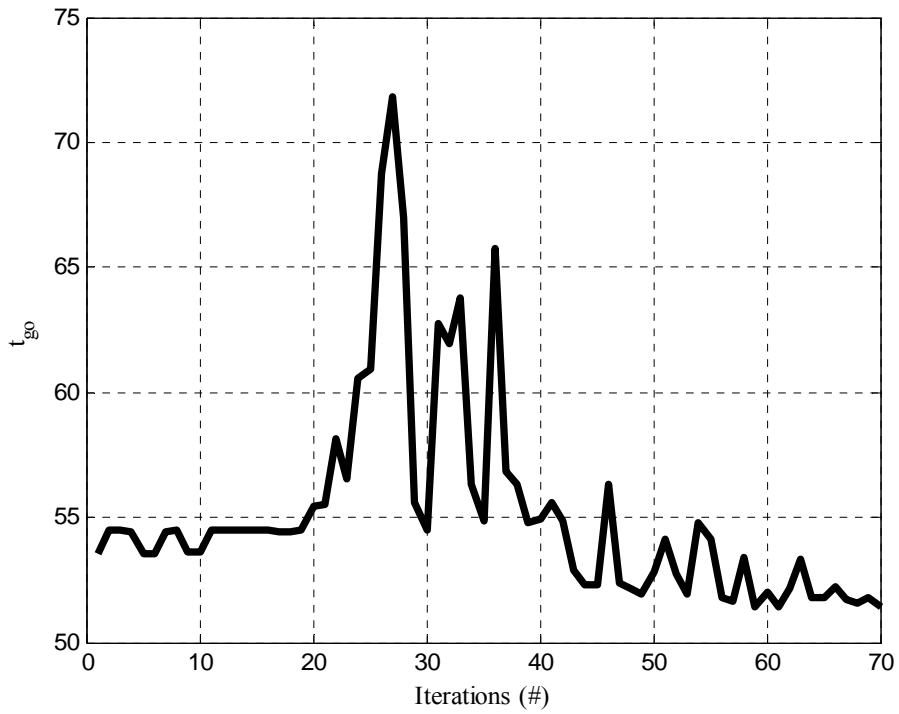


Figure 42. Iterative Value of Intercept Time

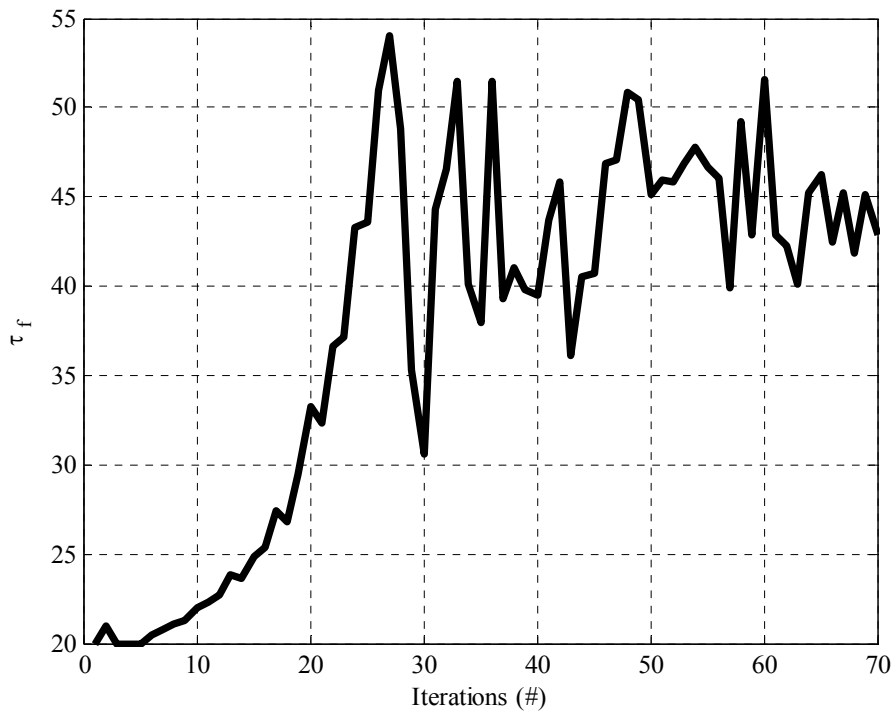


Figure 43. Iterative Value of τ_f

It can therefore be said that the generated flight path is indeed the solution which minimizes the flight path distance, minimizes the time of flight, and maximizes the impact angle – the optimum one for this intercept.

B. APPLICABILITY

This algorithm can easily be incorporated into existing control systems for numerous applications. Yakimenko has shown that for short term spatial maneuvers, the system is extremely robust and capable, and requires only a moderate level of computational power [Ref 19]. The power required for this particular application is slightly more since the final boundary conditions are not fixed but instead vary with the time and flight path conditions. Still, a dedicated system, such as onboard a properly modified SM-6, must be capable of not only deriving the flight path, but also storing the data and executing it. None of these are particularly challenging requirements, as many other missiles in the US inventory complete many of these individual tasks already.

This program cannot take into account the future actions of the target. It is thus not applicable to a target that is capable of maneuvering or deviating from its flight path in a considerable manner. This limits the scope and applicability of the program, but there are currently many very capable guidance laws for these situations. The purpose here was to propose a law that is very specific in its application but which operates far beyond the capabilities of otherwise excellent guidance laws.

C. SUGGESTIONS FOR FUTURE RESEARCH

Several avenues remain unexplored within this area of study. Some weaknesses that may be overcome by further research are:

1. Perform a trade-off analysis of cost function weighting coefficients to determine if the chosen ones are the most influential choices, or if they are redundant, or if other choices may provide better results.
2. Implement a second-order prediction model of the Ballistic Missile path in the development of the final boundary conditions to improve the accuracy of the interception.

3. Perform robustness analysis using the developed 6DOF high-fidelity model and auto-pilot model in the presence of disturbances.
4. Perform Monte Carlo simulation on launch-interception scenario to determine the limitations on the algorithm.

THIS PAGE INTENTIONALLY LEFT BLANK

APPENDIX A: MODELING PROGRAMS

A. 3DOF TARGET

1. BRParams3.m

```
function [BR_mass,dia,length]=BRParams3(t)
% Written by LT John A. Lukacs IV, Naval Postgraduate School, June 2006

% This function calculates the mass of the rocket, assuming a cruciform
% rocket in two stages plus an unpowered nosecone stage. This function
% also returns the reference (base) diameter of the missile.

%% Notes:
% The first stage last 125 seconds, the second stage lasts an
% additional 110 seconds. The stages separate upon completion.

%% Variable List
% BR_mass      =total rocket mass
% BR_nose      =total mass of nosecone section
% BR_st1_bt    =burntime for stage 1
% BR_st1_fcr   =consumption rate of stage 1 fuel
% BR_st1_fuel  =remaining stage 1 fuel based on time and
%              consumption rate
% BR_st1_str   =total mass of stage 1 structural material
% BR_st1_tfm   =total mass of stage 1 fuel
% BR_st2_bt    =burntime for stage 2
% BR_st2_fcr   =consumption rate of stage 2 fuel
% BR_st2_fuel  =remaining stage 2 fuel based on time and
%              consumption rate
% BR_st2_str   =total mass of stage 2 structural material
% BR_st2_tfm   =total mass of stage 2 fuel
% dia          =reference diameter, base diameter
% t           =time

%% Structural Components
BR_nose=250;
BR_st2_str=2288;
BR_st1_str=9000;

%% Fuel Components
BR_st1_tfm=50970;
BR_st1_bt=125;
BR_st1_fcr=BR_st1_tfm/BR_st1_bt;
BR_st2_tfm=12912;
BR_st2_bt=110;
BR_st2_fcr=BR_st2_tfm/BR_st2_bt;

if t<125
    %% Stage 1 - Stage 1 Fuel is consumed; Stage 2 Fuel is not used.
    BR_st1_fuel=BR_st1_tfm-BR_st1_fcr*t;
    BR_mass=BR_nose+BR_st1_str+BR_st1_fuel+BR_st2_str+BR_st2_tfm;
    dia=2.2;
    length=2+14+16;
```

```

elseif t<240;
    %% Stage 2 - Stage 1 has separated; Stage 2 Fuel is consumed.
    BR_st2_fuel=BR_st2_tfm-BR_st2_fcr*(t-125);
    BR_mass=BR_nose+BR_st2_str+BR_st2_fuel;
    dia=1.3;
    length=2+14;

else
    %% Stage 3 - Stage 2 has separated; unpowered nosecone remains.
    BR_mass=BR_nose;
    dia=1.3;
    length=2;

end
return

```

2. BRFlight3.m

```

%% Script File
% Written by LT John A. Lukacs IV, Naval Postgraduate School, June 2006

% This script integrates the position, velocity, and acceleration
values
% at each time step to determine the flight path of a ballistic missile
% in a gravity turn. The script calls BRParams3.m, ZLDragC.m, and
% SAtmos.m

%% Variable List
% acc      =total acceleration
% alt      =altitude
% ax       =x component of acceleration
% ay       =y component of acceleration
% az       =z component of acceleration
% CD       =drag coefficient
% dia      =reference diameter (base diameter)
% Drag     =total drag force
% dt       =time step interval
% g        =gravity force, based on WGS-84 value of gravitational
%          attraction and altitude
% gm       =initial launch angle
% i        =interval count
% m_r      =rocket mass
% Mspd     =rocket speed in Mach (relative to local speed of sound)
% num_BR   =number of iterations conducted (used for plotting)
% nx       =axial force
% press    =local atmospheric pressure
% px       =x component of position
% py       =y component of position
% pz       =z component of position
% Re       =WGS-84 value for Earth's radius
% ro       =local atmospheric density
% spd      =rocket speed in m/s
% Sref     =planar reference area (for drag calculations)
% t        =time

```

```

% temp      =local atmospheric temperature
% Thrust    =thrust generated by motor
% vx       =x component of velocity
% vy       =y component of velocity
% vz       =z component of velocity
% Acc_BR   =index-based vector of acceleration values
% Forces_BR=index-based vector of force values
% Pos_BR   =index-based vector of position values
% time_BR  =index-based vector of time values
% Vel_BR   =index-based vector of velocity values
% All_BR   =index based vector of all rocket values

%% Initialize Variables
t=0; dt=0.5; i=0;
Re=6.378137e6;

%% Initial Conditions
px=0;
py=0;
pz=Re;
gm=75*pi/180;
vx=cos(gm);
vy=0;
vz=sin(gm);

%% Ballistic Flight Path
for t=0:0.5:2219.5
    i=i+1;

    % Speed, Mach Number
    spd=norm([vx;vy;vz]);
    alt=norm([px;py;pz])-Re;
    if alt<86000
        [ro,press,temp]=Statmos(alt);
    else
        [ro,press,temp]=Statmos(86000);
    end
    Mspd=spd/sqrt(1.402*287*temp);

    % Forces
    g=3.986004418e14/norm([px;py;pz])^2;
    [m_r,dia]=BRParams3(t);
    [CD]=ZLDragC(Mspd,t);

    if t<125
        Thrust=105000*9.81;
        CD=CD(1);
    elseif t<240
        Thrust=29950*9.81;
        CD=CD(1);
    else
        Thrust=0;
        CD=CD(2);
    end
    Sref=pi*dia^2/4;
    Drag=ro*spd^2*CD*Sref/2;

```

```

nx=(Thrust-Drag)/m_r;

% Accelerations
g=3.986004418e14*pz/norm([px;py;pz])^3;
ax=nx*cos(gm);
ay=0;
az=nx*sin(gm)-g;
acc=norm([ax;ay;az]);

% Collect Variables
time_BR(i,1)=t;
Pos_BR(i,1)=px;
Pos_BR(i,2)=py;
Pos_BR(i,3)=pz;
Pos_BR(i,4)=norm([px;py;pz]);
Vel_BR(i,1)=vx;
Vel_BR(i,2)=vy;
Vel_BR(i,3)=vz;
Vel_BR(i,4)=spd;
Vel_BR(i,5)=Mspd;
Acc_BR(i,1)=ax;
Acc_BR(i,2)=ay;
Acc_BR(i,3)=az;
Acc_BR(i,4)=acc;
Acc_BR(i,5)=nx;
Forces_BR(i,1)=Thrust;
Forces_BR(i,2)=m_r;
Forces_BR(i,3)=Drag;

% Time Step
px=px+dt*vx;
py=py+dt*vy;
pz=pz+dt*vz;
vx=vx+dt*ax;
vy=vy+dt*ay;
vz=vz+dt*az;
num_BR=length(time_BR);
end

AllBR=[time_BR Forces_BR Pos_BR Vel_BR Acc_BR];

clear CD Drag Mspd Re Sref Thrust acc alt ax ay az dia dt
clear g gm h i m_r nx press px py pz ro spd t temp vx vy vz

```

B. 3DOF INTERCEPTOR

1. SMPParams3.m

```
function [SM_mass,dia]=SMPParams3(t)
% Written by LT John A. Lukacs IV, Naval Postgraduate School, June 2006

% This function calculates the J Matrix and Mass of the interceptor,
% assuming a cruciform rocket in two stages to intercept. This
% function also returns the reference (base) diameter of the missile.

%% Notes:
% The first stage last 6 seconds, the second stage lasts an additional
% 10 seconds. Stage 1 (booster) separates upon completion. Stage 2
% does not separate after completion

% Variable List
% dia          =reference diameter, base diameter
% l            =length, varies by component
% p_SM_st1_fuel=density of stage 1 rocket fuel
% p_SM_st2_fuel=density of stage 2 rocket fuel
% p_SMstr      =density of structural material
% r            =radius, varies by component
% ro           =outer radius, varies by component
% ri           =inner radius, varies by component
% SM_mass      =total rocket mass
% SM_nose      =total mass of nosecone section
% SM_st1_fcr   =consumption rate of stage 1 fuel
% SM_st1_fuel  =remaining stage 1 fuel based on time and
%              consumption rate
% SM_st1_str   =total mass of stage 1 structural material
% SM_st1_tfm   =total mass of stage 1 fuel
% SM_st2_fcr   =consumption rate of stage 2 fuel
% SM_st2_fuel  =remaining stage 2 fuel based on time and
%              consumption rate
% SM_st2_str   =total mass of stage 2 structural material
% SM_st2_tfm   =total mass of stage 2 fuel
% t            =time
% th           =structural thickness
% V_body       =volume of body structural material
% V_nose_str   =volume of nosecone structural material
% V_nose_str0  =volume of nosecone structural material,
%              intermediate value
% V_nose_str1  =volume of nosecone structural material,
%              intermediate value
% V_st1_fuel   =volume of stage 1 fuel
% V_st1_str    =volume of stage 1 structural material
% V_st2_fuel   =volume of stage 2 fuel
% V_st2_str    =volume of stage 2 structural material

%% Structural Components
p_SMstr=4225;
th=.0208;

% Mass of Nosecone
l=.8255;
```

```

r=0.34/2;
V_nose_str0=pi*(1*((r^2+l^2)/(2*r))^2-l^3/3-(((r^2+l^2)/...
    (2*r))-r)*((r^2+l^2)/(2*r))^2*asin(1/((r^2+l^2)/(2*r))));
l=.8255-th;
r=0.34/2-th;
V_nose_str1=pi*(1*((r^2+l^2)/(2*r))^2-l^3/3-(((r^2+l^2)/...
    (2*r))-r)*((r^2+l^2)/(2*r))^2*asin(1/((r^2+l^2)/(2*r))));
V_nose_str=V_nose_str0-V_nose_str1+pi*r^2*th;
SM_nose=1.3*V_nose_str*p_SMstr;

% Mass of Body/Warhead Section
l=.849;
ro=0.34/2;
ri=0.34/2-th;
V_body=l*pi*(ro^2-ri^2);
SM_body=V_body*p_SMstr+115;

% Mass of Stage 1 (Mk72 Booster)
l=1.72;
ro=0.53/2;
ri=0.53/2-th;
V_st1_str=l*pi*(ro^2-ri^2)+2*pi*ro^2*th;
SM_st1_str=V_st1_str*p_SMstr;

% Mass of Stage 2 (Mk104 Engine)
l=2.88-2*th;
ro=0.34/2;
ri=0.34/2-th;
V_st2_str=l*pi*(ro^2-ri^2)+2*pi*ro^2*th;
SM_st2_str=V_st2_str*p_SMstr;

%% Fuel Components
% Stage 1 Solid Fuel is HTPB/AP/Al
l=1.72;
ri=0.53/2-th;
V_st1_fuel=0.80*l*pi*ri^2;
p_SM_st1_fuel=1860;
SM_st1_tfm=468;
SM_st1_fcr=468/6;
% Stage 2 Solid Fuel is TP-H1205/6
l=2.88;
ri=0.34/2-th;
V_st2_fuel=0.60*l*pi*ri^2;
SM_st2_tfm=360;
p_SM_st2_fuel=SM_st2_tfm/V_st2_fuel;
SM_st2_fcr=360/15;

if t<6
    % Stage 1 - Stage 1 Fuel is consumed; Stage 2 Fuel is not used.
    SM_st1_fuel=SM_st1_tfm - SM_st1_fcr * t;
    SM_mass=SM_nose+SM_body+SM_st2_str+SM_st2_tfm+SM_st1_str+...
        SM_st1_fuel;
    dia=0.53;

elseif t<21
    % Stage 2 - Stage 1 has separated; Stage 2 Fuel is consumed.

```

```

SM_st2_fuel=SM_st2_tfm - SM_st2_fcr * (t-6);
SM_mass=SM_nose+SM_body+SM_st2_str+SM_st2_fuel;
dia=0.34;

else
    %% Stage 3 - The unpowered nosecone and Stage 2 remains.
    SM_mass=SM_nose+SM_body+SM_st2_str;
    dia=0.34;

end
return

```

2. SMFlight3.m

```

%% Script File
% Written by LT John A. Lukacs IV, Naval Postgraduate School, June 2006

% This script develops and tracks the flight path of the interceptor
% missile. For the first ten seconds it integrates a series of
% acceleration commands to simulate a vertical launch and tip over.
% Upon activation of the guidance law, it sends the known values to the
% guidance law and receives back the future time history of the optimal
% flight path. This script then implements that optimal path. It
% updates the final conditions and recalculates the optimal flight path
% at an (modifiable) interval of 10 seconds. The script calls
% SMPParams3.m, ZLDragC.m, and SStatmos.m

%% Variable List
% Acc_SM =index-based vector of acceleration values
% AllSM =index based vector of all interceptor values
% alt =altitude
% CD =drag coefficient
% count =counting variable to determine guidance law update
% interval
% dia =reference diameter (base diameter)
% dist =cumulative distance traveled
% Drag =total drag force
% Forces_SM=index-based vector of force values
% g =gravity force, based on WGS-84 value of
% gravitational attraction and altitude
% i =interval count
% m_i =interceptor mass
% Model_SM =index-based vector of internal values
% MV =interceptor speed in Mach (relative to local speed of
% sound)
% N1 =variable used to compare optimal vector length
% N2 =variable used to compare optimal vector length
% num_SM =number of iterations conducted (used for plotting)
% nx =axial acceleration command, body frame x
% nx_Op =index based vector of the optimal flight path values
% ny =axial acceleration command, body frame y
% ny_Op =index based vector of the optimal flight path values
% nz =axial acceleration command, body frame z
% nz_Op =index based vector of the optimal flight path values

```



```

% path      =returned time history of the optimal path
% Pos_SM    =index-based vector of position values
% press     =local atmospheric pressure
% psi       =heading angle
% psi_old   =heading angle (used in the time step)
% psi_Op    =index based vector of the optimal flight path values
% psidot    =rate of change of heading angle
% psidot_Op=index based vector of the optimal flight path values
% px        =x component of position
% px_old    =x component of position (used in the time step)
% px_Op     =index based vector of the optimal flight path values
% py        =y component of position
% py_old    =y component of position (used in the time step)
% py_Op     =index based vector of the optimal flight path values
% pz        =z component of position
% pz_old    =z component of position (used in the time step)
% pz_Op     =index based vector of the optimal flight path values
% q         =counting variable (used in another program)
% Re        =WGS-84 Earth's radius
% ro        =local atmospheric density
% spot      =counting variable (used for plotting)
% spot2     =counting variable (used for plotting)
% Sref      =planar reference area (for drag calculations)
% state     =the state of the interceptor
% t         =time
% target    =the state of the rocket
% temp      =local atmospheric temperature
% tgo       =time to go to intercept
% th        =flight path angle
% th_old    =flight path angle (used in the time step)
% th_Op     =index based vector of the optimal flight path values
% thdot     =rate of change of flight path angle
% thdot_Op  =index based vector of the optimal flight path values
% Thrust    =thrust generated by motor
% time_Op   =index based vector of the optimal flight path values
% time_SM   =index-based vector of time values
% update    =number of updates to the guidance law conducted
% V         =velocity of the interceptor
% V_old     =velocity of the interceptor (used in the time step)
% V_Op      =index based vector of the optimal flight path values
% Vdot      =rate of change of the velocity
% Vdot_Op   =index based vector of the optimal flight path values
% Vel_SM    =index-based vector of velocity values
% w         =counting variable (used in another program)

```

BRFlight3

```

global tgo q states xf xpf spot spot2 j path N1 update trys
global spot spot2 w Pos_BR Pos_SM

```

```

% Initialize Variables

```

```

t=0; dt=0.5;
i=0; ii=0; w=120; q=0; qq=0; rr=0;
count=30; update=0;
spot=13; spot2=81;
Re=6.378137e6;

```

```

tgo=85;
V=1;
psi=-130*pi/180;
th=90*pi/180;
V_old=V;
psi_old=psi;
th_old=th;

px=100000;
py=100000;
pz=Re;
px_old=px;
py_old=py;
pz_old=pz;
dist=0;

%% Flight Path
for i=1:1:1000
    t=t+dt;

% True APN Guidance
if t<10
    % Speed, Mach Number
    alt=norm([px;py;pz])-Re;
    if alt<86000
        [ro, press, temp]=Statmos(alt);
    else
        [ro, press, temp]=Statmos(86000);
    end
    MV=V/sqrt(1.402*287*temp);

    % Forces
    g=3.986004418e14/norm([px;py;pz])^2;
    [m_i,dia]=SMPParams3(t);
    [CD]=ZLDragC(MV,t);
    if t<6
        Thrust=206500;
        CD=CD(1);
    elseif t<20
        Thrust=95300;
        CD=CD(1);
    else
        Thrust=0;
        CD=CD(2);
    end
    Sref=pi*dia^2/4;
    Drag=ro*V^2*CD*Sref/2;
    nx=(Thrust-Drag)/m_i/g;

    % Guidance
    if t<=6
        psidot=0;
        thdot=0;
        ny=V/g*cos(th)*psidot;
        nz=V/g*thdot+cos(th);
    % Boost Phase Vertical Launch

```

```

else                                     % Boost Phase Pitch over
    psidot=0;
    thdot=-0.075;
    ny=V/g*cos(th)*psidot;
    nz=V/g*thdot+cos(th);
end

% Kinematics
Vdot=g*(nx-sin(th));
psidot=ny*g/V/cos(th);
thdot=g*(nz-cos(th))/V;

% Collect Variables
time_SM(i,1)=t;
Forces_SM(i,1)=nx;
Forces_SM(i,2)=ny;
Forces_SM(i,3)=nz;
Model_SM(i,1)=V;
Model_SM(i,2)=Vdot;
Model_SM(i,3)=th;
Model_SM(i,4)=thdot;
Model_SM(i,5)=psi;
Model_SM(i,6)=psidot;
Pos_SM(i,1)=px;
Pos_SM(i,2)=py;
Pos_SM(i,3)=pz;
Pos_SM(i,4)=dist;
Vel_SM(i,1)=V*cos(th)*cos(psi);
Vel_SM(i,2)=V*cos(th)*sin(psi);
Vel_SM(i,3)=V*sin(th);
Acc_SM(i,1)=Vdot*cos(th)*cos(psi)-V*cos(th)*sin(psi)*psidot...
    -V*sin(th)*cos(psi)*thdot;
Acc_SM(i,2)=Vdot*cos(th)*sin(psi)+V*cos(th)*cos(psi)*psidot...
    +V*sin(th)*sin(psi)*thdot;
Acc_SM(i,3)=Vdot*sin(th)+V*cos(th)*thdot;

% Time Step
V=V_old+Vdot*dt;
psi=psi_old+psidot*dt;
th=th_old+thdot*dt;

px=px_old+V*cos(th)*cos(psi)*dt;
py=py_old+V*cos(th)*sin(psi)*dt;
pz=pz_old+V*sin(th)*dt;

dist=(dist+abs(norm([px-px_old;py-py_old;pz-pz_old]))));

V_old=V;
psi_old=psi;
th_old=th;

px_old=px;
py_old=py;
pz_old=pz;

```

```

else                                                    % Optimal Guidance
    if count==30
        display('Starting SMGuidance Update')
        update=update+1;
        state=[px;py;pz;V;th;psi;Vdot;thdot;psidot];
        target=[Pos_BR(i+w,1);Pos_BR(i+w,2);Pos_BR(i+w,3);
                Vel_BR(i+w,1);Vel_BR(i+w,2);Vel_BR(i+w,3)];
        [path]=SMGuidance(t,state,target,i);
        if update==1;
            N1=length(path(:,1)); N2=N1;
        else
            N2=length(path(:,1));
        end
        % Identify Variables
        time_Op(:,update)=[path(:,1);zeros(N1-N2,1)];
        px_Op(:,update)=[path(:,2);zeros(N1-N2,1)];
        py_Op(:,update)=[path(:,3);zeros(N1-N2,1)];
        pz_Op(:,update)=[path(:,4);zeros(N1-N2,1)];
        V_Op(:,update)=[path(:,5);zeros(N1-N2,1)];
        th_Op(:,update)=[path(:,6);zeros(N1-N2,1)];
        psi_Op(:,update)=[path(:,7);zeros(N1-N2,1)];
        Vdot_Op(:,update)=[path(:,8);zeros(N1-N2,1)];
        thdot_Op(:,update)=[path(:,9);zeros(N1-N2,1)];
        psidot_Op(:,update)=[path(:,10);zeros(N1-N2,1)];
        nx_Op(:,update)=[path(:,11);zeros(N1-N2,1)];
        ny_Op(:,update)=[path(:,12);zeros(N1-N2,1)];
        nz_Op(:,update)=[path(:,13);zeros(N1-N2,1)];
        count=1;
    end

    t=time_Op(count,update);
    nx=nx_Op(count,update);
    ny=ny_Op(count,update);
    nz=nz_Op(count,update);
    V=V_Op(count,update);
    Vdot=Vdot_Op(count,update);
    th=th_Op(count,update);
    thdot=thdot_Op(count,update);
    psi=psi_Op(count,update);
    psidot=psidot_Op(count,update);
    px=px_Op(count,update);
    py=py_Op(count,update);
    pz=pz_Op(count,update);

    % Collect Variables
    time_SM(i,1)=t;
    Forces_SM(i,1)=nx;
    Forces_SM(i,2)=ny;
    Forces_SM(i,3)=nz;
    Model_SM(i,1)=V;
    Model_SM(i,2)=Vdot;
    Model_SM(i,3)=th;
    Model_SM(i,4)=thdot;
    Model_SM(i,5)=psi;
    Model_SM(i,6)=psidot;
    Pos_SM(i,1)=px;

```

```

    Pos_SM(i,2)=py;
    Pos_SM(i,3)=pz;
    Pos_SM(i,4)=dist;
    Vel_SM(i,1)=V*cos(th)*cos(psi);
    Vel_SM(i,2)=V*cos(th)*sin(psi);
    Vel_SM(i,3)=V*sin(th);
    Acc_SM(i,1)=Vdot*cos(th)*cos(psi)-V*cos(th)*sin(psi)*psidot...
        -V*sin(th)*cos(psi)*thdot;
    Acc_SM(i,2)=Vdot*cos(th)*sin(psi)+V*cos(th)*cos(psi)*psidot...
        +V*sin(th)*sin(psi)*thdot;
    Acc_SM(i,3)=Vdot*sin(th)+V*cos(th)*thdot;
    Update(i,1)=update;

    % Time Step
    count=count+1;
    dist=(dist+abs(norm([px-px_old;py-py_old;pz-pz_old])));
    V_old=V;
    psi_old=psi;
    th_old=th;
    px_old=px;
    py_old=py;
    pz_old=pz;
end

num_SM=length(time_SM);
end

AllSM= [time_SM Forces_SM Model_SM Pos_SM Vel_SM Acc_SM update];

```

C. 6DOF MODEL

1. BRDetails6.m

```

%% Script File
% Written by LT John A. Lukacs IV, Naval Postgraduate School, June 2006

% This script defines mass and fuel parameters of the Ballistic Rocket,
% as extracted from several open source materials relating to the
% North Korean Taepo-Dong II missile project.

% This script calculates the volume of structural material and
% therefore the weight of the structural components, assuming
% structural steel as the primary structural material. The process to
% determine the average thickness of the structure was an iterative
% process based on the known information of launch weight, some fuel
% data, payload, and burn times.

%% Variables List
% BR_fuel_p =density of rocket fuel
% BR_str_p =density of structural material
% BR_nose =total mass of nosecone section
% BR_stl_bt =burn time of stage 1 fuel
% BR_stl_fcr =consumption rate of stage 1 fuel
% BR_stl_str =total mass of stage 1 structural material
% BR_stl_tfm =total mass of stage 1 fuel

```

```

% BR_st2_bt =burn time of stage 2 fuel
% BR_st2_fcr =consumption rate of stage 2 fuel
% BR_st2_str =total mass of stage 2 structural material
% BR_st2_tfm =total mass of stage 2 fuel
% l =length, varies by component
% r =radius, varies by component
% ri =outer radius, varies by component
% ro =inner radius, varies by component
% tctc =total vs. chamber thrust comparison, used to
% extrapolate fuel consumption rate for stage 1
% from stage 2
% th =thickness of structural material
% V_nose_str =volume of nosecone structural material
% V_nose_str0=volume of nosecone structural material,
% intermediate value
% V_nose_str1=volume of nosecone structural material,
% intermediate value
% V_st1_str =volume of stage 1 structural material
% V_st2_str =volume of stage 2 structural material

global BR_str_p BR_fuel_p BR_nose BR_st2_str BR_st1_str
global BR_st2_tfm BR_st1_tfm BR_st1_fcr BR_st2_fcr

%% Structural Components
BR_str_p=7682;
th=.012;

%% Mass of Nosecone
l=2;
r=1.3/2;
V_nose_str0=pi*(1*((r^2+l^2)/(2*r))^2+l^3/3-(((r^2+l^2)/(2*r))-r)*...
((r^2+l^2)/(2*r))^2*asin(1/((r^2+l^2)/(2*r))));
l=2-th;
r=1.3/2-th;
V_nose_str1=pi*(1*((r^2+l^2)/(2*r))^2+l^3/3-(((r^2+l^2)/(2*r))-r)*...
((r^2+l^2)/(2*r))^2*asin(1/((r^2+l^2)/(2*r))));
V_nose_str=V_nose_str0-V_nose_str1;
BR_nose=250+V_nose_str*BR_str_p;

%% Mass of Stage 2
l=14;
r0=1.3/2;
ri=1.3/2-th;
V_st2_str=l*pi*(r0^2-ri^2);
BR_st2_str=V_st2_str*BR_str_p;

%% Mass of Stage 1
l=16;
r0=2.2/2;
ri=2.2/2-th;
V_st1_str=l*pi*(r0^2-ri^2);
BR_st1_str=V_st1_str*BR_str_p;

%% Fuel Components
BR_fuel_p=801.164+1544.9/4.05;

```

```

% Fuel mass, rate, burntime
BR_st2_tfm=12912;
BR_st2_bt=110;
BR_st2_fcr=BR_st2_tfm/BR_st2_bt;
tctc=103000/30432;
BR_st1_fcr=BR_st2_fcr*tctc;
BR_st1_bt=125;

BR_st1_tfm=BR_st1_fcr*BR_st1_bt;

```

2. BRParams6.m

```

function [J,BR_mass,dia,length]=BRParams6(t)
% Written by LT John A. Lukacs IV, Naval Postgraduate School, June 2006

% This function calculates the J Matrix and Mass of the rocket,
% assuming a cruciform rocket in two stages plus an unpowered nosecone
% stage. This function also returns the reference (base) diameter of
% the missile.

%% Notes:
% All CGs are measured from the tip of the nosecone.
% The rocket is divided into five components: the nosecone and payload,
% stage one structure, stage one fuel, stage 2 structure, stage 2 fuel.
% Liquid fuel is assumed to remain at the rear of the fuel tanks. Both
% stages utilize the same fuel. Fuel is consumed at a constant rate.
% The first stage last 130 seconds, the second stage lasts an
% additional 110 seconds. The stage separates upon completion.
% No Parallel axis theorem is required for Jx due to symmetry. Parallel
% axis theorem is required from CG for Jy and Jz.

% Variable List
% BR_fuel_L      =Length of remaining fuel in the stage
% BR_fuel_p      =density of rocket fuel
% BR_mass        =total rocket mass
% BR_nose        =total mass of nosecone section
% BR_str_p       =density of structural material
% BR_st1_fcr     =consumption rate of stage 1 fuel
% BR_st1_fuel    =remaining stage 1 fuel based on time and
%                consumption rate
% BR_st1_str     =total mass of stage 1 structural material
% BR_st1_tfm     =total mass of stage 1 fuel
% BR_st2_fcr     =consumption rate of stage 2 fuel
% BR_st2_fuel    =remaining stage 2 fuel based on time and
%                consumption rate
% BR_st2_str     =total mass of stage 2 structural material
% BR_st2_tfm     =total mass of stage 2 fuel
% CG             =total rocket center of gravity
% CG_nose        =nosecone center of gravity
% CG_st1         =stage 1 center of gravity
% CG_st2         =stage 2 center of gravity
% dia           =reference diameter, base diameter
% J             =Matrix of moment of inertia
% Jx            =total rocket moment of inertia, x-axis

```

```

% Jx_nose      =nosecone moment of inertia, x-axis
% Jx_st1_fuel  =stage 1 fuel moment of inertia, x-axis
% Jx_st1_str   =stage 1 structure moment of inertia, x-axis
% Jx_st2_fuel  =stage 2 fuel moment of inertia, x-axis
% Jx_st2_str   =stage 2 structure moment of inertia, x-axis
% Jy          =total rocket moment of inertia, y-axis
% Jy_nose     =nosecone moment of inertia, y-axis
% Jy_st1_fuel =stage 1 fuel moment of inertia, y-axis
% Jy_st1_str  =stage 1 structure moment of inertia, y-axis
% Jy_st2_fuel =stage 2 fuel moment of inertia, y-axis
% Jy_st2_str  =stage 2 structure moment of inertia, y-axis
% Jz         =total rocket moment of inertia, z-axis
% t         =time

global BR_str_p BR_fuel_p BR_nose BR_st2_str BR_st1_str
global BR_st2_tfm BR_st1_tfm BR_st1_fcr BR_st2_fcr

if t<130
% Stage 1 - Stage 1 Fuel is consumed; Stage 2 Fuel is not used.
BR_st1_fuel=BR_st1_tfm-BR_st1_fcr*t;
BR_fuel_L=BR_st1_fuel/(BR_fuel_p*pi*1.0^2);
CG_nose=BR_nose*10/8;
CG_st1=BR_st1_str*24+BR_st1_fuel*(32-BR_fuel_L);
CG_st2=BR_st2_str*9+BR_st2_tfm*9;
BR_mass=BR_nose+BR_st1_str+BR_st1_fuel+BR_st2_str+BR_st2_tfm;
CG=(CG_nose+CG_st1+CG_st2)/BR_mass;

FF=(BR_st1_fuel+BR_st2_tfm)/BR_mass;

Jx_nose=BR_nose*3*(0.65^2)/10;
Jx_st1_str=BR_st1_str*(1.1^2+1.025^2)/2;
Jx_st1_fuel=BR_st1_fuel*(1.025^2)/2;
Jx_st2_str=BR_st2_str*(0.65^2+0.575^2)/2;
Jx_st2_fuel=BR_st2_tfm*(0.575^2)/2;
Jx=Jx_nose+Jx_st1_str+Jx_st1_fuel+Jx_st2_str+Jx_st2_fuel;

Jy_nose=BR_nose*3*(.25*1.3^2+2^2)+BR_nose*(CG-10/8)^2;
Jy_st1_str=BR_st1_str*(16^2/12+(1.1^2+1.025^2)/4)+ ...
BR_st1_str*(CG-24)^2;
Jy_st1_fuel=BR_st1_fuel*(1.025^2/4 + BR_fuel_L^2/12) + ...
BR_st1_fuel*(CG-(32-BR_fuel_L/12))^2;
Jy_st2_str=BR_st2_str*(14^2/12+(0.65^2+0.575^2)/4)+ ...
BR_st2_str*(CG-9)^2;
Jy_st2_fuel=BR_st2_tfm*(0.575^2/4+7^2/12) + ...
BR_st2_tfm*(CG-9)^2;
Jy=Jy_nose+Jy_st1_str+Jy_st1_fuel+Jy_st2_str+Jy_st2_fuel;
Jz=Jy;

dia=2.2;
length=2+14+16;

elseif t<240;
% Stage 2 - Stage 1 has separated; Stage 2 Fuel is consumed.
BR_st2_fuel=BR_st2_tfm-BR_st2_fcr*(t-130);
BR_fuel_L=BR_st2_fuel/(BR_fuel_p*pi*0.575^2);

```



```

CG_nose=BR_nose*10/8;
CG_st2=BR_st2_str*9+BR_st2_fuel*(14-BR_fuel_L);
BR_mass=BR_nose+BR_st2_str+BR_st2_fuel;
CG=(CG_nose+CG_st2)/BR_mass;

Jx_nose=BR_nose*3*(0.65^2)/10;
Jx_st2_str=BR_st2_str*(0.65^2+0.575^2)/2;
Jx_st2_fuel=BR_st2_fuel*(0.575^2)/2;
Jx=Jx_nose+Jx_st2_str+Jx_st2_fuel;

Jy_nose=BR_nose*3*(1.3^2/4+2^2)+BR_nose*(CG-10/8)^2;
Jy_st2_str=BR_st2_str*(14^2/12+(0.65^2+0.575^2)/4)+ ...
            BR_st2_str*(CG-9)^2;
Jy_st2_fuel=BR_st2_fuel*(0.575^2/4+BR_fuel_L^2/12)+ ...
            BR_st2_fuel*(CG-(16-BR_fuel_L/2))^2;
Jy=Jy_nose+Jy_st2_str+Jy_st2_fuel;
Jz=Jy;

dia=1.3;
length=2+14;
else
% Stage 3 - Stage 2 has separated; only the unpowered nosecone remains.
BR_fuel_L=0;
CG_nose=BR_nose*10/8;
BR_mass=BR_nose;
CG=(CG_nose)/BR_mass;

Jx=BR_nose*3*(0.65^2)/10;
Jy=BR_nose*3*(1.3^2/4+2^2)+BR_nose*(CG-10/8)^2;
Jz=Jy;

dia=1.3;
length=2;

end

%% Combining the results into output variables.
J=[Jx  0  0;
   0  Jy  0;
   0  0  Jz];

return

```

3. BRFlight6.m

```
function [udot]=BRFlight6(u)
% Written by LT John A. Lukacs IV, Naval Postgraduate School, June 2006

% This script integrates the position, velocity, and acceleration
% values at each time step to determine the flight path of a ballistic
% missile in a gravity turn. The script calls BRParams6.m, ZLDragC.m,
% and SAtmos.m

% Variable List:
% [ACoeff] =Vector of 13 coefficients returned from Aerocoeff.m
% Aa      =angle of attack
% As      =sideslip angle
% Cd      =aerodynamic coefficient
% Cl      =aerodynamic coefficient
% Cm      =aerodynamic coefficient
% CN      =aerodynamic coefficient
% Cn      =aerodynamic coefficient
% CY      =aerodynamic coefficient
% delta_h =iterative value for determination of altitude
% dia     =reference diameter, base diameter
% dP      =Pitch control surface deflection
% dPdot   =Pitch control surface deflection derivative
% Drag    =Total drag force
% dY      =Yaw control surface deflection
% dYdot   =Yaw control surface deflection derivative
% egm     =intermediate value for gravity calculations
% Force   =Total force on the center of mass
% g       =Gravity
% h       =Altitude above the Earth surface
% J       =Mass Moment of Inertia Matrix
% latgc   =Geocentric Latitude
% latgd   =Geodetic Latitude
% lm_g    =Celestial Longitude
% Mach    =Ballistic Rocket speed in Mach
% Mspd    =Local Speed of Sound
% N       =iterative value for determination of altitude
% Nh      =iterative value for determination of altitude
% P       =Roll Rate
% p       =Ballistic Rocket Position vector, [px;py;pz]
% pdot    =Ballistic Rocket Position derivative vector
% phi     =Euler Roll wrt ECEF
% press   =atmospheric pressure
% psy     =Euler Yaw wrt ECEF
% px      =X Position
% py      =Y Position
% pz      =Z Position
% Q       =Pitch Rate
% q       =quaternion vector
% q0      =Quaternion's 0th component
% q1      =Quaternion's 1st component
% q2      =Quaternion's 2nd component
% q3      =Quaternion's 3rd component
% qdot    =Quaternion derivative
% qnorm   =Normalization of Quaternion
% Qro     =Atmospheric density
```

```

% R      =Yaw Rate
% R_b2e  =Rotation Matrix
% R_i2b  =Rotation Matrix
% R_i2e  =Rotation Matrix
% R_n2b  =Rotation Matrix
% Rm     =Ballistic Rocket current mass
% ro     =local atmospheric density
% rp     =iterative value for gravity
% speed  =velocity of the rocket in m/s
% t      =time
% theta  =Euler Pitch wrt ECEF
% temp   =local atmospheric temperature
% Thrust =thrust vector
% Torque =torque vector
% u      =input vector
% udot   =output vector, to be integrated
% vb     =velocity vector
% vdot   =velocity vector derivative
% vx     =X Velocity
% vy     =Y Velocity
% vz     =Z Velocity
% wb     =angular velocity
% Wbwi   =cross product matrix
% wdot   =angular velocity derivative
% Wewi   =cross product matrix
% Wq     =cross product matrix

global lLong Re WzE Eps2 Gravity R_e2n runcount dq dr

% Variable Definitions and Quaternion Normalization
px=u(1);
py=u(2);
pz=u(3);
vx=u(4);
vy=u(5);
vz=u(6);
P =u(7);
Q =u(8);
R =u(9);
qnorm=norm(u(10:13),2);
q0=u(10)/qnorm;
q1=u(11)/qnorm;
q2=u(12)/qnorm;
q3=u(13)/qnorm;
t =u(14);
dq=u(15);
dr=u(16);

% Vector Definitions
p =[px;py;pz];
vb=[vx;vy;vz];
wb=[P;Q;R];
q =[q0;q1;q2;q3];

% Geocentric Latitude and Celestial Longitude from [p]
latgc=atan(pz/sqrt(px^2+py^2));

```

```

lm_g=(atan2(py,px)+lLong-WzE*t);
if lm_g > pi
    lm_g=lm_g-pi;
elseif lm_g < -pi
    lm_g=lm_g+pi;
end

% Geodetic Latitude and Altitude about the Earth's Geoid from [p]
h=0; N=Re; Nh=N+h; delta_h=Re;
while abs(delta_h) > .1
    latgd=atan(pz/sqrt(px^2+py^2)/(1-N*Eps2/Nh));
    N=Re/sqrt(1-Eps2*sin(latgd)^2);
    Nh=sqrt(px^2+py^2)/cos(latgd);
    delta_h=Nh-N-h;
    h=h+delta_h;
end

% Gravity, Atmosphere from EGM1996
rp=norm(p,2);
egm=diag([1;1;3]);
g=-Gravity*3.986004418e14/rp^2*(eye(3)+1.5*1.0826267e-3*(Re/rp)^2*...
    (egm-5*(pz/rp)^2*eye(3)))*p/rp;
[ro,press,temp]=STatmos(h);

% Speed, Mach Number, Angles
speed=norm(vb,2);
Mspd=sqrt(1.402*287*temp);
Mach=speed/Mspd;

Aa=atan2(vz,vx);
As=atan2(vy,speed);
if As<1e-3
    As=0;
end

% Moment Matrix, Aerodynamic Coefficients
[J,Rm,dia,length]=BRParams(t);
CD=ZLDragC(Mach,t);
Sref=pi*dia^2/4;
Drag=ro*speed*vb*CD*Sref/2;
Qro=0.5*ro*speed^2;

[CN_Aa Cm_Aa CY_As Cn_As Cl_dp CY_dp Cn_dp...
    Cl_dr CY_dr Cn_dr Cl_As CN_dq Cm_dq]=AeroCoeff(Aa,h,dq,t);

CY=CY_As*As+CY_dr*dr;
CN=CN_Aa*Aa+CN_dq*dq;
Cl=Cl_As*As+Cl_dr*dr+dia/2*speed*[-0.5*P];
Cm=Cm_Aa*Aa+Cm_dq*dq+dia/2*speed*[-0.5*Q];
Cn=Cn_As*As+Cn_dr*dr+dia/2*speed*[-0.5*R];

% Force, Torque
if t < 130
    Thrust=[103500*9.81;0;0];
elseif t < 240

```

```

    Thrust=[26200*9.81;0;0];
else
    Thrust=[0;0;0];
end

Force=Sref*Qro.*[0;CY;-CN]+Thrust-Drag;
Torque=Sref*Qro.*[dia*Cl;100*length*Cm;dia*Cn];

% Quaternion from ECI to Body Centered
R_i2b=[q0^2+q1^2-q2^2-q3^2  2*(q1*q2+q0*q3)  2*(q1*q3-q0*q2);
        2*(q1*q2-q0*q3)    q0^2-q1^2+q2^2-q3^2  2*(q2*q3+q0*q1);
        2*(q1*q3+q0*q2)    2*(q2*q3-q0*q1)    q0^2-q1^2-q2^2+q3^2];

% Rotation from ECI to ECEF and from {b} to ECEF
R_i2e=[ cos(lLong+WzE*t) sin(lLong+WzE*t) 0;
        -sin(lLong+WzE*t) cos(lLong+WzE*t) 0;
         0 0 1];
R_b2e=R_i2e*R_i2b';
R_n2b=(R_e2n*R_b2e)';

% Euler Angles wrt {n}
phi=atan2(R_n2b(2,3),R_n2b(3,3));
theta=asin(-R_n2b(1,3));
psy=atan2(R_n2b(1,2),R_n2b(1,1));

% Cross-Product matrices
Wewi=[ 0 -WzE 0;
        WzE 0 0;
        0 0 0];
Wbwi=[0 -R Q;
        R 0 -P;
        -Q P 0];
Wq=[0 -P -Q -R;
     P 0 R -Q;
     Q -R 0 P;
     R Q -P 0];

% State Equations
pdot=Wewi*p+R_i2b'*vb;
vdot=R_i2b*(g-Wewi^2*p)-(Wbwi+2*R_i2b*Wewi*R_i2b')*vb+Force/Rm;
wdot=inv(J)*Torque-inv(J)*Wbwi*J*wb;
qdot=Wq*q/2;

for ind=1:3
    if wdot(ind)<1e-5
        wdot(ind)=0;
    end
end

% Output Vector udot
udot=[pdot;vdot;wdot;qdot;
       phi;theta;psy;Aa;As;speed;
       latgd;lm_g;h];

```

3. SMDetails6.m

```
%% Script File
% Written by LT John A. Lukacs IV, Naval Postgraduate School, June 2006

% This script defines mass and fuel parameters of the SM-6 interceptor
% missile, as extracted from several open source materials relating to
% the Raytheon SM-6 ERAAW interceptor missile project.

% This script calculates the volume of structural material and
% therefore weight of the structural components, assuming structural
% steel as the primary structural material. The process to determine
% the average thickness of the structure was an iterative process based
% on the known information of launch weight, some fuel data, payload,
% and burn times.

%% Variables List
% l          =length, varies by component
% p_SM_st1_fuel=density of stage 1 rocket fuel
% p_SM_st2_fuel=density of stage 2 rocket fuel
% p_SMstr    =density of structural material
% r          =radius, varies by component
% r0        =outer radius, varies by component
% ri        =inner radius, varies by component
% SM_body   =total mass of body section
% SM_nose   =total mass of nosecone section
% SM_st1_fr =fuel consumption rate of stagel
% SM_st1_str =total mass of stage 1 structural material
% SM_st1_tfm =total fuel mass of stage 1
% SM_st2_fr =fuel consumption rate of stage2
% SM_st2_str =total mass of stage 2 structural material
% SM_st2_tfm =total fuel mass of stage 2
% th        =thickness of structural material
% V_body    =volume of body structural material
% V_nose_str =volume of nosecone structural material
% V_nose_str0 =volume of nosecone structural material,
%             intermediate value
% V_nose_str1 =volume of nosecone structural material,
%             intermediate value
% V_st1_fuel =volume of stage 1 fuel
% V_st1_str  =volume of stage 1 structural material
% V_st2_fuel =volume of stage 2 fuel
% V_st2_str  =volume of stage 2 structural material

global p_SMstr p_SM_st2_fuel p_SM_st1_fuel SM_nose SM_st2_str
global SM_st1_str SM_body SM_st2_tfm SM_st1_tfm SM_st1_fr SM_st2_fr

%% Structural Components
p_SMstr=7682;
th=.007;

% Mass of Nosecone
l=.8255;
r=0.34/2;
```

```

V_nose_str0=pi*(1*((r^2+l^2)/(2*r))^2+l^3/3-(((r^2+l^2)/(2*r))-r)*...
((r^2+l^2)/(2*r))^2*asin(1/((r^2+l^2)/(2*r))));
l=.8255-th;
r=0.34/2-th;
V_nose_str1=pi*(1*((r^2+l^2)/(2*r))^2+l^3/3-(((r^2+l^2)/(2*r))-r)*...
((r^2+l^2)/(2*r))^2*asin(1/((r^2+l^2)/(2*r))));
V_nose_str=V_nose_str0-V_nose_str1;
SM_nose=V_nose_str*p_SMstr;

% Mass of Body/Warhead Section
l=3.729-2.88;
r0=0.34/2;
ri=0.34/2-th;
V_body=l*pi*(r0^2-ri^2);
SM_body=V_body*p_SMstr+115;

% Mass of Stage 2 (Mk104 Engine)
l=2.88;
r0=0.34/2;
ri=0.34/2-th;
V_st2_str=l*pi*(r0^2-ri^2);
SM_st2_str=V_st2_str*p_SMstr;

% Mass of Stage 1 (Mk72 Booster)
l=1.72;
r0=0.53/2;
ri=0.53/2-th;
V_st1_str=l*pi*(r0^2-ri^2);
SM_st1_str=V_st1_str*p_SMstr;

%% Fuel Components
% Stage 2
V_st2_fuel=0.70*l*pi*ri^2;
SM_st2_tfm=360;
p_SM_st2_fuel=SM_st2_tfm/V_st2_fuel;
SM_st2_fr=360/20;

% Stage 1
V_st1_fuel=0.70*l*pi*ri^2;
p_SM_st1_fuel=1860;
SM_st1_tfm=468;
SM_st1_fr=468/6;

```

5. SMParams6.m

```
function [J,SM_mass,C]=SMParams6(t)
% Written by LT John A. Lukacs IV, Naval Postgraduate School, June 2006

% This function calculates the J Matrix and Mass of the interceptor,
% assuming a cruciform rocket in two stages to intercept. This
% function also returns the reference (base) diameter of the missile.

%% Notes:
% All CGs are measured from the tip of the nosecone.
% The rocket is divided into five components: the nosecone and payload,
% stage one structure, stage one fuel, stage 2 structure, stage 2 fuel.
% Solid fuel is assumed to burn from the centerline radially outward.
% A constant burn profile is assumed, such as a star grain produces.
% See description in SMDetail.m for specific derivation of reasons.
% The first stage last 6 seconds, the second stage lasts an additional
% 15 seconds. Stage 1 (booster) separates upon completion. Stage 2
% does not separate after completion.

% Variable List:
% SM_mass      =total rocket mass
% SM_nose      =total mass of nosecone section
% SM_st1_fcr    =consumption rate of stage 1 fuel
% SM_st1_fuel   =remaining stage 1 fuel based on time and
%               consumption rate
% SM_st1_str    =total mass of stage 1 structural material
% SM_st1_tfm    =total mass of stage 1 fuel
% SM_st2_fcr    =consumption rate of stage 2 fuel
% SM_st2_fuel   =remaining stage 2 fuel based on time and
%               consumption rate
% SM_st2_str    =total mass of stage 2 structural material
% SM_st2_tfm    =total mass of stage 2 fuel
% CG            =total rocket center of gravity
% CG_nose      =nosecone center of gravity
% CG_st1       =stage 1 center of gravity
% CG_st2       =stage 2 center of gravity
% dia          =reference diameter, base diameter
% J            =Matrix of moment of inertia
% Jx           =total rocket moment of inertia, x-axis
% Jx_nose      =nosecone moment of inertia, x-axis
% Jx_st1_fuel  =stage 1 fuel moment of inertia, x-axis
% Jx_st1_str   =stage 1 structure moment of inertia, x-axis
% Jx_st2_fuel  =stage 2 fuel moment of inertia, x-axis
% Jx_st2_str   =stage 2 structure moment of inertia, x-axis
% Jy           =total rocket moment of inertia, y-axis
% Jy_nose      =nosecone moment of inertia, y-axis
% Jy_st1_fuel  =stage 1 fuel moment of inertia, y-axis
% Jy_st1_str   =stage 1 structure moment of inertia, y-axis
% Jy_st2_fuel  =stage 2 fuel moment of inertia, y-axis
% Jy_st2_str   =stage 2 structure moment of inertia, y-axis
% Jz           =total rocket moment of inertia, z-axis
% L_SMfuel     =Length of remaining fuel in the stage
% p_SMfuel     =density of rocket fuel
% p_SMstr      =density of structural material
```



```

% t          =time

global p_SMstr p_SM_st1_fuel p_SM_st2_fuel SM_nose SM_st2_str
global SM_st1_str SM_body SM_st2_fuel_mass SM_st1_fuel_mass
global SM_st1_fuel_rate SM_st2_fuel_rate

% Moment Matrix
if t<6
% Stage 1 - Stage 1 Fuel is consumed; Stage 2 Fuel is not used.
SM_st1_fuel=SM_st1_fuel_mass-SM_st1_fuel_rate*t;
ri=sqrt(0.258^2-SM_st1_fuel/(p_SM_st1_fuel*1.72*pi));

CG_nose=3/4*0.8255*SM_nose;
CG_body=(0.8255+0.8445/2)*SM_body;
CG_st2=(1.67+2.88/2)*(SM_st2_str+SM_st2_fuel_mass);
CG_st1=(4.55+1.72/2)*(SM_st1_str+SM_st1_fuel);

SM_mass=SM_nose+SM_body+SM_st2_str+SM_st2_fuel_mass+SM_st1_str+...
SM_st1_fuel;
CG=(CG_nose+CG_body+CG_st2+CG_st1)/SM_mass;

Jx_nose=SM_nose*3/10*0.17^2;
Jx_body=SM_body*0.17^2/2;
Jx_st2_str=SM_st2_str*(0.17^2+0.163^2)/2;
Jx_st2_fuel=SM_st2_fuel_mass*(0.163^2+0.091^2)/2;
Jx_st1_str=SM_st1_str*(0.265^2+0.258^2)/2;
Jx_st1_fuel=SM_st1_fuel*(0.258^2+0.141^2)/2;
Jx=Jx_nose+Jx_body+Jx_st2_str+Jx_st2_fuel+Jx_st1_str+Jx_st1_fuel;

Jy_nose=SM_nose*(12*0.17^2+3*0.8255^2)/80+SM_nose*(CG-3*0.8255/4)^2;
Jy_body=SM_body*(0.17^2/4+0.8445^2/12)+SM_body*...
(CG-(0.8255+0.8445/2))^2;
Jy_st2_str=SM_st2_str*((0.17^2+0.163^2)/4+2.88^2/12)+SM_st2_str*...
(CG-(1.67+2.88/2))^2;
Jy_st2_fuel=SM_st2_fuel_mass*((0.163^2+0.091^2)/4+2.88^2/12)+...
SM_st2_fuel_mass*(CG-(1.67+2.88/2))^2;
Jy_st1_str=SM_st1_str*((0.265^2+0.258^2)/4+2.88^2/12)+SM_st1_str*...
(CG-(4.55+1.72/2))^2;
Jy_st1_fuel=SM_st1_fuel*((0.258^2+0.141^2)/4+2.88^2/12)+...
SM_st1_fuel*(CG-(4.55+1.72/2))^2;
Jy=Jy_nose+Jy_body+Jy_st2_str+Jy_st2_fuel+Jy_st1_str+Jy_st1_fuel;
Jz=Jy;

dia=0.53;

elseif t<26
% Stage 2 - Stage 1 has separated; Stage 2 Fuel is consumed.
SM_st2_fuel=SM_st2_fuel_mass-SM_st2_fuel_rate*t;
ri=sqrt(0.17^2-SM_st2_fuel/(p_SM_st2_fuel*2.88*pi));

CG_nose=3/4*0.8255*SM_nose;
CG_body=(0.8255+0.8445/2)*SM_body;
CG_st2 =(1.67+2.88/2)*(SM_st2_str+SM_st2_fuel);

SM_mass=SM_nose+SM_body+SM_st2_str+SM_st2_fuel;

```

```

CG=(CG_nose+CG_body+CG_st2)/SM_mass;

Jx_nose=SM_nose*3/10*0.17^2;
Jx_body=SM_body*0.17^2/2;
Jx_st2_str=SM_st2_str*(0.17^2+0.163^2)/2;
Jx_st2_fuel=SM_st2_fuel*(0.163^2+0.091^2)/2;
Jx=Jx_nose+Jx_body+Jx_st2_str+Jx_st2_fuel;

Jy_nose=SM_nose*(12*0.17^2+3*0.8255^2)/80+SM_nose*...
    (CG-3*0.8255/4)^2;
Jy_body=SM_body*(0.17^2/4+0.8445^2/12)+SM_body*...
    (CG-(0.8255+0.8445/2))^2;
Jy_st2_str=SM_st2_str*((0.17^2+0.163^2)/4+2.88^2/12)+...
    SM_st2_str*(CG-(1.67+2.88/2))^2;
Jy_st2_fuel=SM_st2_fuel*((0.163^2+0.091^2)/4+2.88^2/12)+...
    SM_st2_fuel*(CG-(1.67+2.88/2))^2;
Jy=Jy_nose+Jy_body+Jy_st2_str+Jy_st2_fuel;
Jz=Jy;

dia=0.34;

else
% Stage 3 - Stage 2 has not separated; entire missile is unpowered.
CG_nose=3/4*0.8255*SM_nose;
CG_body=(0.8255+0.8445/2)*SM_body;
CG_st2 =(1.67+2.88/2)*SM_st2_str;

SM_mass=SM_nose+SM_body+SM_st2_str;
CG=(CG_nose+CG_body+CG_st2)/SM_mass;

Jx_nose=SM_nose*3/10*0.17^2;
Jx_body=SM_body*0.17^2/2;
Jx_st2_str=SM_st2_str*(0.17^2+0.163^2)/2;
Jx=Jx_nose+Jx_body+Jx_st2_str;

Jy_nose=SM_nose*(12*0.17^2+3*0.8255^2)/80+SM_nose*...
    (CG-3*0.8255/4)^2;
Jy_body=SM_body*(0.17^2/4+0.8445^2/12)+SM_body*...
    (CG-(0.8255+0.8445/2))^2;
Jy_st2_str=SM_st2_str*((0.17^2+0.163^2)/4+2.88^2/12)+SM_st2_str*...
    (CG-(1.67+2.88/2))^2;
Jy=Jy_nose+Jy_body+Jy_st2_str;
Jz=Jy;

dia=0.34;

end

% Combining the results into output variables.
J=[Jx  0  0;
   0  Jy  0;
   0  0  Jz];

return

```

6. SMFlight6.m

```
function [udot]=SMFlight6(u)
% Written by LT John A. Lukacs IV, Naval Postgraduate School, June 2006

% This script integrates the position, velocity, and acceleration
values
% at each time step to determine the flight path of a SM-6 missile
% under guidance. The script calls SMParams6.m, ZLDragC.m, and
% SAtmos.m

% Variable List:
% [ACoeff] =Vector of 13 coefficients returned from Aerocoeff.m
% Aa      =angle of attack
% As      =sideslip angle
% Cd      =aerodynamic coefficient
% Cl      =aerodynamic coefficient
% Cm      =aerodynamic coefficient
% CN      =aerodynamic coefficient
% Cn      =aerodynamic coefficient
% CY      =aerodynamic coefficient
% delta_h =iterative value for determination of altitude
% dia     =reference diameter, base diameter
% dP      =Pitch control surface deflection
% dPdot   =Pitch control surface deflection derivative
% Drag    =Total drag force
% dY      =Yaw control surface deflection
% dYdot   =Yaw control surface deflection derivative
% egm     =intermediate value for gravity calculations
% Force   =Total force on the center of mass
% g       =Gravity
% h       =Altitude above the Earth surface
% J       =Mass Moment of Inertia Matrix
% latgc   =Geocentric Latitude
% latgd   =Geodetic Latitude
% lm_g    =Celestial Longitude
% Mach    =speed in Mach
% Mspd    =Local Speed of Sound
% N       =iterative value for determination of altitude
% Nh      =iterative value for determination of altitude
% P       =Roll Rate
% p       =Position vector, [px; py; pz]
% pdot    =Position derivative vector
% phi     =Euler Roll wrt ECEF
% press   =atmospheric pressure
% psy     =Euler Yaw wrt ECEF
% px      =X Position
% py      =Y Position
% pz      =Z Position
% Q       =Pitch Rate
% q       =quaternion vector
% q0      =Quaternion's 0th component
% q1      =Quaternion's 1st component
% q2      =Quaternion's 2nd component
% q3      =Quaternion's 3rd component
% qdot    =Quaternion derivative
% qnorm   =Normalization of Quaternion
```

```

% Qro      =Atmospheric density
% R        =Yaw Rate
% R_b2e    =Rotation Matrix
% R_i2b    =Rotation Matrix
% R_i2e    =Rotation Matrix
% R_n2b    =Rotation Matrix
% Rm       =current mass
% ro       =local atmospheric density
% rp       =iterative value for gravity
% speed    =velocity in m/s
% t        =time
% theta    =Euler Pitch wrt ECEF
% temp     =local atmospheric temperature
% Thrust   =thrust vector
% Torque   =torque vector
% u        =input vector
% udot     =output vector, to be integrated
% vb       =velocity vector
% vdot     =velocity vector derivative
% vx       =X Velocity
% vy       =Y Velocity
% vz       =Z Velocity
% wb       =angular velocity
% Wbwi     =cross product matrix
% wdot     =angular velocity derivative
% Wewi     =cross product matrix
% Wq       =cross product matrix

global lLong Re WzE Eps2 Gravity R_e2n runcount dq dr

% Variable Definitions and Quaternion Normalization
px=u(1);
py=u(2);
pz=u(3);
vx=u(4);
vy=u(5);
vz=u(6);
P =u(7);
Q =u(8);
R =u(9);
qnorm=norm(u(10:13),2);
q0=u(10)/qnorm;
q1=u(11)/qnorm;
q2=u(12)/qnorm;
q3=u(13)/qnorm;
t =u(14);
dq=u(15);
dr=u(16);

% Vector Definitions
p =[px;py;pz];
vb=[vx;vy;vz];
wb=[P;Q;R];
q =[q0;q1;q2;q3];

% Geocentric Latitude and Celestial Longitude from [p]

```

```

latgc=atan(pz/sqrt(px^2+py^2));
lm_g=(atan2(py,px)+lLong-WzE*t);
if lm_g > pi
    lm_g=lm_g-pi;
elseif lm_g < -pi
    lm_g=lm_g+pi;
end

% Geodetic Latitude and Altitude about the Earth's Geoid from [p]
h=0; N=Re; Nh=N+h; delta_h=Re;
while abs(delta_h) > .1
    latgd=atan(pz/sqrt(px^2+py^2)/(1-N*Eps2/Nh));
    N=Re/sqrt(1-Eps2*sin(latgd)^2);
    Nh=sqrt(px^2+py^2)/cos(latgd);
    delta_h=Nh-N-h;
    h=h+delta_h;
end

% Gravity, Atmosphere from EGM1996
rp=norm(p,2);
egm=diag([1;1;3]);
g=-Gravity*3.986004418e14/rp^2*(eye(3)+1.5*1.0826267e-...
    3*(Re/rp)^2*(egm-5*(pz/rp)^2*eye(3)))*p/rp;
[ro,press,temp]=SStatmos(h);

% Speed, Mach Number, Angles
speed=norm(vb,2);
Mspd=sqrt(1.402*287*temp);
Mach=speed/Mspd;

Aa=atan2(vz,vx);
As=atan2(vy,speed);
if As<1e-3
    As=0;
end

% Moment Matrix, Aerodynamic Coefficients
[J,Rm,dia,length]=SMPParams6(t);
CD=ZLDragC(Mach,t);
Sref=pi*dia^2/4;
Drag=ro*speed*vb*CD*Sref/2;
Qro=0.5*ro*speed^2;

[CN_Aa Cm_Aa CY_As Cn_As Cl_dp CY_dp Cn_dp...
    Cl_dr CY_dr Cn_dr Cl_As CN_dq Cm_dq]=AeroCoeff(Aa,h,dq,t);

CY=CY_As*As+CY_dr*dr;
CN=CN_Aa*Aa+CN_dq*dq;
Cl=Cl_As*As+Cl_dr*dr+dia/2*speed*[-0.5*P];
Cm=Cm_Aa*Aa+Cm_dq*dq+dia/2*speed*[-0.5*Q];
Cn=Cn_As*As+Cn_dr*dr+dia/2*speed*[-0.5*R];

% Force, Torque
if t < 130
    Thrust=[206500;0;0];

```

```

elseif t < 240
    Thrust=[95300;0;0];
else
    Thrust=[0;0;0];
end

Force=Sref*Qro.*[0;CY;-CN]+Thrust-Drag;
Torque=Sref*Qro.*[dia*Cl;100*length*Cm;dia*Cn];

% Quaternion from ECI to Body Centered
R_i2b=[q0^2+q1^2-q2^2-q3^2  2*(q1*q2+q0*q3)  2*(q1*q3-q0*q2);
       2*(q1*q2-q0*q3)    q0^2-q1^2+q2^2-q3^2  2*(q2*q3+q0*q1);
       2*(q1*q3+q0*q2)    2*(q2*q3-q0*q1)    q0^2-q1^2-q2^2+q3^2];

% Rotation from ECI to ECEF and from {b} to ECEF
R_i2e=[ cos(lLong+WzE*t) sin(lLong+WzE*t) 0;
       -sin(lLong+WzE*t) cos(lLong+WzE*t) 0;
         0 0 1];
R_b2e=R_i2e*R_i2b';
R_n2b=(R_e2n*R_b2e)';

% Euler Angles wrt {n}
phi=atan2(R_n2b(2,3),R_n2b(3,3));
theta=asin(-R_n2b(1,3));
psy=atan2(R_n2b(1,2),R_n2b(1,1));

% Cross-Product matrices
Wewi=[ 0 -WzE 0;
       WzE 0 0;
       0 0 0];
Wbwi=[ 0 -R Q;
       R 0 -P;
       -Q P 0];
Wq=[ 0 -P -Q -R;
     P 0 R -Q;
     Q -R 0 P;
     R Q -P 0];

% State Equations
pdot=Wewi*p+R_i2b'*vb;
vdot=R_i2b*(g-Wewi^2*p)-(Wbwi+2*R_i2b*Wewi*R_i2b')*vb+Force/Rm;
wdot=inv(J)*Torque-inv(J)*Wbwi*J*wb;
qdot=Wq*q/2;

for ind=1:3
    if wdot(ind)<1e-5
        wdot(ind)=0;
    end
end

% Output Vector udot
udot=[pdot;vdot;wdot;qdot;
      phi;theta;psy;Aa;As;speed;
      latgd;lm_g;h;];

```

7. ACoeff.m

```
function [CN_Aa Cm_Aa CY_As Cn_As Cl_dp CY_dp Cn_dp...
        Cl_dr CY_dr Cn_dr Cl_As CN_dq Cm_dq]=AeroCoeff(Aa,h,dq,t)
% Written by LT John A. Lukacs IV, Naval Postgraduate School, June 2006

% This function interpolates to determine several aerodynamic
% coefficients to be utilized by the BRFlight.m function for
% calculation
% of forces and moments acting on the missile.

% The tables used were point-plotted from the book:
% Tactical Missile Aerodynamics: General Topics, M.J.Hemsch
% (Editor)
% Progress in Astronautics and Aeronautics, Vol.141, c1992
% Chapter 2, Aerodynamic Considerations for Autopilot Design,
% L.L.Cronvich, Figures 8,10,14,17,18,19,23 from pp.47-59

% Variable List:
% Aa      =angle of attack, function input.
% CY_As   =aerodynamic side force coefficient.
% CY_dr   =aerodynamic yaw control force derivative.
% CY_dp   =aerodynamic yaw control coupling derivative.
% CN_Aa   =aerodynamic normal force coefficient,
%         requires multiple interpolations.
% CN_dq   =aerodynamic pitch control force derivative.
% Cl_As   =aerodynamic side moment coefficient.
% Cl_dr   =aerodynamic roll control coupling derivative.
% Cl_dp   =aerodynamic roll control moment derivative.
% Cm_Aa   =aerodynamic pitching moment coefficient,
%         requires multiple interpolations.
% Cm_dq   =aerodynamic pitch control moment derivative.
% Cn_As   =aerodynamic yaw moment coefficient.
% Cn_dr   =aerodynamic yaw control moment derivative.
% Cn_dp   =aerodynamic yaw control coupling derivative.
% dq      =pitch controlling surface deflection, utilized to
%         calculate variables requiring multiple interpolations,
%         function input.
% sign(dq) =utilized to create symmetric response to dq commands.
%         Obtains a value of +1 if dq>0, -1 if dq<0.
% h       =altitude in meters, converted to km, function input.
% n00,n10,n20=tabular value of dq from point plots. Utilized for
%         initial interpolation of CN_Aa, Cm_Aa, and Cl_As to create
%         the secondary interpolation tables. The actual input
%         value of dq is then used to interpolate between the three
%         values.

AoA =[ 0      4      8      12      16      20      24      ];
Alt =[ 0      3.048  6.096  9.144  12.192  15.24  18.288  86      ];
Tdq =[ 0      10      20      ];

Aa=Aa*180/pi;
dq=dq*180/pi;
h=h/1000;
```

```

if dq == abs(dq) % Assume the coefficient values are symmetrical
    sign=1;      % around the mean line of the control surface.
else
    sign=-1;
end

%% Tables
% Fig 8 - Stability Data, Pitch Plane
T_CN_Aa_dqn00=[ 0      0.545  1.212  2.061  3.212  4.424  5.697 ];
T_CN_Aa_dqn10=[ -0.424  0.061  0.727  1.576  2.727  3.879  5.152 ];
T_CN_Aa_dqn20=[ -0.969 -0.485  0.242  1.182  2.242  3.455  4.606 ];
T_Cm_Aa_dqn00=[ 0      -0.394 -0.848 -1.394 -1.969 -2.545 -3.212 ];
T_Cm_Aa_dqn10=[ 2.061  1.697  1.273  0.788  0.303 -0.182 -0.667 ];
T_Cm_Aa_dqn20=[ 4.545  3.909  3.273  2.606  2.121  1.818  1.667 ];

% Fig 10 - Yaw Stability Derivatives
T_CY_As=[ -0.114 -0.118 -0.127 -0.136 -0.152 -0.177 -0.207 ];
T_Cn_As=[ 0.106  0.085  0.042 -0.015 -0.042 -0.021  0.042 ];

% Fig 14 - Roll Derivative
T_Cl_dp=[ 0.08  0.08  0.082  0.084  0.086  0.088  0.09  ];

% Fig 17 - Roll Control Coupling Derivatives
T_CY_dp=[ 0 -0.002 -0.005 -0.009 -0.016 -0.024 -0.032 ];
T_Cn_dp=[ 0 0.0078 0.019 0.039 0.068 0.104 0.141 ];

% Fig 18 - Yaw Control Derivatives
T_Cl_dr=[ 0      -0.001 -0.004 -0.009 -0.016 -0.023 -0.031 ];
T_CY_dr=[ 0.050  0.050  0.050  0.051  0.053  0.056  0.059 ];
T_Cn_dr=[ -0.209 -0.217 -0.223 -0.231 -0.241 -0.250 -0.266 ];

% Fig 19 - Effect of Pitch Control on Roll Stability
T_Cl_As_dqn00=[ 0 0.011 0.039 0.106 0.123 0.082 0.021 ];
T_Cl_As_dqn10=[ 0 0.033 0.102 0.227 0.269 0.219 0.167 ];

% Fig 23 - Pitch Control Derivatives for Aeroelastic Missile
T_CN_dq=[ 0.1634 0.1649 0.1656 0.1662 0.1665 0.1667 0.1668...
          0.167 ];
T_Cm_dq=[ 0.0689 0.0827 0.0921 0.0985 0.1033 0.1061 0.1076...
          0.110 ];

%% Calculation of Coefficient Values
% Angle of Attack based values
CN_Aa_dqn00=interp1(AoA,T_CN_Aa_dqn00,Aa,'spline');
CN_Aa_dqn10=interp1(AoA,T_CN_Aa_dqn10,Aa,'spline');
CN_Aa_dqn20=interp1(AoA,T_CN_Aa_dqn20,Aa,'spline');
Cm_Aa_dqn00=interp1(AoA,T_Cm_Aa_dqn00,Aa,'spline');
Cm_Aa_dqn10=interp1(AoA,T_Cm_Aa_dqn10,Aa,'spline');
Cm_Aa_dqn20=interp1(AoA,T_Cm_Aa_dqn20,Aa,'spline');
CY_As=interp1(AoA,T_CY_As,Aa,'spline');
Cn_As=interp1(AoA,T_Cn_As,Aa,'spline');
Cl_dp=interp1(AoA,T_Cl_dp,Aa,'spline');
CY_dp=interp1(AoA,T_CY_dp,Aa,'spline');
Cn_dp=interp1(AoA,T_Cn_dp,Aa,'spline');

```



```

Cl_dr=interp1(AoA,T_Cl_dr,Aa,'spline');
CY_dr=interp1(AoA,T_CY_dr,Aa,'spline');
Cn_dr=interp1(AoA,T_Cn_dr,Aa,'spline');
Cl_As_dqn00=interp1(AoA,T_Cl_As_dqn00,Aa,'spline');
Cl_As_dqn10=interp1(AoA,T_Cl_As_dqn10,Aa,'spline');

% Altitude based values
CN_dq=interp1(Alt,T_CN_dq,h,'linear');
Cm_dq=interp1(Alt,T_Cm_dq,h,'linear');

%% Further Interpolation of dq variables
T2_CN_Aa=[ CN_Aa_dqn00 CN_Aa_dqn10 CN_Aa_dqn20 ];
T2_Cm_Aa=[ Cm_Aa_dqn00 Cm_Aa_dqn10 Cm_Aa_dqn20 ];
T2_Cl_As=[ Cl_As_dqn00 Cl_As_dqn10 Cl_As_dqn10 ];

CN_Aa_1=interp1(Tdq,T2_CN_Aa,abs(dq),'spline');
CN_Aa=CN_Aa_1;
Cm_Aa_1=interp1(Tdq,T2_Cm_Aa,abs(dq),'spline');
Cm_Aa=Cm_Aa_1;
Cl_As_1=interp1(Tdq,T2_Cl_As,abs(dq),'spline');
Cl_As=Cl_As_1;

return

```

8. Animation.m

```

%% Script File
% This script 'animates' the data received after Ballistic Missile
Model
% run. It requires six vectors of parameters:
%         speed - defining missile's full speed time history,
%   psy,theta,phi - defining Euler angles histories (orientation of {b}
%                   wrt {n}),
%   alpha,beta - defining angle of attack and sideslip angle
%                   histories,
%   E-mail:      oayakime@nps.edu

clc
d2r=pi/180;
NumbofFrs=length(theta);    % Number of available data points (frames)

psyI=pi+psy;
thetaI=theta;
phiI=phi;
alphaI=alpha;
betaI=beta;
speedI=speed;

%% Define Ballistic Missile's geometry (3 stages)
% The geometry is defined for a half of the missile
xBMs{1}=[0 0 2 3 16 19 30 32];

```

```

yBMs{1}=[0 1.85 1.85 1.1 1.1 0.65 0.65 0];
xBMs{2}=[0 0 1 2 14 16];
yBMs{2}=[0 1.31 1.31 0.65 0.65 0];
xBMs{3}=[0 0 2];
yBMs{3}=[0 0.65 0];
% Define geometry for the second half
for iMS=1:3
nP=length(xBMs{iMS});
for i=1:nP-1
xBMs{iMS}=[xBMs{iMS} xBMs{iMS}(nP-i)];
yBMs{iMS}=[yBMs{iMS} -yBMs{iMS}(nP-i)];
end
% Place the missile to the center of the image and scale it so that it
% occupies 2/3 of the screen
sca=max(xBMs{iMS})-min(xBMs{iMS});
xbm=3*(xBMs{iMS}-sca/2)/sca; % Missile geometry is defined in NED
ybm=3*yBMs{iMS}/sca; % frame {b} (x-axis is pointed North)
% The final (full, centered and scaled) geometry
Missile{iMS}(:,1)=xbm'; Missile{iMS}(:,2)=ones(length(xbm),1);
Missile{iMS}(:,3)=ybm';
end

%% Define Interceptor's geometry (2 stages)
% The geometry is defined for a half of the missile
xIMs{1}=[0 0 1.6 1.7 1.74 1.83 2 2.1 2.6 2.8 4.5 4.7 6 6.63];
yIMs{1}=[0 0.265 0.265 0.17 0.17 0.29 0.33 0.17 0.17 0.3 0.3 0.17 ...
0.17 0];
xIMs{2}=[0 0 0.04 0.13 0.3 0.4 0.9 1.1 2.8 3 4.3 4.93];
yIMs{2}=[0 0.17 0.17 0.29 0.33 0.17 0.17 0.3 0.3 0.17 0.17 0];
% Define geometry for the second half
for iIS=1:2
nP=length(xIMs{iIS});
for i=1:nP-1
xIMs{iIS}=[xIMs{iIS} xIMs{iIS}(nP-i)];
yIMs{iIS}=[yIMs{iIS} -yIMs{iIS}(nP-i)];
end
% Place the missile to the center of the image and scale it so that it
% occupies 2/3 of the screen
sca=max(xIMs{iIS})-min(xIMs{iIS});
xim=3*(xIMs{iIS}-sca/2)/sca; % Missile geometry is defined in NED
yim=3*yIMs{iIS}/sca; % frame {b} (x-axis is pointed North)
% The final (full, centered and scaled) geometry
Interceptor{iIS}(:,1)=xim'; Interceptor{iIS}(:,2)=ones(length(xim),1);
Interceptor{iIS}(:,3)=yim';
end

%% Define the initial frame for Missile
figure('Name','Side-View Animation')
subplot(1,2,1)
R_psy =[ cos(psy(1)) sin(psy(1)) 0;
-sin(psy(1)) cos(psy(1)) 0;
0 0 1];
R_theta=[ cos(theta(1)) 0 -sin(theta(1))
0 1 0;
sin(theta(1)) 0 cos(theta(1))];
R_phi =[1 0 0;
0 1 0;
0 0 1];

```

```

        0   cos(phi(1))   sin(phi(1));
        0  -sin(phi(1))   cos(phi(1))];
Rm_n2b=R_phi*R_theta*R_psy;           % Rotation from {n} to {b}
imMis=Rm_n2b'*Missile{1}';           % Missile's coordinates in {n}
Mis=fill(imMis(2,:),-imMis(3,:), 'c');% Projection onto y-z plane of {n}
set(Mis, 'EraseMode', 'xor')
axis(2*[-1 1 -1 1]); axis equal
hold on
plot(0,0, 'r.')                       % Center of the figure
plot([0 0],[0 -.1], 'Color', 'k', 'LineWidth', 2) % Gravity vector
R_beta = [ cos(beta(1))   sin(beta(1))   0;
          -sin(beta(1))   cos(beta(1))   0;
           0               0               1];
R_alpha=[ cos(-alpha(1))  0  -sin(-alpha(1))
          0                1    0;
          sin(-alpha(1))  0   cos(-alpha(1))];
Rm_n2v=R_alpha*Rm_n2b;                 % Rotation from {n} wrt {v}
Speed=[speed(1); 0; 0]/1000;           % Speed magnitude in {v}
imSpd=Rm_n2v'*Speed;                   % Projection onto y-z plane of {n}
SpM=plot([0 imSpd(2)],[0 -imSpd(3)], 'Color', 'r', 'LineWidth', 2);
set(SpM, 'EraseMode', 'xor');
textSpeed=text(imSpd(2)+.1,-imSpd(3), 'Speed');
set(textSpeed, 'EraseMode', 'xor');
xlabel('East (y_{LTP})'), ylabel('Up (-z_{LTP})')
set(gca, 'XTickLabel', {}), set(gca, 'YTickLabel', {})
title('Ballistic Missile Attitude')
%% Display initial frame and time
textFrame=text('Color', [0.8471 0.1608 0], 'FontAngle', 'italic', ...
              'Position', [1 1.75], 'String', ['Frame ' num2str(1) ' out of ' ...
              num2str(NumbofFrs)]);
textTime=text('Color', [0.8471 0.1608 0], 'FontAngle', 'italic', ...
              'Position', [1 1.45], 'String', ['Time ' num2str(time(1), '%.2f') ...
              ' sec']);

%% Define the initial frame for Interceptor
subplot(1,2,2)
R_psy = [ cos(psyI(1))   sin(psyI(1))   0;
         -sin(psyI(1))   cos(psyI(1))   0;
          0               0               1];
R_theta=[cos(thetaI(1))  0  -sin(thetaI(1))
         0                1    0;
         sin(thetaI(1))  0   cos(thetaI(1))];
R_phi = [1   0   0;
         0   cos(phiI(1))   sin(phiI(1));
         0  -sin(phiI(1))   cos(phiI(1))];
Ri_n2b=R_phi*R_theta*R_psy;           % Rotation from {n} to {b}
imInt=Ri_n2b'*Interceptor{1}';        % Interceptor's coordinates in {n}
Int=fill(imInt(2,:),-imInt(3,:), 'r');% Projection onto y-z plane of {n}
set(Int, 'EraseMode', 'xor');
axis(2*[-1 1 -1 1]); axis equal
hold on
plot(0,0, 'r.')                       % Center of the figure
plot([0 0],[0 -.1], 'Color', 'k', 'LineWidth', 2) % Gravity vector
R_beta = [ cos(betaI(1))   sin(betaI(1))   0;
          -sin(betaI(1))   cos(betaI(1))   0;
           0               0               1];
R_alpha=[ cos(-alphaI(1))  0  -sin(-alphaI(1))
          0                1    0;
          sin(-alphaI(1))  0   cos(-alphaI(1))];

```

```

            0          1          0;
            sin(-alphaI(1)) 0 cos(-alphaI(1))];
Ri_n2v=R_alpha*Ri_n2b; % Rotation from {n} wrt {v}
Speed=[speedI(1); 0; 0]/1000; % Speed magnitude in {v}
imSpd=Ri_n2v'*Speed; % Projection onto y-z plane of {n}
SpI=plot([0 imSpd(2)],[0 -imSpd(3)], 'Color', 'r', 'LineWidth', 2);
set(SpI, 'EraseMode', 'xor');
textSpeedI=text(imSpd(2)+.1, -imSpd(3), 'Speed');
set(textSpeedI, 'EraseMode', 'xor');
xlabel('East (y_{LTP})'), ylabel('Up (-z_{LTP})')
set(gca, 'XTickLabel', {}), set(gca, 'YTickLabel', {})
title('Interceptor Attitude')

%% Add the 'Next Frame' and 'Auto' buttons
uicontrol('string', 'Next Frame', ...
    'units', 'normal', 'pos', [.66, .15, .13, .06], ...
    'callback', 'set(gcf, 'userdata', 1)');
auto=uicontrol('style', 'toggle', 'units', 'norm', 'pos', ...
    [.8 .15, .08, .06], 'string', 'Auto', 'callback', 'set(gcf, ...
    'userdata', 1)');
set(gcf, 'userdata', 0); goFlag=0;

%% Start animation
for j=2:NumbofFrs
%% i) Define current stage for Missile and Interceptor
if time(j)<6 % Interceptor booster burns out
    iMS=1; iIS=1;
elseif time(j)<130 % Missile 1st stage burns out
    iMS=1; iIS=2;
elseif time(j)<240 % Missile 2nd stage burns out
    iMS=2; iIS=2;
else
    iMS=3; iIS=2;
end

%% ii) Define rotation matrix from {n} to {b} and rotate the missile
R_psy = [ cos(psy(j)) sin(psy(j)) 0;
         -sin(psy(j)) cos(psy(j)) 0;
           0          0          1];
R_theta=[cos(theta(j)) 0 -sin(theta(j))
          0          1          0;
          sin(theta(j)) 0 cos(theta(j))];
R_phi = [1 0 0;
          0 cos(phi(j)) sin(phi(j));
          0 -sin(phi(j)) cos(phi(j))];
Rm_n2b=R_phi*R_theta*R_psy; % Rotation from {n} to {b}
imMis=Rm_n2b'*Missile{iMS}'; % Missile's coordinates in {n}
set(Mis, 'XData', imMis(2, :), 'YData', -imMis(3, :)); % y-z plane projection

%% iii) Define rotation matrix for the Missile's speed vector
%% and rotate it
R_beta = [ cos(beta(j)) sin(beta(j)) 0;
          -sin(beta(j)) cos(beta(j)) 0;
            0          0          1];
R_alpha=[ cos(-alpha(j)) 0 -sin(-alpha(j))
           0          1          0;
           0          0          0];

```

```

        sin(-alpha(j)) 0 cos(-alpha(j))];

Rm_n2v=R_alpha*Rm_n2b;           % Rotation from {n} wrt {v}
Speed=[speed(j); 0; 0]/1000;     % Speed magnitude in {v}
imSpd=Rm_n2v'*Speed;            % Projection onto y-z plane of {n}
set(SpM, 'XData',[0 imSpd(2)], 'YData',[0 -imSpd(3)]);
set(textSpeed, 'Position',[imSpd(2)+.1 -imSpd(3) 0]);

%% iv) Define rotation matrix from {n} to {b} and rotate the
interceptor
R_psy =[ cos(psyI(j)) sin(psyI(j)) 0;
        -sin(psyI(j)) cos(psyI(j)) 0;
         0 0 1];
R_theta=[cos(thetaI(j)) 0 -sin(thetaI(j))
          0 1 0;
          sin(thetaI(j)) 0 cos(thetaI(j))];
R_phi =[1 0 0;
        0 cos(phiI(j)) sin(phiI(j));
        0 -sin(phiI(j)) cos(phiI(j))];
Ri_n2b=R_phi*R_theta*R_psy;     % Rotation from {n} to {b}
imInt=Ri_n2b'*Interceptor{iIS}'; % Interceptor coordinates in
{n}
set(Int, 'XData',imInt(2,:), 'YData',-imInt(3,:)); % y-z plane projection

%% v) Define rotation matrix for the Interceptor's speed vector
%% and rotate it
R_beta =[ cos(betaI(j)) sin(betaI(j)) 0;
          -sin(betaI(j)) cos(betaI(j)) 0;
          0 0 1];
R_alpha=[ cos(-alphaI(j)) 0 -sin(-alphaI(j))
          0 1 0;
          sin(-alphaI(j)) 0 cos(-alphaI(j))];

Ri_n2v=R_alpha*Ri_n2b;         % Rotation from {n} wrt {v}
SpeedI=[speedI(j); 0; 0]/1000; % Speed magnitude in {v}
imSpdI=Ri_n2v'*SpeedI;        % Projection onto y-z plane of {n}
set(SpI, 'XData',[0 imSpdI(2)], 'YData',[0 -imSpdI(3)]);
set(textSpeedI, 'Position',[imSpdI(2)+.1 -imSpdI(3) 0]);

%% vi) Count frames
set(textFrame, 'String', ['Frame ' num2str(j) ' out of ' ...
                          num2str(NumbofFrs)]);
set(textTime, 'String', ['Time ' num2str(time(j), '%.2f') ' sec']);

%% vii) Wait for any control button to be pushed
while goFlag==0
    if get(auto, 'value')==1
        goFlag=1;
    elseif get(gcf, 'userdata')==1
        goFlag=1;
        set(gcf, 'userdata', 0)
    else
        pause(.25)
    end
end
goFlag=0;

```

```
pause(0.1)
end
```

D. COMMON PROGRAMS

1. ZLDragC.m

```
function [Drag]=ZLDragC(M,t)
% Written by LT John A. Lukacs IV, Naval Postgraduate School, June 2006

% This function interpolates to determine drag coefficient based on the
% Mach number and the boost or glide phase of the rocket to be utilized
% in the BRFlight.m and SMFlight.m programs for the calculation of
% forces acting on the rocket/missile.

% The tables used were point-plotted from Prof Hutchinson's ME4703
% "Missile Flight Analysis" Class Notes

% Variable List
% BDrag=boost phase drag interpolation table
% GDrag=glide phase drag interpolation table
% M=mach number
% Mach=mach number interpolation table
% t=time

%% Tables:
Mach= [ 0      0.90  1.1   1.2   1.5   2.0   2.5   3.0...
        3.5   5.0   6.0];
BDrag=[ 0.1444 0.1444 0.2778 0.2778 0.2308 0.1778 0.1481 0.1296...
        0.1185 0.1000 0.0950];
GDrag=[ 0.2461 0.2461 0.4615 0.4615 0.3615 0.2846 0.2500 0.2192...
        0.2000 0.1500 0.1300];

%% Calculation of Drag Coefficient Values:
if M>6.0
    M=6.0;
end

BDrag=interp1(Mach,BDrag,M,'cubic');
GDrag=interp1(Mach,GDrag,M,'cubic');;

Drag=[BDrag;GDrag];

return
```

2. SAtmos.m

```
function [Density, Pressure, Temperature]=SAtmos(alt)
% Calculation of the 1976 standard atmosphere up to 86 km
% Code source: http://www.pdas.com/atmos.htm
% Run ezplot('SAtmos(x)',0,86000) to see the plot of density vs
```

```

% altitude

% Author: Yakimenko, Oleg A.
% Date:   September, 27 2005
% E-mail: oayakime@nps.edu
%
alt=alt/1000;           % Convert altitude from m to km
%% --- Initialize values for 1976 atmosphere
REARTH=6369.0;         % Earth radius (km), depends on Latitude
GMR=34.163195;        % Gas Constant
htab=[0.0, 11.0, 20.0, 32.0, 47.0, 51.0, 71.0, 84.852]; % Geometric alt
ttab=[288.15, 216.65, 216.65, 228.65, 270.65,... % Temperature
      270.65, 214.65, 186.946];
ptab=[1.0, 2.233611E-1, 5.403295E-2, 8.5666784E-3,... % Relative pres
      1.0945601E-3, 6.6063531E-4, 3.9046834E-5, 3.68501E-6];
gtab=[-6.5, 0.0, 1.0, 2.8, 0.0, -2.8, -2.0, 0.0]; % Temp gradient
P0=101325.0; Ro0=1.225;

%%--- Convert geometric to geopotential altitude
if alt>250
    alt=100
end

h=alt*REARTH/(alt+REARTH);

% --- Binary search for altitude interval
i=1;
j=8;

while j > i+1
    k=fix((i+j)/2);
    if h<htab(k);
        j=k;
    else
        i=k;
    end
end

% --- Calculate local temperature
tgrad=gtab(i);
tbase=ttab(i);
deltah=h-htab(i);
tlocal=tbase+tgrad*deltah;
theta=tlocal/ttab(1);

% --- Calculate local pressure
if (tgrad == 0.0)
    delta=ptab(i)*exp(-GMR*deltah/tbase); % Isothermal layers
else
    delta=ptab(i)*(tbase/tlocal)^(GMR/tgrad); % Non-isothermal layers
end

% --- Calculate local density
sigma=delta/theta;

```

```
%% --- Current atmosphere parameters corresponding to Altitude alt
Temperature=tlocal; Density=Ro0*sigma; Pressure=P0*delta;
```

```
return
```


THIS PAGE INTENTIONALLY LEFT BLANK

APPENDIX B: GUIDANCE PROGRAMS

A. DEMONSTRATION

```
%% Script File
% Written by LT John A. Lukacs IV, Naval Postgraduate School, June 2006

% This script generates the plots used to demonstrate the power of the
% developed algorithm to change the path and derivatives of the path
% by varying the boundary conditions and virtual arc, tau. The output
% is two charts, with four sub-charts each, that show the path for the
% variation of the third derivative of the initial condition and tau.

% This script is modeled after one developed by Oleg Yakimenko for the
% ME4903 course, Spring 2006

%% Variable List
% A          = matrix of reference equations
% x1         = first coordinate axis
% x2         = second coordinate axis
% tf         = variable placeholder for tau
% x0         = initial position [x1;x2] boundary condition
% xp0        = initial 1st derivative of position boundary condition
% xpp0       = initial 2nd derivative of position boundary condition
% xppp0      = initial 3rd derivative of position boundary condition
% xf         = final position [x1;x2] boundary condition
% xpf        = final 1st derivative of position boundary condition
% xppf       = final 2nd derivative of position boundary condition
% xpppf      = final 3rd derivative of position boundary condition
% tau        = virtual arc variable
% N          = length of tau
% a1         = x1 boundary conditions vector
% a2         = x2 boundary conditions vector
% ax1        = x1 boundary conditions reference equation
% ax2        = x2 boundary conditions reference equation
% bx1        = x1 1st derivative of boundary conditions reference
%             equation
% bx2        = x2 1st derivative of boundary conditions reference
%             equation
% px1        = inversion of ax1
% px2        = inversion of ax2
% x1         = x1 reference trajectory
% x2         = x2 reference trajectory
% vx1        = inversion of bx1
% vx2        = inversion of bx2
% v1         = x1 1st derivative of reference trajectory
% v2         = x2 1st derivative of reference trajectory
% v          = norm of [v1;v2]

syms tf x0 xp0 xpp0 xppp0 xf xpf xppf xpppf real
A=[1 0 0 0 0 0 0 0 0;
   0 1 0 0 0 0 0 0 0;
   0 0 1 0 0 0 0 0 0;
   0 0 0 1 0 0 0 0 0;
```

```

1 tf tf^2/2 tf^3/6 tf^4/24 tf^5/60 tf^6/120 tf^7/210;
0 1 tf      tf^2/2 tf^3/6  tf^4/12 tf^5/20  tf^6/30;
0 0 1      tf      tf^2/2  tf^3/3  tf^4/4  tf^5/5;
0 0 0      1      tf      tf^2    tf^3    tf^4];
b=[x0 xp0 xpp0 xppp0 xf xpf xppf xpppf]';
a=A\b;
a=collect(a,tf)

for j=1:1:4
xppp0=0.3*j-0.7;
for tf=1:1:10;

a1=subs(a,{'x0','xp0','xpp0','xppp0','xf','xpf','xppf','xpppf','tf'},...
.
        {0,.2,.2,xppp0,1,0.1,0.1,0.1,tf});

a2=subs(a,{'x0','xp0','xpp0','xppp0','xf','xpf','xppf','xpppf','tf'},...
.
        {0,1,0.1,0.1,1,-1,0.1,0.1,tf});
ax1=diag([1,1,1/2,1/6,1/24,1/60,1/120,1/210])*a1;
ax2=diag([1,1,1/2,1/6,1/24,1/60,1/120,1/210])*a2;
bx1=diag([0,1,1,1/2,1/6,1/12,1/20,1/30])*a1;
bx2=diag([0,1,1,1/2,1/6,1/12,1/20,1/30])*a2;
tau=[0:.05:tf];
N=length(a);

figure(1)
subplot(2,2,j)
for i=1:N
px1(i)=ax1(N+1-i);
px2(i)=ax2(N+1-i);
end
x1=polyval(px1,tau);
x2=polyval(px2,tau);
line(x1,x2,'Linewidth',2)
axis([0 2 0 6])
xlabel('x_1'), ylabel('x_2')
text(1.1,2,'\tau_f=var')
title(['d^3x/dt^3|_0=' num2str(xppp0)])
grid on;

figure(2)
subplot(2,2,j)
for i=1:N-1
vx1(i)=bx1(N+1-i);
vx2(i)=bx2(N+1-i);
end
v1=polyval(vx1,tau);
v2=polyval(vx2,tau);
v=sqrt(v1.^2+v2.^2);
line(tau,v,'Linewidth',2)
axis([0 10 0 4])
xlabel('\tau'), ylabel('\surd(x_1^2+x_2^2)')
text(1.1,2,'\tau_f=var')
title(['d^3x/dt^3|_0=' num2str(xppp0)])
grid on

```

end

end

B. GUIDANCE ALGORITHMS

1. SMGuidance.m

```
function [path]=SMGuidance(time,state,target,i);
% Written by LT John A. Lukacs IV, Naval Postgraduate School, June 2006

% This function takes in the state of the interceptor and target and
% generates an initial guess at the final conditions (position,
% orientation angles, range, and time to intercept) through a first-
% order
% trajectory assumption and iterative process. It then calls the
% fminsearch function using those initial guesses. Finally, it plots
% the
% returned optimal flight path and associated variables.

%% Variable List
% best      = vector of the variables in the optimal path returned from
%            the fminsearch function
% const     = variables that fminsearch cannot modify, including system
%            constraints
% cost      = cost function value returned from SMGuidanceCost.m
% costs     = array of the value of the cost variables at each
iteration
% delta     = difference between the tgo1 and tgo2 values (used in the
%            iteration of initial guesses)
% free      = variables that fminsearch can modify, specifically
%            [tau;tgo;thf;psif]
% init      = vector of initial estimates
% J         = vector of cost function variable values
% N         = length of the path vector (used for plotting)
% nmax      = maximum acceleration capability of the interceptor,
%            altitude dependent
% options   = modifiable options for the fminsearch function (MATLAB
%            help file is under "optimset")
% path      = returned time history of the optimal path
% psi       = initial interceptor heading angle
% psidot    = initial rate of change of interceptor heading angle
% psif      = final interceptor heading angle, calculated from final
%            conditions estimate
% psit      = target heading angle
% Py        = penalty function on the y acceleration
% Pz        = penalty function on the z acceleration
% q         = counting variable
% qq        = counting variable
% range     = estimate of distance between target and interceptor
% state     = state of the interceptor missile, sent from SMGuidance.m
%            [px;py;pz;V;th;psi;Vdot;thetadot;psidot];
% states    = array of the values of all processes in SMGuidance.m
% target    = state of the rocket, sent from SMGuidance.m
%            [Pos_BR(i+j,1);Pos_BR(i+j,2);Pos_BR(i+j,3);
```

```

%           Vel_BR(i+j,1);Vel_BR(i+j,2);Vel_BR(i+j,3)] where 'i+j'
%           is the time synchronization function between BRFlight.m
%           and SMFlight.m
% tau_f     = value of the virtual arc
% tgo       = time to go to intercept
% tgo1      = estimate of time to go to intercept, iterative value
% tgo2      = estimate of time to go to intercept, iterative value
% th        = initial interceptor flight path angle
% thdot     = initial rate of change of interceptor flight path angle
% thf       = final interceptor flight path angle
% tht       = target flight path angle
% tic..toc  = MATLAB function to track run time
% trys      = vector of optimal path and derivative values
% V         = initial interceptor velocity
% V_f       = final interceptor velocity
% Vave      = average interceptor velocity
% Vdot      = initial interceptor acceleration
% x0        = initial interceptor position
% xd0       = initial interceptor velocity
% xdd0      = initial interceptor acceleration
% xdf       = final interceptor position
% xdt       = current target velocity
% xf        = final interceptor acceleration
% xmult     = ratio value (used for plotting)
% xt        = current target position
% ymult     = ratio value (used for plotting)
% zmult     = ratio value (used for plotting)

```

```

global costs q qq states tgo trys update

```

```

% Initialize Variables

```

```

Re=6.378137e6;

```

```

q=q+1;

```

```

% SM Initial State

```

```

x0=state(1:3);

```

```

V=state(4);

```

```

th=state(5);

```

```

psi=state(6);

```

```

Vdot=state(7);

```

```

thdot=state(8);

```

```

psidot=state(9);

```

```

% SM Initial Velocities and Accelerations

```

```

xd0=[V*cos(th)*cos(psi);

```

```

      V*cos(th)*sin(psi);

```

```

      V*sin(th)];

```

```

xdd0=[Vdot*cos(th)*cos(psi)-V*cos(th)*sin(psi)*psidot-V*sin(th)*...
      cos(psi)*thdot;

```

```

      Vdot*cos(th)*sin(psi)+V*cos(th)*cos(psi)*psidot-V*sin(th)*...
      sin(psi)*thdot;

```

```

      Vdot*sin(th)+V*cos(th)*thdot];

```

```

% BR Initial State

```

```

xt=target(1:3);

```

```

xdt=target(4:6);

```

```

tht=atan2(xdt(3),norm(xdt(1:2)));

```

```

psit=atan2(xdt(2),xdt(1));

% Estimate Final Conditions
tgo1=100; delta=5;
while delta>1
    if tgo1>26
        V_f=3500-10*(tgo1-26);
        Vave=(26*3500/2+(tgo1-26)*(3500+V_f)/2)/tgo1;
    else
        V_f=tgo1*3500/26;
        Vave=V_f/2;
    end
    xf=xt+xdt.*tgo1;
    tgo2=sqrt((xf(1)-x0(1))^2+(xf(2)-x0(2))^2+(xf(3)-x0(3))^2)...
        /(norm(xdt)+Vave);
    delta=abs(tgo2-tgo1);
    tgo1=(tgo1+tgo2)/2;
end
tgo=tgo1;

range=sqrt((xf(1)-x0(1))^2+(xf(2)-x0(2))^2+(xf(3)-x0(3))^2)
tau_f=30-10*q;
thf=-tht;
psif=psit+pi;
init=[tau_f;tgo;thf;psif];

% Collect Constraints
free=init;
const=[x0;xd0;xdd0;time;xt;xdt;init];

% Search for Minimum Cost function
tic
options=optimset('MaxIter',100,'Tolfun',10,'TolX',10);
best = fminsearch(@(x) SMGuidanceCost(x,const),free,options);
toc
[path]=SMTrajectory(best,const);
[cost,J,Py,Pz]=SMGuidanceCost(best,const)

tau_f=best(1);
tgo=best(2);
thf=best(3);
psif=best(4);

N=length(path(:,1));
V_f=path(N,5)
xf=path(N,2:4)
xdf=[V_f*cos(thf)*cos(psif);
     V_f*cos(thf)*sin(psif);
     V_f*sin(thf)];

%% Plot Every Iteration
xmult=20000/(norm(xd0)+norm(xdt));
ymult=20000/(norm(xd0)+norm(xdt));
zmult=20000/(norm(xd0)+norm(xdt));
nmax=40+(40-10)/(0-50000)*(path(:,4)-Re);

```

```

figure
plot3(path(:,2),path(:,3),path(:,4),'-k','Linewidth',3)
hold on;grid;
plot3(x0(1),x0(2),x0(3),'*b','linewidth',5)
plot3([x0(1)-xmult*xd0(1);x0(1)+xmult*xd0(1)],...
      [x0(2)-ymult*xd0(2);x0(2)+ymult*xd0(2)],...
      [x0(3)-zmult*xd0(3);x0(3)+zmult*xd0(3)], '-b','Linewidth',3)
plot3(x0(1)+xmult*xd0(1),x0(2)+xmult*xd0(2),x0(3)+xmult*xd0(3),...
      'ob','linewidth',3)
plot3(xf(1),xf(2),xf(3),'*r','linewidth',5)
plot3([xf(1)-xmult*xdt(1);xf(1)+xmult*xdt(1)],...
      [xf(2)-ymult*xdt(2);xf(2)+ymult*xdt(2)],...
      [xf(3)-zmult*xdt(3);xf(3)+zmult*xdt(3)], '-r','Linewidth',3)
plot3(xf(1)+xmult*xdt(1),xf(2)+xmult*xdt(2),xf(3)+xmult*xdt(3),...
      'or','linewidth',3)
%axis([0 250000 -150000 200000 6300000 6550000])
xlabel('X position (m)','FontName','Times New Roman')
ylabel('Y position (m)','FontName','Times New Roman')
zlabel('Z position (m)','FontName','Times New Roman')
title('Interception Geometery','FontName','Times New Roman',...
      'FontSize',12.5)

```

```

figure
plot3(path(:,2),path(:,3),path(:,4)-Re,'-k','Linewidth',3)
hold on;grid;
plot3(x0(1),x0(2),x0(3)-Re,'*b','linewidth',5)
plot3([x0(1)-xmult*xd0(1);x0(1)+xmult*xd0(1)],...
      [x0(2)-ymult*xd0(2);x0(2)+ymult*xd0(2)],...
      [x0(3)-Re-zmult*xd0(3);x0(3)-Re+zmult*xd0(3)], '-b','Linewidth',3)
plot3(x0(1)+xmult*xd0(1),x0(2)+xmult*xd0(2),x0(3)-Re+xmult*xd0(3),...
      'ob','linewidth',3)
plot3(xf(1),xf(2),xf(3)-Re,'*r','linewidth',5)
plot3([xf(1)-xmult*xdt(1);xf(1)+xmult*xdt(1)],...
      [xf(2)-ymult*xdt(2);xf(2)+ymult*xdt(2)],...
      [xf(3)-Re-zmult*xdt(3);xf(3)-Re+zmult*xdt(3)], '-r','Linewidth',3)
plot3(xf(1)+xmult*xdt(1),xf(2)+xmult*xdt(2),xf(3)-Re+xmult*xdt(3),...
      'or','linewidth',3)
%axis([0 250000 -150000 200000 6300000 6550000])
xlabel('X position (m)','FontName','Times New Roman')
ylabel('Y position (m)','FontName','Times New Roman')
zlabel('Z position (m)','FontName','Times New Roman')

```

```

figure
plot(path(:,2),path(:,3),'-k','Linewidth',3)
hold on;grid;%axis equal;
plot(x0(1),x0(2),'*b','linewidth',5)
plot([x0(1)-xmult*xd0(1);x0(1)+xmult*xd0(1)],...
      [x0(2)-ymult*xd0(2);x0(2)+ymult*xd0(2)], '-b','Linewidth',3)
plot(x0(1)+xmult*xd0(1),x0(2)+xmult*xd0(2),'ob','linewidth',3)
plot(xf(1),xf(2),'*r','linewidth',5)
plot([xf(1)-xmult*xdt(1);xf(1)+xmult*xdt(1)],...
      [xf(2)-ymult*xdt(2);xf(2)+ymult*xdt(2)], '-r','Linewidth',3)
plot(xf(1)+xmult*xdt(1),xf(2)+xmult*xdt(2),'or','linewidth',3)
xlabel('X position (m)','FontName','Times New Roman')
ylabel('Y position (m)','FontName','Times New Roman')

```

```

figure
plot(path(:,3),path(:,4)-Re, '-k', 'Linewidth', 3)
hold on;grid;%axis equal;
plot(x0(2),x0(3)-Re, '*b', 'linewidth', 5)
plot([x0(2)-ymult*xd0(2);x0(2)+ymult*xd0(2)],...
      [x0(3)-Re-zmult*xd0(3);x0(3)-Re+zmult*xd0(3)], '-b', 'Linewidth', 3)
plot(x0(2)+xmult*xd0(2),x0(3)-Re+xmult*xd0(3), 'ob', 'linewidth', 3)
plot(xf(2),xf(3)-Re, '*r', 'linewidth', 5)
plot([xf(2)-ymult*xdt(2);xf(2)+ymult*xdt(2)],...
      [xf(3)-Re-zmult*xdt(3);xf(3)-Re+zmult*xdt(3)], '-r', 'Linewidth', 3)
plot(xf(2)+xmult*xdt(2),xf(3)-Re+xmult*xdt(3), 'or', 'linewidth', 3)
xlabel('Y position (m)', 'FontName', 'Times New Roman')
ylabel('Z position (m)', 'FontName', 'Times New Roman')

```

```

figure
plot(path(:,2),path(:,4)-Re, '-k', 'Linewidth', 3)
hold on;grid;%axis equal;
plot(x0(1),x0(3)-Re, '*b', 'linewidth', 5)
plot([x0(1)-xmuilt*xd0(1);x0(1)+xmuilt*xd0(1)],...
      [x0(3)-Re-zmult*xd0(3);x0(3)-Re+zmult*xd0(3)], '-b', 'Linewidth', 3)
plot(x0(1)+xmuilt*xd0(1),x0(3)-Re+xmuilt*xd0(3), 'ob', 'linewidth', 3)
plot(xf(1),xf(3)-Re, '*r', 'linewidth', 5)
plot([xf(1)-xmuilt*xdt(1);xf(1)+xmuilt*xdt(1)],...
      [xf(3)-Re-zmult*xdt(3);xf(3)-Re+zmult*xdt(3)], '-r', 'Linewidth', 3)
plot(xf(1)+xmuilt*xdt(1),xf(3)-Re+xmuilt*xdt(3), 'or', 'linewidth', 3)
xlabel('X position (m)', 'FontName', 'Times New Roman')
ylabel('Z position (m)', 'FontName', 'Times New Roman')

```

```

figure
hold on
plot(path(:,1),path(:,5), '-b', 'Linewidth', 3)
plot(path(:,1),path(:,8), '--k', 'Linewidth', 3)
grid
xlabel('time (s)', 'FontName', 'Times New Roman')
ylabel('V', 'FontName', 'Times New Roman')
legend('V', 'Vdot', 'Location', 'EastOutside')

```

```

figure
hold on
plot(path(:,1),path(:,6), '-b', 'Linewidth', 3)
plot(path(:,1),path(:,7), '--k', 'Linewidth', 3)
grid
xlabel('time (s)', 'FontName', 'Times New Roman')
ylabel('th, psi (rad)', 'FontName', 'Times New Roman')
legend('th', 'psi', 'Location', 'EastOutside')

```

```

figure
hold on
plot(path(:,1),path(:,12), '--b', 'Linewidth', 3)
plot(path(:,1),path(:,13), '-k', 'Linewidth', 3)
plot(path(:,1),nmax(:), '--r', 'Linewidth', 3)
plot(path(:,1),-nmax(:), '--r', 'Linewidth', 3)
grid
xlabel('time (s)', 'FontName', 'Times New Roman')
ylabel('force (g)', 'FontName', 'Times New Roman')

```



```

legend('ny', 'nz', 'Location', 'EastOutside')

figure
subplot(3,1,1)
plot(path(:,1),trys(:,1), '-k', 'Linewidth', 2);
legend('x(1)')
grid
subplot(3,1,2)
plot(path(:,1),trys(:,5), '-k', 'Linewidth', 2);
ylabel('Flight Path', 'FontName', 'Times New Roman')
legend('x^(1)')
grid
subplot(3,1,3)
plot(path(:,1),trys(:,9), '-k', 'Linewidth', 2);
legend('x^^(1)')
grid
xlabel('time', 'FontName', 'Times New Roman')

figure
subplot(3,1,1)
plot(path(:,1),trys(:,2), '-k', 'Linewidth', 2);
grid
legend('x(2)')
subplot(3,1,2)
plot(path(:,1),trys(:,6), '-k', 'Linewidth', 2);
ylabel('1st Dirivative of Flight Path', 'FontName', 'Times New Roman')
legend('x^(2)')
grid
subplot(3,1,3)
plot(path(:,1),trys(:,10), 'k', 'Linewidth', 2);
legend('x^^(2)')
grid

figure
subplot(3,1,1)
plot(path(:,1),trys(:,3), '-k', 'Linewidth', 2);
legend('x(3)')
grid
subplot(3,1,2)
plot(path(:,1),trys(:,7), '-k', 'Linewidth', 2);
ylabel('2nd Derivative of Flight Path', 'FontName', 'Times New Roman')
legend('x^(3)')
grid
subplot(3,1,3)
plot(path(:,1),trys(:,11), '-k', 'Linewidth', 2);
legend('x^^(3)')
grid
xlabel('time (s)', 'FontName', 'Times New Roman')

figure
plot(costs(:,1), '-k', 'Linewidth', 3);grid
xlabel('Iterations (#)', 'FontName', 'Times New Roman')
ylabel('Cost Function Value', 'FontName', 'Times New Roman')

figure
plot(costs(:,2), '-k', 'Linewidth', 3);grid

```

```

xlabel('Iterations (#)', 'FontName', 'Times New Roman')
ylabel('/tau _f', 'FontName', 'Times New Roman')

figure
plot(costs(:,3), '-k', 'Linewidth', 3);grid
xlabel('Iterations (#)', 'FontName', 'Times New Roman')
ylabel('t_g_o to Intercept', 'FontName', 'Times New Roman')

figure;hold on;
plot(costs(:,5), '-b', 'Linewidth', 3)
grid
plot(costs(:,6), '-k', 'Linewidth', 3)
hold off
xlabel('Iterations (#)', 'FontName', 'Times New Roman')
ylabel('Penalty Values', 'FontName', 'Times New Roman')
legend('Py', 'Pz')

figure
plot(180/pi*acos(costs(:,4)/100), '-k', 'Linewidth', 3);grid
xlabel('Iterations (#)', 'FontName', 'Times New Roman')
ylabel('Impact Angle', 'FontName', 'Times New Roman')
axis([0 qq 0 100])
%%
states{q,1}=path;
states{q,2}=const;
states{q,3}=free;
states{q,4}=best;
states{q,5}=[cost;J;Py;Pz];

return

```

2. SMGuidanceCost.m

```

function [cost,J,Py,Pz]=SMGuidanceCost(free,const)
% Written by LT John A. Lukacs IV, Naval Postgraduate School, June 2006

% This function calculates the cost of the proposed trajectory returned
% from the SMTrajectory.m function based on the optimization parameters
% and penalty parameters defined herein. This is a sub-function of the
% SMGuidance.m function's fminsearch. This cost value is used to
% determine whether the proposed trajectory is optimal. The trajectory
% that returns the minimum value of J is the optimal function.

%% Variable List
% calccost = a global variable of the value of the J function (used
%           for plotting)
% const    = variables that fminsearch cannot modify, including system
%           constraints, specifically [x0;xd0;xdd0;time;xt;xdt;init]
% cost     = cost function value returned from SMGuidanceCost.m
function
% costs   = vector of values of the cost variables at each iteration
% dist    = cumulative distance traveled
% free    = variables that fminsearch can modify, specifically

```

```

%           [tau;tgo;thf;psif]
% init      = vector of initial estimates
% J         = vector of cost function variable values
% N         = length of the path vector (used for plotting)
% nmax      = maximum acceleration capability of the interceptor,
%           altitude dependent
% nx        = axial acceleration command, body frame x
% ny        = axial acceleration command, body frame y
% nz        = axial acceleration command, body frame z
% path      = returned time history of the optimal path, specifically
%           [time' X(1:3,:) ' V' th' psi' Vdot' thdot' psidot' nx' ny'
%           nz']
% psi       = initial interceptor heading angle
% psidot    = initial rate of change of interceptor heading angle
% psif      = final interceptor heading angle, calculated from final
%           conditions estimate
% Py        = penalty function on the y acceleration
% Pz        = penalty function on the z acceleration
% qq        = counting variable
% t         = current time
% tau_f     = value of the virtual arc
% tgo;      = time to go to intercept
% th        = initial interceptor flight path angle
% thdot     = initial rate of change of interceptor flight path angle
% thf       = final interceptor flight path angle
% time      = optimal path time history
% V         = initial interceptor velocity
% V_f       = final interceptor velocity
% Vdot      = initial interceptor acceleration
% X         = the optimal path time history in Cartesian coordinates
% x0        = initial interceptor position
% xd0       = initial interceptor velocity
% xdd0      = initial interceptor acceleration
% xdf       = final interceptor velocity
% xdt       = current target velocity
% xt        = current target position

```

```
[path]=SMTrajectory(free,const);
```

```
global calccost costs q qq tgo trys
```

```
% Initialize Variables
```

```
qq=qq+1;
dist=0;
Re=6.378137e6;
```

```
%% Identify Variables
```

```
time=path(:,1);
X=path(:,2:4);
V=path(:,5);
th=path(:,6);
psi=path(:,7);
Vdot=path(:,8);
thdot=path(:,9);
psidot=path(:,10);
nx=path(:,11);
```

```

ny=path(:,12);
nz=path(:,13);
N=length(path(:,1));

tau_f=free(1);
tgo=free(2);
thf=free(3);
psif=free(4);

x0=const(1:3);
xd0=const(4:6);
xdd0=const(7:9);
t=const(10);
xt=const(11:13);
xdt=const(14:16);
init=const(17:19);

V_f=path(N,5);
xdf=[V_f*cos(thf)*cos(psif);
      V_f*cos(thf)*sin(psif);
      V_f*sin(thf)];
tgo=path(N,1);

for i=2:1:N
    dist=dist+abs(norm([X(i,1)-X(i-1,1);X(i,2)-X(i-1,2);X(i,3)-X(i-
1,3);]));
end
nmax=40+(40-10)/(0-50000)*(path(:,4)-Re);

%% Calculate Cost of the chosen trajectory
J=[ tau_f;
    tgo;
    100*abs(dot(xdf,xdt)/norm(xdf)/norm(xdt))];
Py=sum(max(0,abs(ny)-nmax).^2);
Pz=sum(max(0,abs(nz)-nmax).^2);

cost=0.33*ones(1,3)*J+norm([Py;Pz]);
costs(qq,1:6)=[cost;J;Py;Pz];
calccost=cost;

return

```

3. SMTrajectory.m

```

function [path]=SMTrajectory(free,const)
% Written by LT John A. Lukacs IV, Naval Postgraduate School, June 2006

% This function proposes a trajectory based on the input parameters
% "free" and "const". This is a sub-function of the SMGuidance.m
% function's fminsearch. This function creates a 7th order set of
% equations and evaluates that equation at the boundary conditions
% supplied by the inputs. It then calculates the time history of all
% the flight vehicle variables, including controls and reactions,

```

```

% necessary to develop that flight path. A plot command set at the end
% of this function will plot a chart of the iterations at the end of
% run if desired.

```

```

%% Variable List

```

```

% A      = matrix of reference equations
% Ax     = boundary condition reference equation (1 for each axis)
% Axp    = 1st derivative of boundary conditions reference equation
%        (1 for each axis)
% Axpp   = 2nd derivative of boundary conditions reference equation
%        (1 for each axis)
% Axppp  = 3rd derivative of boundary conditions reference equation
%        (1 for each axis)
% BND    = boundary condition vector (1 for each axis)
% BR_diff = iterative variable (used for plotting)
% BR_end  = iterative variable (used for plotting)
% const  = variables that fminsearch cannot modify, including system
%        constraints, specifically [x0;xd0;xdd0;time;xt;xdt;init]
% Cx     = inversion of Ax (1 for each axis)
% Cxp    = inversion of Axp (1 for each axis)
% Cxpp   = inversion of Axpp (1 for each axis)
% Cxppp  = inversion of Axppp (1 for each axis)
% dtau   = tau step value
% dtime  = time step value
% free   = variables that fminsearch can modify, specifically
%        [tau;tgo;thf;psif]
% g      = gravitational force
% i      = index for coordinate axis
% init   = vector of initial estimates
% L      = lambda, virtual speed
% Lf     = final lambda, defined as Vf
% Li     = initial lambda, defined as V0
% Lpf   = 1st derivative of final lambda
% Lpi   = 1st derivative of initial lambda
% nmax   = maximum acceleration capability of the interceptor,
%        altitude dependent
% nX     = norm of reference trajectory
% nx     = axial acceleration command, body frame x
% nXp    = norm of 1st derivative of reference trajectory
% nXpp   = norm of 2nd derivative of reference trajectory
% nXppp  = norm of 3rd derivative of reference trajectory
% ny     = axial acceleration command, body frame y
% nz     = axial acceleration command, body frame z
% path   = returned time history of the optimal path, specifically
%        [time' X(1:3,:) V' th' psi' Vdot' thdot' psidot' nx'...
%        ny' nz']
% psi    = interceptor heading angle
% psidotf = final rate of change of interceptor heading angle
% psif   = final interceptor heading angle
% psip   = 1st derivative of heading angle
% qq     = counting variable
% t      = current time
% tau    = virtual arc variable
% tau_f  = value of the virtual arc
% tgo    = time to go to intercept
% th     = initial interceptor flight path angle
% thdotf = final rate of change of interceptor flight path angle

```

```

% thf      = final interceptor flight path angle
% thp      = 1st derivative of flight path angle
% time     = optimal path time history
% trys     = collection of norms [X nX Xp nXp Xpp nXppp] (used for
%           plotting)
% V        = velocity
% Vdotf    = final acceleration
% Vdoti    = initial acceleration
% Vf       = final velocity
% Vi       = initial velocity
% Vp       = 1st derivative of velocity
% X        = reference trajectory (1 for each axis)
% x0       = initial interceptor position
% xd0      = initial interceptor velocity
% xdd0     = initial interceptor acceleration
% xddf     = final interceptor position
% xdf      = final interceptor velocity
% xdt      = current target velocity
% xf       = estimate of intercept position
% xF       = final position [x1;x2] boundary condition
% xI       = initial position [x1;x2] boundary condition
% Xp       = 1st derivative of reference trajectory (1 for each axis)
% xp0      = 1st derivative of initial boundary conditions
% xpf      = 1st derivative of final boundary conditions
% xpF      = final 1st derivative of position boundary condition
% xpI      = initial 1st derivative of position boundary condition
% Xpp      = 2nd derivative of reference trajectory (1 for each axis)
% xpp0     = 2nd derivative of initial boundary conditions
% xppf     = 2nd derivative of final boundary conditions
% xppF     = final 2nd derivative of position boundary condition
% xppI     = initial 2nd derivative of position boundary condition
% Xppp     = 3rd derivative of reference trajectory (1 for each axis)
% xppp0    = 3rd derivative of initial boundary conditions
% xpppf    = 3rd derivative of final boundary conditions
% xpppF    = final 3rd derivative of position boundary condition
% xpppI    = initial 3rd derivative of position boundary condition
% xt       = current target position

```

```

global update trys q qq Pos_BR Pos_SM calccost
Re=6.378137e6;

```

```

%% Define Terms

```

```

tau_f=free(1);
tgo=free(2);
thf=free(3);
psif=free(4);

x0=const(1:3);
xd0=const(4:6);
Vi=norm(xd0);
Li=Vi;
xdd0=const(7:9);
Vdoti=norm(xdd0);
Lpi=Vdoti/Vi;
t=const(10);
xt=const(11:13);

```

```

xdt=const(14:16);
init=const(17:19);

Vf=3500-10*tgo;
Lf=Vf;
xf=xt+xdt.*(2.5*tgo);
xdf=[Vf*cos(thf)*cos(psif);
     Vf*cos(thf)*sin(psif);
     Vf*sin(thf)];
Vdotf=-5.9578;
thdotf=0;
psidotf=0;
xddf=[Vdotf*cos(thf)*cos(psif)-Vf*cos(thf)*sin(psif)*psidotf-...
      Vf*sin(thf)*cos(psif)*thdotf;
      Vdotf*cos(thf)*sin(psif)+Vf*cos(thf)*cos(psif)*psidotf-...
      Vf*sin(thf)*sin(psif)*thdotf;
      Vdotf*sin(thf)+Vf*cos(thf)*thdotf];
Lpf=Vdotf/Vf;

%% Calculate Coefficients
xp0=xd0/Li;
xpp0=(xdd0-xd0*Lpi)/Li^2;
xppp0=[0;0;0];
xpf=xdf/Lf;
xppf=(xddf-xdf*Lpf)/Lf^2;
xpppf=[0;0;0];

xp0=xd0;
xpp0=xdd0;
xpf=xdf;
xppf=xddf;

syms tau_F xI xpI xppI xpppI xF xpF xppF xpppF real
A=[ 1  0  0  0  0  0  0  0  0...
    0  0  0;
    0  1  0  0  0  0  0  0  0...
    0  0  0;
    0  0  1  0  0  0  0  0  0...
    0  0  0  0;
    1  tau_F tau_F^2/2 tau_F^3/6 tau_F^4/24 tau_F^5/60...
    tau_F^6/120 tau_F^7/210;
    0  1 tau_F tau_F^2/2 tau_F^3/6 tau_F^4/12...
    tau_F^5/20 tau_F^6/30;
    0  0 1 tau_F tau_F^2/2 tau_F^3/3...
    tau_F^4/4 tau_F^5/5;
    0  0 0 1 tau_F tau_F^2...
    tau_F^3 tau_F^4];
b=[xI xpI xppI xpppI xF xpF xppF xpppF]';
a=A\b;
a=collect(a,tau_F);
N=length(a);

%% Define Boundary Conditions
% {'xI','xpI','xppI','xF','xpF','xppF','tau_F'}

```

```

BND{1}={x0(1),xp0(1),xpp0(1),xppp0(1),xf(1),xpf(1),xppf(1),...
    xpppf(1),tau_f}; %x1
BND{2}={x0(2),xp0(2),xpp0(2),xppp0(2),xf(2),xpf(2),xppf(2),...
    xpppf(2),tau_f}; %x2
BND{3}={x0(3),xp0(3),xpp0(3),xppp0(3),xf(3),xpf(3),xppf(3),...
    xpppf(3),tau_f}; %x3
dtau=tau_f/99;
tau=[0:dtau:tau_f]; % 100 data points

clear A
%% Calculate trajectories (2+1 4th order case)
for i=1:3
    A{i}=subs(a,{'xI','xpI','xppI','xpppI','xF','xPF','xppF',...
        'xpppF','tau_F'},BND{i});
    Ax{i}=diag([ 1, 1, 1/2, 1/6, 1/24, 1/60, 1/120, 1/210 ])...
        *A{i};
    Axp{i}=diag([ 0, 1, 1, 1/2, 1/6, 1/12, 1/20, 1/30 ])...
        *A{i};
    Axpp{i}=diag([ 0, 0, 1, 1, 1/2, 1/3, 1/4, 1/5 ])...
        *A{i};
    Axppp{i}=diag([ 0, 0, 0, 1, 1, 1, 1, 1 ])...
        *A{i};
    Cx(i,:)=Ax{i}([N:-1:1]);
    Cxp(i,:)=Axp{i}([N:-1:2]);
    Cxpp(i,:)=Axpp{i}([N:-1:3]);
    Cxppp(i,:)=Axppp{i}([N:-1:4]);
    X(i,:)=polyval(Cx(i,:),tau);
    Xp(i,:)=polyval(Cxp(i,:),tau);
    Xpp(i,:)=polyval(Cxpp(i,:),tau);
    Xppp(i,:)=polyval(Cxppp(i,:),tau);
end

%% Compute the States
g=3.986004418e14/norm(X(1:3,1)+[0;0;Re])^2;
V(1)=Vi;
Vp(1)=Vdoti;
th(1)=atan2(Xp(3,1),norm(Xp(1:2,1)));
psi(1)=atan2(Xp(2,1),Xp(1,1));

L(1)=V(1);
time(1)=t; dtime(1)=0.1;
tau(1)=0;

for j=2:length(tau);
    g=3.986004418e14/norm(X(1:3,j-1)+[0;0;Re])^2;
    if norm(X(:,j-1))<86000
        [ro,press,temp]=Statmos(norm(X(:,j-1)));
    else
        [ro,press,temp]=Statmos(86000);
    end
    MV=V(j-1)/sqrt(1.402*287*temp);
    [m_i,dia]=SMPParams3(time(j-1));
    [CD]=ZLDragC(MV,time(j-1));
    if time(j-1) < 6
        Thrust=206000;
        CD=CD(1);
    end
end

```



```

elseif time(j-1) < 26
    Thrust=95300;
    CD=CD(1);
else
    Thrust=0;
    CD=CD(2);
end
Sref=pi*dia^2/4;
Drag=ro*V(j-1)^2*CD*Sref/2;
nx(j-1)=(Thrust-Drag)/m_i/g;

th(j-1)=atan2(Xp(3,j-1),norm(Xp(1:2,j-1)));
psi(j-1)=atan2(Xp(2,j-1),Xp(1,j-1));
Vp(j-1)=g*(nx(j-1)-sin(th(j-1)));

thp(j-1)=cos(th(j-1)^2)*(Xpp(3,j-1)*(Xp(1,j-1)^2+Xp(2,j-1)^2)-...
    Xp(3,j-1)*(Xpp(1,j-1)+Xpp(2,j-1)))/(Xp(1,j-1)^2+...
    Xp(2,j-1)^2)^1.5;
psip(j-1)=cos(psi(j-1)^2)*(Xp(1,j-1)*Xpp(2,j-1)-Xpp(1,j-1)*...
    Xp(2,j-1))/(Xp(1,j-1)^2+Xp(2,j-1)^2);
ny(j-1)=V(j-1)/g*cos(th(j-1))*psip(j-1);
nz(j-1)=V(j-1)/g*thp(j-1)+cos(th(j-1));

V(j)=V(j-1)+Vp(j-1)*dtime(j-1);

tau(j)=tau(j-1)+dtau;
ddist(j)=sqrt((X(1,j)-X(1,j-1))^2+(X(2,j)-X(2,j-1))^2+...
    (X(3,j)-X(3,j-1))^2);
dtime(j)=2*ddist(j)/(V(j)+V(j-1));
L(j)=dtau/dtime(j-1);

time(j)=time(j-1)+dtime(j-1);
end
N=length(X(1,:));
for i=1:1:N
    nX(i)=norm(X(1:3,i));
    nXp(i)=norm(Xp(1:3,i));
    nXpp(i)=norm(Xpp(1:3,i));
end
dtime(N)=dtime(N-1);
th(N)=th(N-1);
psi(N)=psi(N-1);
Vp(N)=Vp(N-1);
thp(N)=thp(N-1);
psip(N)=psip(N-1);
nx(N)=nx(N-1);
ny(N)=ny(N-1);
nz(N)=nz(N-1);

trys=[X' nX' Xp' nXp' Xpp' nXpp'];
path=[time' X(1:3,:) ' V' th' psi' Vp' thp' psip' nx' ny' nz' tau'...
    ddist' dtime' L'];

%% Plot every iteration
nmax=40+(40-10)/(0-50000)*(path(:,4)-Re);

```

```

BR_end=time(N)*2+1;
BR_diff=BR_end;
while BR_diff>1
    BR_diff=BR_diff-1;
end
BR_end=BR_end-BR_diff;

figure(100)
figurepalette('hide')
subplot(3,6,[1 2 7 8])
plot3(X(1,:),X(2,:),X(3,:)-Re,'Linewidth',3);grid on
hold on;
plot3(Pos_BR(1:300,1),Pos_BR(1:300,2),Pos_BR(1:300,3)-Re,':k',...
'LineWidth',2)
plot3(Pos_BR(140+BR_end,1),Pos_BR(140+BR_end,2),...
Pos_BR(140+BR_end,3)-Re,'ok','LineWidth',3)
plot3(Pos_BR(140,1),Pos_BR(140,2),Pos_BR(140,3)-Re,'*k','LineWidth',2)
plot3(xf(1),xf(2),xf(3)-Re,'*r','LineWidth',2)
plot3(Pos_SM(1:19,1),Pos_SM(1:19,2),Pos_SM(1:19,3)-Re,'--b',...
'LineWidth',2)
view(-102,8)
hold off;
axis([0 1.1e5 -1e4 1.1e5 0 7e4])
title('3D Flight Path')
subplot(3,6,[13 14])
plot(path(:,1),path(:,12),'--b','LineWidth',3)
hold on;grid on
plot(path(:,1),path(:,13),'-k','LineWidth',3)
plot(path(:,1),nmax(:),'--r','LineWidth',3)
plot(path(:,1),-nmax(:),'--r','LineWidth',3)
axis([10 time(N) -45 45]);
title('Control Effort')
hold off
subplot(3,6,3)
plot(time,X(1,:),'Linewidth',3);grid on
axis([10 time(N) 1e4 1.1e5])
title('X(1)')
subplot(3,6,9)
plot(time,X(2,:),'Linewidth',3);grid on
axis([10 time(N) -1e4 1.1e5])
title('X(2)')
subplot(3,6,15)
plot(time,X(3,:)-Re,'Linewidth',3);grid on
axis([10 time(N) 0 7e4])
title('X(3)')
subplot(3,6,4)
plot(time,Xp(1,:),'Linewidth',3);grid on
axis([10 time(N) -45 45]);axis 'auto y'
title('X_p(1)')
subplot(3,6,10)
plot(time,Xp(2,:),'Linewidth',3);grid on
axis([10 time(N) -45 45]);axis 'auto y'
title('X_p(2)')
subplot(3,6,16)
plot(time,Xp(3,:),'Linewidth',3);grid on
axis([10 time(N) -45 45]);axis 'auto y'
title('X_p(3)')

```

```

subplot(3,6,5)
plot(time,Xpp(1,:), 'Linewidth',3);grid on
axis([10 time(N) -45 45]);axis 'auto y'
title('X_p_p(1)')
subplot(3,6,11)
plot(time,Xpp(2,:), 'Linewidth',3);grid on
axis([10 time(N) -45 45]);axis 'auto y'
title('X_p_p(2)')
subplot(3,6,17)
plot(time,Xpp(3,:), 'Linewidth',3);grid on
axis([10 time(N) -45 45]);axis 'auto y'
title('X_p_p(3)')
subplot(3,6,6)
hold on
plot(qq,time(N), '*k', 'Linewidth',1);grid on
hold off
axis([0 200 0 60]);
title('Time to go')
if qq>1
subplot(3,6,[12 18])
hold on
plot(qq,calccost, '*k', 'Linewidth',1);grid on
axis([0 200 0 100]);axis 'auto y'
hold off
title('Functional Cost')
end

return

```

LIST OF REFERENCES

1. Alway, Peter, "Tartar Missile Dimensions",
<http://yellowjacketsystems.com/alway/images/tartar.gif>, Accessed 1/10/2006
2. Bardanis, Florios, "Kill Vehicle Effectiveness for Boost Phase Interception of Ballistic Missiles", NPS Masters Thesis, 2004
3. Lennox, Duncan, "Ballistic Missile Defense," Jane's Strategic Weapon Systems 40, p. 4, November 27, 2003
4. Federation of American Scientists, "Taep'o-dong 2",
<http://www.fas.org/nuke/guide/dprk/missile/td-2.htm>, Accessed 08/27/2005
5. Google Earth™ distance calculator, Accessed 06/10,2006
6. Jane's Strategic Advisory Services, "RIM-66/-67/-156 Standard SM-1/-2 and RIM-161 SM-3",
<http://www4.janes.com/K2/doc.isp?K2DocKey=/content1/janesdata/binder/isws/isws0208.htm>, Accessed 10/26/2005
7. Hensch, M.J. (editor), Tactical Missile Aerodynamics: General Topics, "Aerodynamic Considerations for Autopilot Design," by L.L.Cronvich, Progress in Astronautics and Aeronautics, Vol.141, 1992
8. Hutchins, Robert, ME4703 "Missile Flight Analysis" Course Notes, Spring 2005
9. Missile Defense Agency, "Ballistic Missile Defense System Overview",
<http://www.mda.mil/mdalink/pdf/bmdsbook.pdf>, Accessed 05/15/2006
10. NASA, "Solid Propellant Grain Design and Internal Ballistics", Document SP-8076, March 1972
11. Raytheon, "Missile Trajectory Phases",
<http://www.raytheonmissiledefense.com/phases/index.html>, Accessed 05/15/2006
12. Raytheon, "Standard Missile 6: Extended Range Active Missile",
http://www.raytheon.com/products/stellent/groups/public/documents/content/cms04_014817.pdf, Accessed 01/10/2006
13. San Jose, Antonio, "Theater Ballistic Missile Defense – Multisensor Fusion, Targeting, and Tracking Techniques", NPS Masters Thesis, 1998
14. Stevens, Brian, and Lewis, Frank, Aircraft Control and Simulation Second Edition, John Wiley and Sons, 2003

15. Springer Online Reference Works, "Calculus of Variations", <http://eom.springer.de/v/v096190.htm>, Accessed 06/10/2006
16. Venik's Aviation, "Russian Space Engines", http://www.aeronautics.ru/archive/reference/Russian_Space_Engines/Russian_Space_Engines_22.htm, Accessed 06/10/2006
17. Wikipedia, "Calculus of Variations", "Galerkin method", "Rayleigh-Ritz method", http://en.wikipedia.org/wiki/Calculus_of_variations, http://en.wikipedia.org/wiki/Galerkin_method, http://en.wikipedia.org/wiki/Rayleigh-Ritz_method, All accessed 06/10/2006
18. Yakimenko, O.A., AE4903 "Direct Method of Calculus of Variations as the Means for Rapid Prototyping of Optimal Trajectories" Course Notes, Winter 2006
19. Yakimenko, O.A., "Direct Methods for Rapid Prototyping of Near-Optimal Aircraft Trajectories", Journal of Guidance, Control, and Dynamics, Vol 23, No. 5, Sep-Oct 2000, pp 865-875
20. Zarchan, Paul, "Ballistic Missile Defense Guidance and Control Issues", Science & Global Security, Volume 8, 1998, pp. 99-124
21. Zarchan, Paul, Tactical and Strategic Missile Guidance Fourth Edition, Vol. 199, American Institute of Aeronautics and Astronautics, Reston, VA, 2002
22. Zipfel, Peter, Modeling and Simulation of Aerospace Vehicle Dynamics, American Institute of Aeronautics and Astronautics, Reston, VA, 2000

INITIAL DISTRIBUTION LIST

1. Defense Technical Information Center
Ft. Belvoir, Virginia
2. Dudley Knox Library
Naval Postgraduate School
Monterey, California
3. Temasek Defence Systems Institute
National University of Singapore
Singapore, Singapore
4. Thomas Hoivik, Associate Chair of Interdisciplinary Activities
Naval Postgraduate School
Monterey, California